SOME STUDIES ON THE ELECTRICAL PROPERTIES OF CHALCOGENIDE AND OXIDE FILMS

A THESIS SUBMITTED TO THE
UNIVERSITY OF POONA

FOR THE DEGREE OF
DOCTOR OF PHILOSOPHY
(IN CHEMISTRY)

BY

ANANDA BALAVANT MANDALE
M. Sc.

STRUCTURE AND THIN FILMS PHYSICS DIVISION
NATIONAL CHEMICAL LABORATORY
POONA - 411 008 (India)

SEPTEMBER 1 9 7 8

CONTENTS

Title	Page
CHAPTER-I : GENERAL INTRODUCTION	
(i) Thin Films	1
(ii) Energy band picture of crystalline solids	4
(iii) Hall effect	9
(iv) Impurity band conduction	14
(v) Scattering mechanism	17
(vi) Thermoelectric power	24
(vii) Fermi energy level	29
(viii) Mean free path	31
(ix) Effective mass	33
(x) Conduction in thin films	33
(xi) Present study	39
REFERENCES	
CHAPTER-II : EXPERIMENTAL TECHNIQUES	
(A) Preparation and measurement technique	
(i) Method of deposition	40
(ii) Substrate and substrate heating	41
(iii) Preparation of samples	42
(iv) Film thickness measurements	43
(v) Electrical contacts	44
(B) Measurements of basic semiconducting parameters	

(i) Resistance and Hall voltage measurements 45

(ii) Measurement technique

(a) Resistance 46

(b) Hall voltage 47

(iii) Thermoelectrical power

(a) Experimental 48

(b) Methods of measurements 49

(C) Structure

REFERENCES

CHAPTER-III : MANGANESE TELLURIDE AND MANGANESE SELENIDE

(A) Introduction 51

(B) Experimental

(i) Preparation of MnTe 54

(ii) Film preparation 55

(a) MnTe

(C) Results

(i) Structure 55

(ii) Resistivity and activation energy 56

(iii) Hall constant 57

(iv) Carrier concentration 58

(v) Mobility 59

(vi) Thermoelectric power 60

(vii) Temperature coefficient of resistance (TCR) 61

(viii) Mean free path 61

(MnS

(b) MnSe

(C) Results

(i) Structure 62

(ii) Resistivity and activation energy 62

(iii) Thermoelectric power 63

(iv) Temperature coefficient of resistance 63

(D) Discussion

REFERENCES

CHAPTER-IV : MERCURY TELLURIDE

(A) Introduction 76

(B) Experimental

(a) Preparation of mercury telluride 83

(b) Film preparation 84

(C) Results

(i) Structure 84

(ii) Resistance, resistivity and activation energy 85

(iii) Hall constant and carrier concentration 86

(iv) Mobility 86

(v) Thermoelectric power 87

(vi) Effective hole mass 88

(vii) Temperature coefficient of resistance (TCR) 89

(viii) Mean free path 89

(D) Discussion 89

REFERENCES

CHAPTER-V : TIN TELLURIDE AND TIN SELENIDE

(A) Introduction 94

(B) Experimental 100

(a) SnTe

(C) Results

(i) Structure 102

(ii) Resistivity 102

(iii) Hall coefficient and carrier concentration 103

(iv) Mobility and potential barrier height 103

(v) Thermoelectric power 104

(vi) Fermi energy level 104

(vii) TCR 105

(viii) Mean free path 106

(b) SnSe

(C) Results

(i) Structure 106

(ii) Resistance, resistivity and activation energy 107

(iii) Thermoelectric power 107

(iv) TCR 108

(D) Discussion

REFERENCES

CHAPTER-VI : LEAD TELLURIDE AND LEAD SELENIDE

(A) Introduction 114

(B) Experimental 120

(C) Results

(i) Structure 122

(a) PbTe

(ii) Resistivity and activation energy 123

(iii) Hall coefficient and carrier concentration 123

(iv) Mobility and potential barrier height 124

(v) Thermoelectric power 125

(vi) Mean free path 126

(b) PbSe

(C) Results

(i) Resistivity and activation energy 127

(ii) Hall constant and carrier concentration 127

(iii) Mobility and potential barrier height 128

(iv) Thermoelectric power 129

(v) Mean free path 130

(D) Discussion 130

REFERENCES

CHAPTER-VII : GALLIUM TELLURIDE, GALLIUM SELENIDE AND INDIUM OXIDE

(1) GALLIUM TELLURIDE AND GALLIUM SELENIDE

(A) Introduction 134

(B) Experimental 137

(a) Ga_2Te_3

(C) Results

(i) Structure 139

(ii) Resistance, resisticity and activation energy 139

(iii) TCR 140

(iv) Thermoelectric power 141

(b) Ga_2Se_3

(C) Results

(i) Structure 141

(ii) Resistivity and activation energy 141

(iii) TCR 142

(D) Discussion 142

REFERENCES

(2) INDIUM OXIDE

(A) Introduction 146

(B) Experimental 149

(C) Results

(i) Structure 149

(ii) Resistance, resistivity and activation energy 150

(iii) TCR 151

(iv) Mean free path 151

(D) Discussion 152

REFERENCES

SUMMARY AND CONCLUSIONS 154

ACKNOWLEDGEMENTS

CHAPTER-I

GENERAL INTRODUCTION

CHAPTER-I

GENERAL INTRODUCTION

(i) Thin Films

Tremendous advances have been made in the science and technology of thin solid films in the last two decades. The great technological developments especially on rockets, missiles, space research and in electronic industries such as rectification, amplification, detection system, miniaturisation of such devices, etc. have been possible due to the appearance of a new class of material known as "semiconductors".

The applications of thin films are numerous and to mention a few are as infrared detectors, microelectronic integrated circuits, optical filters, memories, microwave amplifiers, solar cells, laser devices, discrete components and device elements and many others. The thin films of metals, semiconductors and dielectrics have become the subjects for intensive research work both from applied and basic point of view in many branches of physics, chemistry and electronics. A vast amount of research work is being carried out throughout the world to prepare better thin film materials with special and desirable properties. These films

are not only economical but also easy to make into suitable size and shapes required for different devices than the corresponding bulk materials.

The term "thin film" is not very well defined. This is usually applied to solid layers where one dimension i.e. thickness is much less than the other two and the layer is assumed to be continuous. In many cases it need not be and especially when the layers are very thin the films are generally discontinuous where the thickness is generally less than 1000 A^{o} or so. In metallic cases however the limit may be around 200-500 A^{o}.

Several techniques such as electrodeposition, anodization, electroless deposition, chemical vapour deposition, pyrolysis, d.c. and r.f. sputtering, electron beam or laser bombardments and thermal evaporation in vacuo are used to prepare thin films. In the present investigation films have been prepared by the thermal evaporation technique because of its simplicity. In this the material to be deposited is heated in high vacuum ($\simeq 10^{-5}$ torr or better). As the temperature rises, a stage is reached where the vapour pressure of the material exceeds that of the surroundings and the evaporation takes place. At such low pressures the mean free path of the vapour molecules is sufficiently large so that gaseous molecules can reach the surface of the

substrate and condensed on it to desired film layers.

Electron microscopic examinations of these films show that in the early stages of the growth process, discrete nuclei are formed (Pashley 1963). With the increase of the film thickness, these grew in size and coalesce to another until a continuous film is obtained. During the different stages of the growth, various defects and imperfections such as lattice defects, twinning, voids, dislocations, grain boundaries, misorientation of crystallites, etc. often develop in these films. A change in crystallographic structure, morphological features, phase composition, etc. can also occur. The phenomena like condensation, nucleation and growth of the film are essentially dependent on the deposition conditions such as source geometry, nature of the substrate, rate of evaporation, substrate temperature, chamber pressure, etc. (Neugebauer, 1960; Holland, 1958). Hence because of the predominance of these defects the electrical, dielectric, optical and other properties of these films as well as the basic conduction and scattering mechanism are likely to be different from those of the bulk materials. Phillips (1960) and several other workers showed the presence of these defects such as dislocations, stacking faults, voids, impurities and imperfections, etc. in the deposited films. These defects also play a predominant role

in electrical (Mayer, 1959), dielectric (Weaver, 1962) Harrop and Wanklyn; 1964, Argall and Janschor; 1968), mechanical (Campbell, 1970), optical (Heavens, 1955) and other properties of films. It is well known that the various film properties are influenced by the purity of the material but more so by their preparative conditions. Some of these factors are the rate of deposition, substrate temperature, cleanliness of the substrates, film thickness, ambient gas pressure, annealing temperature, new phase formation, morphological features of the deposits, grain size, etc. Mayer (1959), Neugebauer and Webb (1962) showed that alkali metals, like potassium, sodium, rubidium, cesium, etc. which have positive temperature coefficient of resistance in bulk forms, behaved like semiconductors exhibiting negative TCR in thin film forms.

(ii) Energy band picture of crystalline solids

Band theory originally developed by Bloch (1928) has been used to explain the general electronic behaviour of crystalline solids. Since it deals with a large number of interacting particles in the solid, their interactions give rise to discrete electronic energy levels instead of overlapping thus forming bands.

In the Bloch scheme the conduction electrons are considered to belong to the crystal as a whole rather then to

any particular atom. The nuclei in the solid are essentially at rest, their motion being treated only as a small perturbation to the electronic behaviour. The most important assumption is that the electrons move in a periodic potential field with the periodicity of the crystal lattice. The electronic wave function and the energy can be evaluated from these assumptions. Further details of the theory have been given in several books (Smith, 1960; Hanney, 1959; Dekker, 1957; Kittel, 1971). The consequence of the above is that there will be innumerable numbers of very closely spaced energy levels in a band which can be vacant, occupied or partially so. The general band structure envisages a number of bands in any solids and the topmost completely filled one is called valence band and next higher unoccupied one is the conduction band. These energy bands are separated by gaps is known as forbidden energy gap. Where normally no electron state can exist. On the basis of this band structure crystalline solids can be classified as metals, semimetals, semiconductors and insulators.

In a pure single crystal semiconductor, the valence and conduction bands are separated by an energy band gap (E_g). At absolute zero the conduction band is completely empty whereas the valence band is fully occupied with electrons. With the rise of temperature, electron in the

valence band are thermally excited and if this thermal energy is greater than E_g these will go to the nearest empty conduction band, thus leaving behind an electron deficiency state i.e. holes in valence band. Electron thus excited to the conduction band and also the holes created in the valence band can now carry current when some electric field is applied between the two ends of the semiconductors. Since these are oppositely charged particles they move in opposite direction, thus giving rise to conductivity with the increase of temperature. This conduction in any material is given by the relation

$$= \qquad (1)$$

where = conductivity of the material.

= drift mobility of the charged carriers expressed in $cm^2/v\text{-}sec$.

n = number of charge carrier either electrons or holes.

e = electronic charge of the carrier.

Since the number of electrons excited will increase with the temperature, the number of electron-hole pairs will also increase. When the conduction is purely due to the equal

number of electrons and holes by the thermal excitation. The material is called an intrinsic semiconductor. The relations will then be

$$= e\,(n\mu_n + p\mu_p)$$
$$= e\,(\mu_n + \mu_p)\; n \text{ (or p)} \qquad \ldots \qquad (2)$$
$$= e\,(\mu_n + \mu_p)\; n \text{ (or p)}$$

where is the resistivity of semiconductor and μ_n and μ_p are the drift mobilities of electrons and hole respectively. The number of carrier concentration is then given by

$$n = p = 2\left(\frac{kT}{2\pi h^2}\right)^{3/2} (m_e m_h)^{3/4}\, e^{-E_g/kT} \qquad \ldots \qquad (3)$$

From the above relation it follows that

$$= {}_o\, e^{-E_g/2kT}$$
$$= {}_o\, e^{E_g/2kT} \qquad \ldots \qquad (4)$$
$$\text{or} \qquad R = R_o\, e^{E_g/2kT}$$

where m_e and m_h are the electron and hole mass respectively

E_g, σ, ρ, R and T have the usual meaning. The above equation is the basis for the determination of the energy band gap from conductivity or resistivity data. The temperature dependence of the mobility and conductivity are the most important characteristic of their transport properties. Thus this mobility is also related with the most of the electrons or holes and their relaxation time

$$\mu = \frac{e\tau}{m^x}$$

However, in practice there are many impurities present in the crystal lattice. These will give rise to additional energy levels (donors or acceptors) in the forbidden energy gap. Such material is called extrinsic semiconductors. If the donor concentration is larger than that of the acceptor then the majority carriers are electrons and these will form donor energy levels very close to the conduction band edge but below it. The sample is then called n-type. For the reverse case when acceptor concentration is higher than that of the donor it is p-type and the acceptor level formation will take place near to the valence band. In almost all impurity semiconductors both types of impurities are present, but the majority carriers determine the type of the material.

The band picture in the cases of metals is slightly different. In this case the energy band containing electrons in only partly filled or the completely filled valence band overlaps with the empty conduction band. In semimetals, however, the conduction band is generally only at a slightly higher energy level than the valence band edge and overlap of bands takes place when $k \neq 0$. This overlap gives rise to small concentrations of electrons in conduction band and holes in the valence band. In the case of insulator, however, the forbidden energy gap is too large as compared to semiconductor to be overcome by the thermally excited electrons from the valence band, unless the temperature is very high. Consequently, insignificant or no conduction takes place at the normal range of temperature.

(iii) Hall effect

One of the most important tools for the investigation of semiconductors is the Hall effect. Conductivity measurements alone give information about the product of mobility and carrier concentrations but do not serve to separate these quantities but Hall effect measurements enable to determine these quantities separately. Hall effect is hence a powerful technique for studying the transport properties in solids particularly of semiconductors.

This effect was discovered by E.H. Hall (1879) during

an investigation of the nature of the force acting on a conductor carrying a current in the magnetic field. This effect can be visualised by considering a confined stream of free particles, each having a charge e and initial velocity V_x. When a magnetic field (H) in Z direction perpendicular to both X- and Y direction, is applied the deflection of the charge carriers along Y direction takes place due to Lorentz force which is given by $(\bar{H} \times \bar{V})e$. A charge unbalance is created and this results in the electric field E_g normal to both current and magnetic field. The sign of it depends upon the material its magnitude is proportional to the current and the magnetic field and inversely proportional to thickness of the material.

When particles of the same charge and velocity are no longer deflected a steady state is reached so that

$$(\bar{H} \times \bar{V})e = eE \quad .. \quad (5)$$

current density is given by

$$J = neV \quad .. \quad (6)$$

When n is the carrier concentration from the equations (5) and (6) we have

$$E_y = -\frac{1}{ne} H_z J_x \qquad .. \qquad (7)$$

The Hall field being proportional to current density and magnetic field, we have

$$E_y = R_H J_x H_z \qquad .. \qquad (8)$$

where R_H is a constant known as Hall coefficient. Further from the equations (7) and (8) it follows

$$R_H = \pm \frac{1}{ne} \qquad .. \qquad (9)$$

This equation offers a simple means of determining the carrier concentration. The sign of R_H is negative or positive respectively for electrons or holes as charge carriers. In terms of Hall voltage (V_H) the equation (8) can be written as

$$V_H = \frac{R_H I\ H}{d}$$

$$\text{or} \quad R_H = \frac{V_H x d}{I x H} \qquad .. \qquad (10)$$

where d and I are the sample thickness and current respectively.

The component of electric field parallel to the current is given by the equation

$$J = ne\mu_e Ex \quad .. \quad (11)$$

The angle θ between the current and resulting electric field is then given by

$$\tan\theta = Ey/Ex \quad .. \quad (12)$$

Another important parameter known as Hall mobility (μ_H) is defined as

$$|R_H|\sigma = \mu_H \quad .. \quad (13)$$

The Hall mobility will be equal to the conductivity mobility (μ) only when the relaxation time (τ) is constant. However, in real solids τ is a function of the carrier velocity (or energy) and

$$\mu = \frac{\mu_H}{\gamma} \quad .. \quad (14)$$

and hence $R_H = \pm \dfrac{\gamma}{ne}$ .. (15)

where γ is a constant which varies according to the type of

scattering that predominates and the degree of degeneracy in conduction band. However, in most of the cases it does not differ much from unity so that relation

$$R_H = \pm \frac{1}{ne}$$

generally holds good. The above treatment of Hall effect and conductivity is essentially based on a single carrier model but when both electrons and holes effectively contribute to the conduction mechanism. The material is called mixed semiconductors. In this case

$$\sigma = ne\mu_e + Pe\mu_h \text{ and} \quad .. \quad (16)$$

$$R_H = \frac{P\mu_n^2 - n\mu_e^2}{e(P\mu_n + n\mu_e)^2} \quad .. \quad (17)$$

where n and p are electron and hole concentration.

The intrinsic condition is found by putting $\mu_H = \mu_{H1} = \mu_{H1} - \mu_{H2}$, as easily verified by putting $n = p = n_i$; $\mu_H = 0$. If intrinsic conductivity is equal to the conductivity for the values of n and p which gives zero Hall coefficient.

Carrier concentration (n or p)

The carrier density is also sensitive to temperature since conduction by electrons and holes are provided by thermal excitation in the extrinsic semiconductors. At ordinary temperature electrons can be excited from the donor levels to the conduction band or from the valence band to acceptor levels because the energy required for it is small. Direct excitation from valence band to conduction band is almost still. As the temperature rises, the donor band may become exhausted or the acceptor levels saturated. Once these levels generally contain fewer states then either the conduction band or valence bands. The carrier concentration thus becomes relatively sensitive to temperature. At a still higher temperature, electrons are excited from valence band to conduction band in large number since the sufficient thermal energy so at high temperature extrinsic carrier conduction therefore becomes intrinsic.

(iv) Impurity band conduction

According to band theory the resistivity and Hall coefficient for impurity semiconductors are expected to increase as the temperature is lowered tending to saturate at a very low temperature. However, in many cases it has been observed that though resistivity tends to saturate at

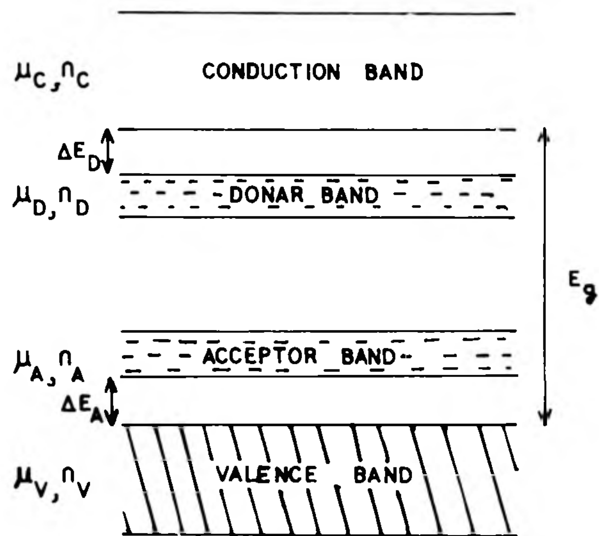

FIG. 1:1

low temperature, Hall coefficient increases as the temperature is lowered but instead of attaining a constant value it starts falling thus showing peak. To explain these features Hung and Gliessman (1954) envisaged the formation of impurity sub-bands among the donor and acceptor levels within the forbidden energy gap (Fig. 1.1).

In this model, a combination of different types of carriers with different mobilities are considered. It was proposed that due to the interaction between impurity states, an impurity band is formed. An electron in such a case can now move from one impurity state to another one in the neighbourhood provided the latter is not occupied and the states are no longer localised. Consequently, conduction can take place within this impurity band.

When simultaneous conduction in the conduction band as well as donor band is considered 'ρ' and 'R_H' are then given by the expressions

$$\rho = (n_C e \mu_C + n_D e \mu_D)^{-1} \quad .. \quad (18a)$$

$$R_H = \frac{\gamma}{e} \times \frac{(n_e \mu_C^2 + n_D \mu_D^2)}{(n_C \mu_C + n_D \mu_D)^2} \quad .. \quad (18b)$$

where the suffix C and D refer to the conduction and donor

bands respectively. Similar expression can also be derived for the hole conduction. The behaviour of R_H with temperature can now be visualised from the contribution of charge carriers from the conduction band and the donor bands. At high temperatures when U_D is much smaller than μ_e, the following conditions emerge

$n_C e \mu_C \gg n_D e \mu_D$ and

$n_C e \mu_C^2 \gg n_D e \mu_D^2$ are filled

Thus from the equations (18a) and (18b) approximate expressions for ρ and R_H

$$\rho = (n_C e \mu_C)^{-1} \quad .. \quad (19)$$

$$R_H = \gamma / n_C e \quad .. \quad (20)$$

These equations are the same as those derived on the basis of single carrier model.

At low temperatures electron concentration in conduction band continue to drop and finally a temperature is reached when

$$n_C e \mu_C^2 << n_D e \mu_D^2 \text{ and}$$

$$n_C e \mu_C << n_D e \mu_D \text{ under these conditions}$$

$$\rho = (n_D e \mu_D)^{-1}, \quad R_H = \gamma/n_D e$$

At low temperature nearly all the electrons will fall back to the donor states and hence R_H will be practically constant, its value being just the same as the R_H when all the electrons are in the conduction band. The flatness in resistivity at low temperature region indicates that mobility in an impurity band is approximately temperature independent. At intermediate temperature since R_H are the same at near room temperature and low temperature R_H must pass through a maximum. The maximum in R_H is found to occur when

$$n_C \mu_C = n_D \mu_D$$

This maximum in the R_H explains the anomaly.

(v) <u>Scattering mechanism</u>

Scattering mechanism in a semiconductor is of great importance since the relaxation time and hence the mobility is governed by the type of scattering of the charge carriers. The scatterings are mainly due to (a) lattice,

(b) ionised impurities, (c) neutral impurities and defects, vacancies, interstetial, (d) dislocations and (e) grain boundaries, etc.

(a) Lattice scattering

This arises due to the thermal vibrations of the lattice, thus giving rise to longitudinal as well as transverse modes. There are two types of lattice scattering viz. (i) phonon or acoustic scattering, and (ii) optical mode or multivalley scattering due to their interaction with the conduction electrons and holes.

(i) Phonons or acoustical mode of scattering

When a semiconductor is exposed to thermal energy, the crystal lattice which is otherwise considered to be at rest starts vibrating. As a result of these vibrations, the lattice potential field is deformed due to the superimposition of the longitudinal phonon waves which are acoustic in nature having wavelengths of the order of the sound waves. This deformation of the potential field leads to a modification of both the valence and conduction band edges, the former rising and the latter falling. According to Bardeen and Shockley (1950) the deformation potential (δE) is then given by the relation

$$\delta E^2 = (E_{1n})^2 \left(\frac{\delta V}{V} \right)^2 = (E_{1n})^2 \cdot \frac{kT}{VB}$$

where B is the modulus of the bulk and E_{1n} is the change in the conduction band per deformation and V is the specific volume. This deformed potential forms a sort of barrier from which electrons are reflected giving rise to a shorter mean free path (l) where

$$l = \pi \hbar^4 C_{11} \Big/ m^{*2} (E_{1n})^2 kT$$

where C is a longitudinal elastic constant. Then the mobility is given by the expression

$$\mu = \frac{2\sqrt{2\pi}}{3} \frac{\hbar^2 C_{11}}{(E_{11})^2 m^{*5/2} K^{3/2}} \cdot T^{-3/2}$$

where $\hbar = \frac{h}{2\pi}$

$$\text{or } \mu \propto T^{-3/2} \quad .. \quad (21)$$

Thus for phonon scattering mobility follows $T^{-3/2}$ law.

(ii) <u>Optical or intervalley mode of scattering</u>

An additional mode of scattering arises from the

thermal vibration is due to the collisions of electromagnetic optical waves with the conduction electrons and holes where the momentum of electron and holes changes from one valley to another by absorption or emission of photons. Electrons and holes are scattered by optical vibration and scattering is proportional to number of phonons, their frequencies and also their coupling constant. Thus mobility

$$\mu \propto \exp \theta_1/T$$

Below Debye temperature θ_D

$$\mu \propto \exp \frac{h\gamma}{kT}$$

But at higher temperature where $T \gg \theta_D$ and $h\gamma \ll kT$,

$1 \propto \frac{\gamma^2}{m^* T}$, where electronic mobility in ionic semiconductor is higher than Debye temperature. Thus

$$\mu \propto m^{*-3/2}\, T^{-1/2} \qquad .. \qquad (22)$$

It may be mentioned here that phonon particle is nothing but electron with its clouds of accompanying phonons.

(b) Impurity ion scattering

In many cases, especially at low temperatures mobility follows an entirely different trend with the lowering of temperature mentioned earlier. This is assumed to be due to the scattering of carriers by ionised impurity centres (Lark-Horovitz, 1946). A theoretical treatment by Conwell and Weisskopf (1950) has been made about the contribution of these ionised impurities to the scattering. In a semiconductor there will be plenty of ionised impurities such as donors or acceptors and they will also scatter the charge carriers moving past by then. The relation for the relaxation time (τ) will then be

$$\tau = \left(\frac{2E}{E_1}\right)^2 \Big/ \ln\left[1 + \left(\frac{2E}{E_1}\right)^2\right]$$

$$= \frac{2a}{\pi V}\left(\frac{2E}{E_1}\right)^2 \ln\left(\frac{2E}{E_1}\right)^2$$

where $E = mV^2/2$, $E_1 = 2e^2/\epsilon d$, ϵ is the dielectric constant and d is the distance between impurity centres. On averaging over the Boltzmann distribution, the mobility due to ionised impurity scattering is given by the relation

$$\mu = \frac{8\sqrt{2}}{\pi^{3/2}} \cdot \frac{\epsilon^2}{N_1 e^3 m^{*1/2}} \cdot \frac{(kT)^{3/2}}{\ln\{1+(3\epsilon kT/e^2 N_1^{1/3})^2\}} \quad .. \quad (23)$$

where N_1 is the number of ionised impurity centres. This leads to the relation $\mu \alpha T^{3/2}$ which is found to be valid generally at the lower temperature region.

(c) Neutral impurities scattering

It is quite likely that neutral impurities such as vacancies, interstetials, etc. may also scatter electrons and holes as in the case of charged impurities. This sort of scattering gives rise to a relation (Pearson and Bardeen, 1949)

$$\mu = T^{-1/2} / 7.6x10^{22} N_n \quad .. \quad (24)$$

where N_n is the density of the neutral impurities. It is here seen that mobility is proportional to $T^{-1/2}$.

(d) Dislocation scattering

Dexter and Seitz (1952) derived a relation based on the strain arising due to the dislocations. The piezo-resistance effect on the material. This assumes the form

$$\Delta \rho = \frac{2\pi^2}{3} \quad \frac{E \lambda^2}{kTh} \cdot \frac{(1-\gamma)}{(1-\gamma)} \cdot \frac{m^*}{m_e} \quad .. \qquad (25)$$

where λ is slip dislocation

γ is Poisson ratio

N is the dislocation density

(e) Grain boundary effect

The effect of grain boundaries on the transport properties is to stipulate a potential barrier at the grain boundary across which the charge carriers must be activated. Pertitz (1956) treated the current in the low field limit through these barriers as a diode current and obtained an effective mobility.

$$\mu^x = \frac{M}{NkT} \exp\left(\frac{-\phi}{kT}\right) \quad .. \qquad (26)$$

M = which depends on the nature of the barrier.

N = density of crystallites per unit length.

ϕ = is the barrier height.

In this model the macroscopic R_H gives a measure of the total carrier concentration in the crystallites and the Hall mobility is approximately equal to μ^x. The plot log μ vs 1/T should give a straight line of slope proportional to $-\phi$.

(vi) Thermoelectric power

When a temperature gradient is established between the two ends of a conductor, the mobile charge carriers have a tendency to travel from the hot to the cold end. This results in an emf across the two ends of the material called "Seebeck voltage". The Seebeck voltage per unit temperature difference developed in an electrically in an isolated sample is known as absolute thermoelectric power (α). This effect amongst the various transport properties is a powerful tool in revealing the distortions of Fermi surface.

In the case of a bipolar semiconductor a thermal emf can also arise due to the following: (1) When the concentration of one type of carriers exceeds the concentration of the opposite type. The flux of first type of the carriers will carry towards the cold end predominantly a charge which will retard their motion and conversely, accelerate the carriers of opposite sign until fluxes of both carriers are equal. An electric field governed by the temperature gradient will thus be established. (2) The difference of charge carrier mobilities forms the second source of thermal emf.

Sommerfield (1928) on the basis of Fermi-Dirac quantum statistics applied to electrons in metals showed that (α) in

metals should be small. This is due to temperature independence of free carriers, the kinetic energy and also the contact potential. In a semiconductor, however, the temperature has pronounced effect on the concentration and kinetic energy of free charge carriers and also on the contact potential. Hence it showed higher values of α than metals.

The thermal emf (α) may be regarded an entropy flux of unit electrical charge and its value is closely related to mobility (μ) which is governed by the same scattering mechanism. For metals, particularly in monovalent metals

$$\alpha = \frac{\pi^2 k^2 T}{3e} \left[\frac{1}{\mu'} + \frac{1}{l} \frac{dl}{dt} \right] \quad .. \quad (27)$$

Here μ' is the chemical potential of electrons, which in the case of metals is equal to Fermi level energy (E_F), and l is the free path of electrons with kinetic energy ε. For metals we assume that l α ε^2 and since the electrons contributing to the current have $\varepsilon = \mu'$

$$\therefore \frac{1}{\mu'} + \frac{1}{l} \frac{dl}{dt} = \frac{3}{\mu'}$$

$$\therefore \alpha = \frac{\pi^2 k^2 T}{e \mu'} \quad .. \quad (28)$$

The value of μ' is almost independent of temperature and α is proportional absolute temperature $\alpha \propto T$.

In semiconductors where possibility of the existence of both free electrons with concentration (n) and holes (p), then

$$\alpha = \frac{1}{\sigma T} \{\mu_- n \, (2kT - \mu) - \mu_+ p (2kT - \mu + \Delta E_o)\} \quad .. \quad (29)$$

where σ = electrical conductivity

μ = mobility and

ΔE_o = width of the forbidden energy band

Pisarenko derived an expression for α which is given by Ioffe (1960)

$$\alpha = \frac{k}{\sigma} \left[\mu_- n \left(A + \ln \frac{2(2\pi m^* kT)^{3/2}}{h^3 n} \right) - \mu_+ p \left(A + \ln \frac{2(2\pi m^* kT)^{3/2}}{h^3 p} \right) \right] \quad .. \quad (30)$$

The value of constant A depends on the electron scattering mechanism. Different values of A, γ and scattering mechanism is given in table (1.1). For a semiconductor with current carriers at only one type the expression (a)

Table-1.1

Scattering modes	X	A	γ
		(constants of α)	
Ionised impurity	3/2	4	1.93
Piezoelectric (ionic lattice)	-1/2	3	1.1
Grain boundary	{(-1 $\{(e^{-1/T})/T\}$	-	-
Lattice or phonons	-3/2	2	1.18
Vibration at constant frequency	-5/2 -3	1 0.5	- -
Ionic lattice	$e^{1/T}$	2.5	-
Degenerate system	-	-	1

may be simplified and replaced by the formula

$$\alpha = \frac{k}{e}\left[A + \ln \frac{2(2\pi m^* kT)^{3/2}}{h^3 n}\right] \quad .. \quad (31a)$$

$$= \frac{k}{e}\left[A + \ln \frac{2(2\pi m^* kT)^{3/2}}{h^3} \cdot \frac{R_H e}{\gamma}\right] \quad .. \quad (31b)$$

For practical purpose it is convenient to write expression (31a) as relationship between α and σ both of which can be measured. By introducing an impurity or an excess of one of the components of compound it is possible to vary the concentration n with wide limits without appreciably affecting the mobility. Therefore the expression for α may be written

$$\alpha = \frac{k}{e}\left[A + \ln \frac{2(2\pi m^* kT)^{3/2} e}{h^3}\right] - \frac{k}{e} \ln (ne\mu)$$

or

$$\alpha = C - 86\times10^{-6} \ln \sigma = C - 2\times10^{-4} \log \sigma \quad .. \quad (32)$$

There is a large group of semiconductors with high electrical conductivity in which concentration does not vary with temperature. The effective mass m* is also independent of

temperature, then

$$\alpha = \frac{k}{e}\left[A + \ln \frac{2(2\pi m^{*}kT)^{3/2}}{h^{3}n}\right] + \frac{3k}{2e}\ln T \quad .. \quad (33)$$

When the semiconductor is completely degenerate then

$$\alpha = \pm \frac{\pi^{2}k}{e}\left(\frac{kT}{E_F}\right)\left(\frac{1}{2} - \frac{1}{3}S\right) \quad .. \quad (34)$$

where S is the exponent of E ($\tau = aE^{-S}$). The Seebeck coefficient for any semiconductor can be expressed as

$$\alpha = \pm \frac{k}{e}\left[A + \frac{E_F}{kT}\right] \quad .. \quad (35)$$

The dependence of A with different type scattering is given in table (1.1).

There are vast applications of thermoelectric power such as (i) thermoelectric generators, (ii) thermoelectric refrigerators and thermoelectric industrial and domestic heating devices are not only of great theoretical interest but present real prospect of practical applications of the basis of the modern science of semiconductors.

Metal semiconductor junctions

In order to measure the theoretical properties of semiconductor it is necessary to make electrical contacts with some metal electrodes. In practice, however, there can be various types of contacts at metal-semiconductor interfaces (i) ohmic contact, (ii) blocking contact, (iii) neutral contact (Azaroff, 1960; Simmons, 1970). The contact potential of both metals and semiconductors is determined by the difference between the energy outside conductor and chemical potential.

Let ϕ_m and ϕ_s be the work function of metal electrode and semiconductor (n-type). In ohmic contact $\phi_m < \phi_s$ because the current passing through obeys ohms law. When $\phi_m > \phi_s$ contact is called blocking contact. If ϕ_m is equal to ϕ_s then the contact formed it called neutral contact.

(vii) Fermi energy level (E_F)

The Fermi-Dirac distribution function is given by

$$f(E) = \frac{1}{1+\exp \frac{E-E_F}{kT}} \quad .. \quad (36)$$

where f(E) is the probability that of a state of energy E is

occupied by electrons, E_F is the Fermi energy, k is the Boltzmann's constant, and T is the absolute temperature. Thus the filling of the bands follows a simple rule. The states of the lowest energy are filled first, then the next lowest and so on and finally, all the electrons have been accommodated. The energy of the highest filled state is called Fermi level. The magnitude of E_F depends on the number of electrons per unit volume in solid and it determines how many electrons must go into bands.

When the concentration of electrons in the conduction band is so high that Fermi level lies above, but very close to the bottom of the conduction band, the semiconductor is said to be "degenerate". The carrier concentration is essentially independent of temperature in a degenerate semiconductor and its conduction is much like that of a metal. When it is about 2kT above the conduction band the sample is almost completely degenerate. The carrier concentration at degenerate temperature is allied degeneracy concentration. The position of Fermi energy can be determined from thermoelectric power (α) and type of scattering mechanism by using the relation

$$\alpha = \pm \frac{k}{e} \left[A + \frac{E_F}{kT} \right]$$

A is the constant depending on the scattering mechanism. For a degenerate semiconductor

$$\alpha = \pm \frac{\pi^2 k}{e} \left(\frac{kT}{E_F}\right)\left(\frac{1}{2} - \frac{1}{3} S\right)$$

where S is the exponent of E ($\tau = aE^{-S}$). A is however related to α and X to mobility of the charge carriers determined by the modes of scattering of the carrier as given in table 1.1.

(viii) Mean free path (l_o)

The average distance travelled by holes or electrons between the two successive collisions. The average time interval between collisions of these particles is called the mean free time (τ). The mean free velocity $\bar{v} = \frac{e^2 E}{m^*}$, where $\bar{v}$ is the mean free velocity, e is the electronic charge, τ is the mean free time, m* is the effective mass. Since $\sigma = ne\mu$ (we have $\sigma = \frac{ne^2}{m^*}$. The mean free path can also be expressed in terms of the collisions time, thermal velocity or total velocity. Then assuming that the kinetic energy is 3/2 kT, thermal velocity $v = l_o / T$. Thus the mobility becomes

$$\mu = \frac{e l_o}{2\sqrt{3m^* kT}} \ \text{cm}^2/\text{V.sec.} \qquad .. \qquad (37)$$

For a more precise determination which takes into account the fact that not all the free paths have the same length and which in effect perform an averaging over all possible free path one has to introduce an additional factor of $\frac{4\sqrt{2}}{\sqrt{3\pi}}$. Thus above relations finally become

$$\mu_0 = \frac{e l_0}{225\sqrt{2\pi m^* kT}} \quad cm^2/V.sec. \qquad .. \qquad (38)$$

and

$$l_0 = 3.54 \times 10^{-10} \mu_0 \sqrt{T} \cdot \sqrt{m^*} \qquad .. \qquad (39)$$

The expression (38) is independent of the electric field. It is clear again that mobility is inversely dependent on the square root of temperature i.e. $\mu = \frac{l_0}{\sqrt{T}}$. The mean free path of electrons in a metal may be expressed as a function of their energy ϵ and the temperature

$$l_0 = \frac{\epsilon^2}{T}$$

The free path in semiconductors with an atomic lattice scattering of electrons does not depend upon velocity of electrons and is inversely proportional to temperature

$$l_o \propto \frac{1}{m^{*2} T}$$

It is also possible to calculate mean free path from the relation (Mayer, 1959),

$$\rho_d = \rho_\infty (d + \frac{3}{8} l_o) \quad .. \quad (40)$$

where d is the film thickness, ρ is the resistivity of the film, l_o is the mean free path of the charge carriers, ρ_∞ is the resistivity of the bulk material having approximately the same number of defects as that of the films.

(ix) Effective mass (m^*)

It is an important basic parameter of semiconducting solid films. The effective electron mass (m^*e) for different materials is generally less than effective hole mass (m^*_h). These have been measured in many bulk materials by the cyclotron resonance technique and generally assumed to be constant. No measurement has yet been reported for effective mass in thin films.

(x) Conduction in thin film

A brief summary of the various parameters governing

the transport properties of bulk material has already been given in the previous sections. However, in thin film states, there appears a number of new factors which may not have any influence on the transport phenomena of bulk and these play an important role in the transport properties of the thin films. To mention a few, physical dimensions especially the film thickness which restrict the movement of the charge carriers, the crystal growth process leading to discontinuous or island type of structure, stacking faults, grain boundaries and continuous film along with the associated morphological features, etc. which are more or less inherent in any film. These features considerably influence the conduction mechanism of the thin films. In the following a brief outline is given of different factors that dominate especially in thin films.

(a) Discontinuous films

Electron transport in thin discontinuous films characterised by very high resistivity and negative TCR has been ascribed to various phenomena such as thermionic emission (Minn, 1960) activated tunneling (Neugebauer and Webb, 1962) tunneling between allowed states (Hartman, 1963), substrate assisted tunneling (Hill, 1964) etc. The model of Naugebauer and Webb (N-W model) has been found applicable for discontinuous films of a smaller particles size and Hill's

theory of substrate assisted tunneling explains observation on large-particle and large-gap film. In the N-W model, a film can be looked upon as planer array of many small, discrete islands of linear dimension and separated by a small average distance. The activation energy in this case is defined as the energy required to transfer a change from one initially neutral islands to another. Only a small number (n) of metal islands are assumed to be charged as a result of losing or gaining an electron to or from initially neutral particles. It has been shown that conductivity of island like film follows an exponential dependence on temperature and is independent of the applied field. In Hill's theory, large number of trap centres between the conduction and valence band of the dielectric substrate are assumed. The charge transfer between the particle thus results either through a trap hopping or through thermionic emission into conduction band of the dielectric which acts as substrate.

(b) Continuous films

Even when the thickness of the films is increased so that the islands coalesce to form a continuous films, the conductivity of these films invariably remains lesser than the starting bulk material. This results from the reduction of the mean free path of the conduction electron which in turn

results from imperfections, impurities and scattering at the surface. This surface scattering is primarily due to the geometrical limitations of one of the dimensions viz. thickness which restricts the movement of the conduction electrons. This effect known as size effect almost invariably influences the properties of continuous films. In the following its effect on conductivity Hall coefficient and mobility is discussed.

Conductivity

The charge carriers are said to be reflected in a specular manner when only the component of their momentum normal to the surface is changed, the parallel momentum component remaining constant. In the case of diffuse scattering the carriers lose the velocities prior to collision with the surfaces and on reflection they have Maxwell-Boltzman distribution. On the basis of the free electron, model Fuchs (1938) proposed the theory of size effect which was extended further by Sondheimar (1950) by taking galvanomagnetic effects into account. However, Funch's theory assumed that scattering coefficient (P) was same for both the surfaces of the film. Lucas (1965) assumed different scattering coefficient p and q for two surfaces and showed that

$$\frac{\sigma_F}{\sigma_\beta} = 1 - \frac{3}{8y}\left(1 - \frac{p+q}{2}\right) \quad (y \gg 1) \qquad .. \qquad (41a)$$

and

$$\frac{\sigma_F}{\sigma_\beta} = \frac{3}{4} \quad \frac{(1+p)\ (1+q)}{(1 - pq)}\ y \quad \ln \frac{1}{y} \ (y \ll 1) \qquad .. \qquad (41b)$$

where σ_F and σ_B are the film and bulk conductivities, $y = d/l$.

Mobility

The mobility of charge carriers is affected considerably by the scattering mechanism dominant in the material. Hence the surface scattering which is dominant in films is bound to have a pronounced influence on the mobility. Assuming a diffuse type of scattering in a n-type material the mean relaxation time of electron in the film is given by

$$\frac{1}{\tau} = \frac{1}{\tau_s} + \frac{1}{\tau_1} \qquad .. \qquad (42)$$

where τ_s is the relaxation time of electrons undergoing diffuse surface scattering and τ_1 is the relaxation time of electrons in the interior of the film. The two relaxation time can be shown to be related by the relation (Wieder, 1970) $\tau_s = \tau_1 (d/l)$ where l is the mean free path. It

follows from the above equation that

$$\frac{\mu}{\mu_1} = \frac{1}{1+l/d} \quad .. \quad (43)$$

where 'μ' is the mean electron mobility and 'μ_1' is the bulk mobility. Thus the mean mobility of the film decreases with decreasing thickness.

For partly specular and partly diffuse scattering the equation (41) becomes

$$\frac{\mu}{\mu_1} = \frac{1}{1+l/d(1-p)} \quad .. \quad (44)$$

where p = 1 is the probability per unit time that an electron reaching the surface will be specularly scattered and p = 0 is the corresponding probability per unit time for completely diffuse scattering.

According to Okyyama (1976) the drift mobility of polycrystalline semiconducting films includes the influence of the (1) surface mobility,(2) mobility due to polycrystalline in nature, (3) lattice scattering mobility, (4) ionised impurity scattering mobility

$$\mu_H^{-1} = \mu_L^{-1} + \mu_S^{-1} + \mu_F^{-1}\, \mu_I^{-1} \quad .. \quad (45)$$

Hall mobility = drift mobility.

(xi) Present study

The above discussion clearly shows that the transport properties of the thin films differ considerably from those of the bulk material. These are mainly due to the presence of various defects, dislocations, crystal imperfections, impurities and also the size effect which are generally present in thin film state.

A general survey of the literature on the thin film transport properties shows a lack of any systematic study of their measurements of their electrical along with the structural properties. Since it is well known that a thin film structure is likely to differ from the bulk, a correlation of electrical properties with structural features is essential for understanding the basic processes involved in the transport mechanism. A detailed investigation on the electrical properties of thin films with some theoretical approach of various properties supported by simultaneous electrons diffraction studies was therefore undertaken in the present work with a view to have a better understanding of the electron transport process in thin films. Such understanding is also likely to give a more consistent and unambiguous picture of the basic phenomena in thin films.

REFERENCES

Argall, F. and Janscher, A.K. (1968), Thin Solid Films, 2, 185.

Azaroff, L.V. (1960), "Introduction to Solids", McGraw-Hill Book Co., Inc. N.Y., p.337.

Bardeen, J. and Shockley, W. (1950), Phys. Rev., 79, 216.

Bloch, F. (1928), Z. Phys., 52, 555.

Campbell, D.S. and Simmons, J.G. (1970) "Handbook of Thin Film Technology" Ed. Maissel, L.I. and Glang, R., McGraw-Hill Book Co., New York, Chapters 4 & 14.

Conwell, E. and Weisskopf, V.F. (1950), Phys. Rev., 77, 388.

Dekker, A.J. (1957) "Solid State Physics", Prentice Hall Inc. N.J.

Dexter, D.L. and Seitz, F. (1952), Phys. Rev., 86, 964.

Fuchs, K. (1938), Proc. Cambridge Phil. Soc., 34, 100.

Hall, E.H. (1879), Amer. J. Math., 2, 287.

Hanney, N.B. (1959) "Semiconductor" Reinhold, New York.

Hartman, T.E. (1963), J. Appl. Phys., 34, 934.

Harrop, P.J. and Wanklyn, J.N. (1964), J. Electrochem. Soc. 111, 1133.

Heavens, O.S. (1955) "Optical properties of thin solid films" Butterworth Scientific Publications, London.

Hill, R.M. (1964), Nature, 204, 35.

Holland, L. (1958) "Vacuum Deposition of Thin Films", John Wiley and Sons, Inc., N.Y.

Hung, C.S. and Gliessman, J.R. (1954), Phys. Rev., 96, 1226.

Ioffe, A.F. (1960) "Physics of Semiconductors" Infosearch Ltd., p.306.

Kittel, C. (1971) "Introduction to Solid State Physics" John Wiley & Sons, Inc. N.Y.

Lark-Horovitz, K. et al (1946), Phys. Rev., 69, 258.

Lucas, M.S.P. (1965), J.Appl.Phys., 36, 1632.

Mayer, H. (1959) "Structure and properties of thin films" Wiley, New York, p.225.

Minn, S.S. (1960), J. Rech. Centre Natl. Rech. Sci. Lab. Bellevue, Paris, 51, 131.

Neugebauer, C.A. (1959) "Structure and Properties of Thin Films", John Wiley and Sons, Inc. N.Y.

Neugebauer, C.A. and Webb, M.B. (1962), J. Appl. Phys., 33, 74.

Okyyama, K. (1976), Thin Solid Films, 33, 165.

Pashley, D.B. (1963), "Seminar of the American Society for Metals", p.59.

Pearson, G.L. and Bardeen, J. (1949), Phys. Rev., 77, 388.

✓ Petritz, R.L. (1956), Phys. Rev., 104, 1508.

Phillips, V.A. (1960), Phil. Mag., 5, 571.

Smith, A.R. (1960) "Semiconductors", University Press, Cambridge.

Shockley, W., (1950) "Electron and Holes in Semiconductors" D. Van. Nostrand Co. (Canada) Ltd.

Sommerfeld, A. (1928), Z. Physik., 47, 1.

Sondheimer, F.H. (1950), Phys. Rev., 80, 401.

Weaver, C. (1962), Advn. Phys., 11, 83.

Wieder, H.H. (1970), "Intermetallic Semiconducting Films" Pergamon Press, Oxford.

CHAPTER-II

EXPERIMENTAL TECHNIQUES

CHAPTER-II

EXPERIMENTAL TECHNIQUES

For studying the electrical properties of thin films, various experimental techniques are used and these are described in detail. It is well known that the properties of thin films depend very much upon the method of their preparation, deposition condition, their post treatment such as ageing, annealing, etc. and for any useful meaning of the measurement and consequent results, the deposition parameters have to be kept as nonvariant as possible. To achieve this necessary care was taken for their preparation, especially as far as possible under the same experimental conditions. In the present case measurements were carried out only after the films were fully stabilised. The general preparation of sample, film thickness measurements, measurements of basic semiconductor parameters, etc. are described below.

(A) Preparation and measurement technique

(i) Method of deposition

All films studied for their electrical and other properties were prepared by the vacuum deposition technique in a conventional coating unit. It consisted of an oil diffusion pump backed by a double stage rotary pump with the

necessary provisions for vacuum and other measurements. The vacuum used was about $5x10^{-5}$ torr or better. The films were prepared by the thermal evaporation method.

The deposition was carried out mostly by the evaporation of the powdered bulk material directly from tungsten or molybdenum boats. Alternatively, the powder bulk material was taken in a micro-conical silica boat which was heated externally by a tungsten coil which was initially flashed in vacuo to remove the surface impurities before inserting the above silica boat with its contents.

(ii) Substrates and substrate heating

Microscopic glass slides (Bluestar) (PIC No.1) cut to the required sizes ($\simeq$ 3x.75 cm^2) were used as substrates. These were initially cleaned with chromic acid, then with distilled water and finally with organic solvents such as distilled acetone, alcohol, etc. These substrates were then dried in an oven for about two hours at about 100^oC. Before deposition, all the glass slides were heated in vacuo at a temperature a little higher than the desired substrate temperature. A suitable ceramic heater was used for heating the substrates and the temperature was measured by a chromel-palumel thermocouple. Sometimes the depositions were also made on the cleavage faces of rocksalt crystal. These were prepared by cleaning them with a clean knife under a

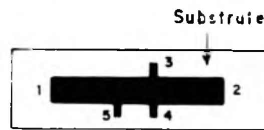

Fig. 2·1

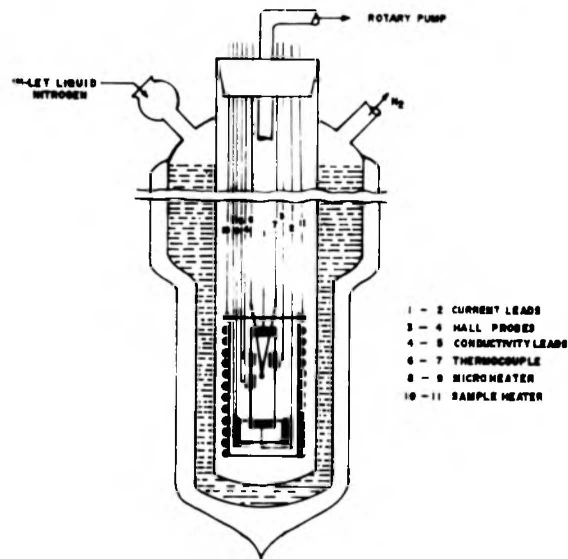

Fig. 2·2

suitable pressure and then using the cleaned surface as substrates. Occasionally these were also etched in running water for a few seconds, dried and then used.

(iii) Preparation of samples

The films were prepared from the powdered bulk material by depositing them in vacuo on to the cleaned glass substrates by using appropriate masks. The shape of the samples prepared for measuring different electrical parameters is shown in Fig. 2.1 (Goswami and Ojha, 1973). A series of samples with graded thicknesses were prepared through a set of masks under the same evaporation conditions by placing one end of the mask plate directly over the evaporating source i.e. by shifting the evaporating source to one side with respect to the mask set. The design of the mask was such that the ratio of length to breadth of the deposited film was about 8:1. These samples were then annealed in vacuo by cycling heating and cooling operation at suitable temperature depending on the nature of films.

Aluminium films were then deposited again through a mask overlapping the two ends of the samples not only to be used as electrodes but also to form a step with the uncoated area for thickness measurement. This will be discussed in details presently.

(iv) Film thickness measurements

The film thickness was generally measured by multiple interference method Tolansky, 1948) and very thick films by weighing method.

(a) Multiple beam interferometry technique

The films already deposited on the glass substrates through the mask covers only a portion of the same but leaving a sharp edge. Over this edge an opaque aluminium film (about 1000 A^{o}) was vacuum deposited thus forming a step at the film edge. This also works as contact lead. An optically flat glass slide having a partially transparent coating of aluminium is then placed on edge of sample so as to form a wedge shaped air gap. A monochromatic light was then allowed to fall on this edge by means of beam splitter and reflected light observed through a microscope. This gives rise to straight line fringes called Fizeau fringes of equal thickness. These, however, are displaced in a step like formation at the edge. The displacement and the fringe width can be measured by a travelling microscope. The film thickness was then determined from the relation,

$$\text{Film thickness (d)} = \frac{\lambda}{2} \times \frac{\text{fringe displacement}}{\text{fringe width}}$$

when λ = wavelength of the monochromatic light (5892 A° for sodium lamp). The above method was found to be suitable for determining the thickness upto about 10000 A°. For thicker films gravimetric method was used.

(b) Gravimetric method

In this method mass of the film was calculated by weighing the substrate before and after deposition on a microbalance (Metlar). Assuming the density (g) of the film to be same to that of the bulk material then 'd' is given by

$$d = \frac{m}{g x A}$$

when m is the mass of deposit, A the area covered by the film.

(v) Electrical contacts

Flexible platinum foils were placed over aluminium electrodes for making electrical contacts with samples as previously described by Goswami and Jog (1964). Each specimen was covered by blank glass slide of the same size with platinum foils in between not only to serve as spacer but also to prevent the damage of sample. Small pressure clamps were then fixed tightly on the glass slide and over the platinum foil. Leads were taken out for connecting the sample to the external circuit.

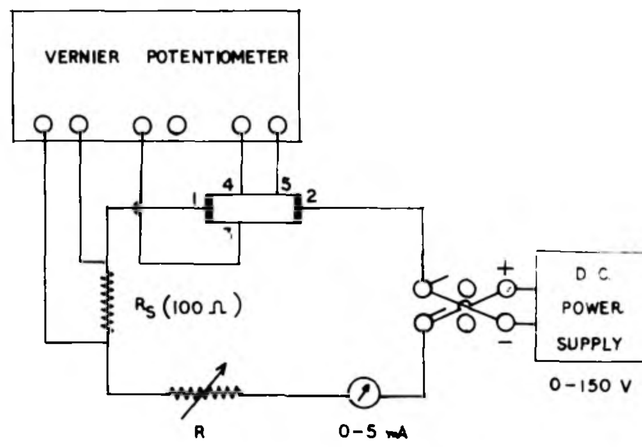

FIG. 2.3

(B) Measurements of basic semiconductor parameters

Resistance (R), Hall voltage (V_H) and thermal emf were measured by different techniques and important parameters such as activation energy (ΔE), Hall coefficient (R_H), carrier concentration (n), mobility (μ), thermoelectric power (α), potential barrier height (ϕ), mean free path (l_o), effective carrier mass (m^*), Fermi energy (ΔE_F), temperature coefficient of resistance (TCR), etc. were then evaluated by using appropriate relations. For determining the variations of above parameters with temperature from 78° to 600°K a suitable cryostat (cf Fig. 2.2) similar to those used by Goswami and Ojha (1973) was used.

(i) Resistance and Hall voltage measurements

The experimental set-up for measuring Hall voltage and resistance is shown in Fig. 2.3.

A suitable d.c. power supply and variable voltage (0.200 V.D.C.) was used for passing the current through terminals (1) and (2) Fig.(2.3)A rheostat for controlling the passing of current was also used. For a rough estimation of current a milliammeter was included in the circuit. The current passing through the sample was, however, determined by measuring the voltage drop across a standard resistance (R_s = 100 ohm) by a vernier potentiometer, the accuracy of

which was ±5 uv. A moving coil galvanometer (sensitivity about 1.5×10^{-9} amp) was used as null detector of field range from 1-8 K.Gauss similar to Deokar and Goswami (1967). The magnetic field was initially calibrated with current passing through the magnets.

In order to measure Hall voltage for different temperatures ranging from liquid nitrogen temperature to 600°K a cryostat used. In this set-up a microheater was inserted along with the sample and temperature was controlled by a variac and the temperatures were measured by using chromel-palumel thermocouple, as shown in Fig. (2.3).

(ii) Measurement techniques

(a) Resistance

The resistance of the specimen was measured from the voltage drop across the terminals 4 and 5 (Fig. 2.3) and also across the standard resistance (100 ohms) which gave the exact value of current passing through sample. Then by using the usual relation of current and voltage, the resistance of the sample was determined. The resistivity of the sample was obtained by using the relation,

$$\rho = \frac{R \times d \times b}{l}$$

where l = distance between 4 and 5 terminals in cm

b = breadth of sample in cm

The voltage drop between the terminals 4 and 5 was used for calculating the exact resistance. The resistance of high resistivity films was measured either by Philips conductivity bridge (PR 9500/) or by ELECO millian megohommeter (model RM-70).

(b) Hall voltage (V_H)

For measuring this the sample was placed in the cryostat which was designed and fabricated in this laboratory (Goswami and Ojha, 1973). After carefully fixing the contacts it was placed between the pole gap of the magnets. The position of the sample was adjusted at first so that plane of the film was exactly parallel to the pole faces. Appropriate current (say about .05 to 5 mA) was passed through the sample when magnetic field was applied, a Hall voltage developed across the terminals 3 and 4. Voltage drop across 4 and 5 was used for determining the resistance of the samples. A d.c. electromagnet (Polytronic Corporation type EMP-75) capable of producing variable field was used for Hall effect measurement. The sample was first cooled to liquid nitrogen temperature and then slowly the temperature was raised by adjusting the microheater current. The sample was then stabilized by repeated heating and cooling cycles

before any Hall voltage and resistance measurements were carried out. The measurements were also made with the change of polarity as well as current passed through the sample and the average of these measurements was used.

The Hall coefficient (R_H) was determined by using the relation

$$R_H = \frac{V_H \times d}{I \times H} \times 10^8 \ cm^3/coulomb \qquad .. \qquad (1)$$

where

V_H = average Hall voltage in volts.

d = thickness of the sample in cm.

I = current passing through the sample in Amperes.

H = magnetic field in Gauss.

All samples have to be vacuum annealed as mentioned before and then the different measurements carried out in vacuo at different temperatures in the above set-up in the manner described in details by Goswami and Ojha (1973).

(iii) Thermoelectric power (α)

(a) Experimental

Thermal emf was measured both by integral and

differential methods. The experimental set-up described by Goswami and Jog (1964) was used for measuring emf. The thin films of semiconducting materials were deposited. Two microheaters were attached to the brass blocks to heat the film from the two ends and two alumel-chromel thermocouples fixed at the two ends. The whole system was placed in the glass tube which was continuously evacuated to vacuum better than 10^{-5} torr. The glass chamber was also uniformly heated by an external electrical heater controlled by a variac. Due to the temperature gradient (ΔT) between the two ends of the samples, thermal emf developed which was measured by a D.C. microvoltmeter (PP 9004 Philips). The temperatures at the two ends were measured to an accuracy of $\pm 1/2^{o}C$. The glass tube was placed inside a Dewar's flask.

(b) Methods of measurement

Integral method

In this method one end of the sample was heated while the other one was held at a constant temperature and the temperature difference (ΔT) between the two ends of the samples and emf were then measured.

Thermoelectric power is calculated from the relation,

$$\alpha_s = \frac{\Delta V}{\Delta T} \text{ in } uV/oK$$

Differential method

Initially a temperature difference was established between the two ends of the sample by two microheaters. Then by adjusting the temperature difference between the two ends by about 10°C by controlling microheaters, thermal emf was measured by the microvoltmeter. The thermal emf due to difference in temperature of the two ends was measured by a vernier potentiometer. It may be mentioned that the difference of temperature between the two ends of the samples was kept more or less constant during the general heating or cooling of the two ends. In this way α was determined for a different temperature. It may be mentioned here that of the two methods, the differential method was more often used because of its relatively better accuracy.

(C) Structure

The structures of vacuum deposited films were studied by the electron diffraction method using transmission as well as reflection techniques. For transmission studies the films were deposited on polycrystalline NaCl tablets and for reflection studies the films were deposited on glass.

The structure of bulk material powder was however studied by X-ray diffraction techniques.

CHAPTER-II

REFERENCES

Deokar, V.D. and Goswami, A. (1967), Ph.D. Thesis, University of Poona.

Goswami, A. and Jog, R.H. (1964), Indian J. Pure and Appl. Phys., **2**, 407.

Goswami, A. and Ojha, S.M. (1973), Thin Solid Films, **16**, 187.

CHAPTER-III

MANGANESE TELLURIDE AND MANGANESE SELENIDE

CHAPTER-III

MANGANESE TELLURIDE AND MANGANESE SELENIDE

(A) INTRODUCTION

Manganese chalcogenides are the binary compounds formed by the suitable combination of Mn with S, Se and Te. These form two types i.e. MnX or MnX_2 where X can be S, Se or Te. Squire (1939) reported that some of these compounds have ferromagnetic and antiferromagnetic properties and thus have found applications in thermomagnetic writing, erasing, magneto-optic read out using a laser, etc. MnSe has three forms namely (i) α- having B_1 type structure (a = 5.44 A^o), (ii) β-cubic (B_3 type, a = 5.82 A^o) and (iii) γ-hexagonal (B_4 type, a = 4.12 A^o). MnTe, on the other hand, has only one form namely the B_8 type structure (a = 4.140 A^o, c = 4.70 A^o).

Uchida and Kondo (1953) investigated the activation energy, Hall voltage and thermoelectric power of bulk MnTe and MnSe in the temperature range of -110^oC to 203^oC in vacuo and found that both the compounds were p-type. However, MnTe showed an antiferromagnetic character upto 50^oC, but beyond 50^oC it became ferromagnetic. Palmer (1954) also measured the resistivity, Hall voltage and magnetoresistance of bulk MnSe and MnTe between 100^oC to 196^oC. Bulk MnTe

showed a high resistivity $\rho = 3x10^3$ ohm.cm. at room temperature and its activation energy for various specimens varied from 0.125 eV to 0.071 eV. MnTe, on the other hand, had low resistivity (ρ = 1 ohm. cm.) and a positive TCR. It was a p-type degenerate semiconductor throughout the temperature range. Uchida et al (1956) studied p-type MnTe from liquid nitrogen temperature to 720°C and observed that it had very high conductivity as compared to other anti-ferromagnetic compounds such as MnSe, MnS, MnO, etc. Electrical properties of bulk MnTe by the addition of p-type promotors (Na or Li) were studied by Fredrick and Manser (1959). They observed that both, the conductivity as well as the thermo-electric power, increased and had negative TCR. Magnetic and transport properties of stoichiometric single crystals of MnTe were studied by Yadaka and others (1962) at various temperatures. They found them to be p-type semiconductors and had intrinsic character above 200°C. Devyakora et al (1964) observed a considerable change in the electrical parameters below and above Neel point and attributed this to the spin-phonon interactions. Wasscher and Hass (1964) also observed a sudden change in thermoelectric power around Neel temperature (310°K) and accounted them as magnon drag due to interaction between current carriers and ion spin. They also reported MnTe to be degenerate semiconductor ($n = 5x10^{19}/cm^3$) and the effective hole mass estimated has about 0.30 m_o at

room temperature. The activation energy of MnSe compound was reported to be about 0.6 eV by Makovestskii and Sirota (1965) for the temperature range of 400 to 570°K and found that it was antiferromagnetic. Valev et al (1960) also studied the electrical properties of MnTe.

Zanmarchi (1967) studied the optical and electrical parameters of single crystals (MnS, MnSe and MnTe) and found them to be p-type semiconductors both below and above T_N. The band energy E_g varied from 1.35 eV to 1.25 eV for the temperature range of 80°K to 300°K. The activation energy as estimated by resistivity measurement in the temperature range of 400°K to 600°K was $\approx$ 0.4 eV. The nuclear magnetic resonance in paramagnetic states of MnO, α-MnS α-MnSe was investigated by Jones (1966). According to Wasscher (1967) Hall constant depends on magnetic field and temperature. Seuter (1967) also measured the various electrical parameters of crystal MnTe and observed an abrupt change in R_H at Neel temperature. It was also p-type semiconductor. Zvyagin et al (1969) observed that the resistance was proportional to $T^{3/2}$ between 100 to 200°K and the phonon scattering mechanism was predominant. Rustamove and others (1970) observed a change in the conductivity and thermoelectric power of MnTe single crystal at Neel temperature and attributed this to a drastic change in carrier concentration.

MnSe and MnS, however, showed the semiconducting behaviour both below and above T_N (-150^oK). The optical and the electrical parameters of MnTe were studied by Zvyagin et al (1971). They found that the activation energy varied from .003 eV to 0.4 eV in the temperature range of 4.2 to 600^oK.

From the above, it is seen that considerable attention has been paid on the bulk transport properties of MnTe and MnSe but no report yet have been published on thin films properties of these compounds. Further, the bulk results are often introductory. Since the properties of thin films often differ from those of the bulk, the same may also be true for MnTe and MnSe films. Hence a detailed investigation on the vacuum deposited films of these compounds has been made in the wide range of temperature.

(B) EXPERIMENTAL

(i) Preparation of MnTe

Manganous telluride (bulk) and manganous selenide (bulk) were prepared from the constituent elements (Mn powder 99.9% supplied by M/s Koch-Light Lab. Ltd., UK) with tellurium powder (specpure, 99.999%) and selenium (99.99%) by mixing them in the stoichiometric proportion (1:1) respectively in and then melting in vacuum sealed silica tube. The content was initially heated to about 400^oC for

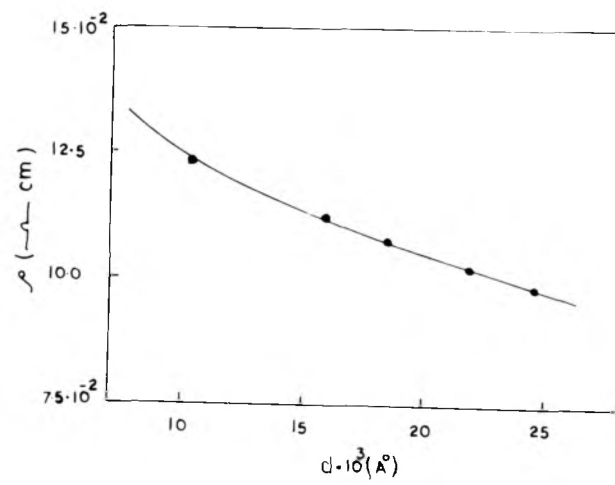

15·10⁻²
12·5
10·0
7·5·10⁻²
ρ (Ω cm)
10
15
20
25
d·10³(Å)

4 hours and finally at about 1350°C for 20 hours. The melt was then cooled slowly to about 400°C and then quenched in water.

(ii) Film preparation

The compounds thus formed were taken out from the silica tube, broken to powder and then deposited at pressure of about 8×10^{-5} torr. The depositions were made from preflashed tungsten filament (basket type) through an appropriate mask on glass substrates at 350°C. The films were annealed at same temperature for about 4 hours and then cooled to room temperature. Similar method was used for preparing manganous selenide films.

(a) MnTe

(C) RESULTS

(i) Structure

Analysis of X-ray powder patterns (table 3.1) revealed that the bulk prepared by the above method had a NiAs type of structure (Fig. 3.1) conforming to the normal i.e. hexagonal phase (a = 4.68 A°, c = 6.82 A°). The vacuum deposited films, however, showed different structures depending on the substrate temperatures. The films formed below 300°C consisted mainly of polycrystalline tellurium often developing a

TABLE-3.1

MnTe

Analysis of the X-ray powder pattern

(Fig. 3.1)

Intensity (I/I_0)	d(A°)	hkl
s	3.10	10.1
s	2.41	10.2
s	2.08	11.1
ms	1.89	10.3
w	1.73	11.2
w	1.65	00.4
w	1.58	00.2
w	1.51	11.3
w	1.35	21.0
w	1.29	11.4
w	1.25	21.2
w	1.05	-

a = 4.68 A° c = 6.82 A°

s - strong
ms - medium strong
w - weak

TABLE-3.1'

MnTe

Analysis of the electron diffraction pattern

(Fig. 3.2)

Intensity (I/I_o)	d (A°)	hkl
s	4.05	-
w	3.57	10.0
vw	3.20	-
vs	3.11	10.1
vs	2.89	-
vw	2.48	10.2
s	2.38	-
w	2.25	00.3
vs	2.13	11.0
vs	1.99	11.1
s	1.90	10.3
w	1.76	11.2
w	1.64	00.4
ms	1.53	00.2
ms	1.50	11.3
w	1.39	20.3
w	1.36	21.0
ms	1.29	11.4
ms	1.25	21.2
s	1.14	30.1
w	1.05	-

a = 4.68 A° c = 6.82 A°

s - strong
vs - very strong
ms - medium strong
w - weak
vw - very weak

1-d orientation. The deposits formed at about 350°C yielded patterns (Fig. 3.2) by transmission conforming to MnTe. These films were quite thick and Fig. 3.3 shows the typical reflection electron diffraction pattern conforming to 1-d{10.3} orientation of MnTe films.

(ii) Resistivity (ρ) and activation energy (ΔE)

Resistance of different film thicknesses of MnTe deposited at 350°C was measured in the temperature range of 78 to 400°K in vacuo. Typical variation of resistivity (ρ) measured at room temperature for different film thicknesses is shown in Fig. 3.4. It is seen that 'ρ' continuously decreased with increasing film thickness with slight tendency to saturate at very high film thickness, suggesting that the above parameter is no longer a constant for films, even though deposited under the same evaporation condition and measured at the same temperature. This is, however, in contrast to bulk where the resistivity remains constant for all film thicknesses.

The resistivity (ρ), however, is strongly dependent upon the temperature. The typical variation of log with 1/T is shown in Fig. 3.5 (semi-log scale). It is interesting to see that 'ρ' increased continuously with decreasing temperature and tend to saturate in the low

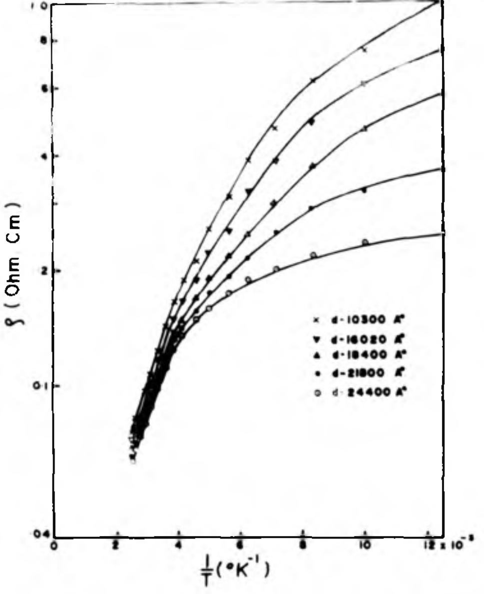

FIG 3.5

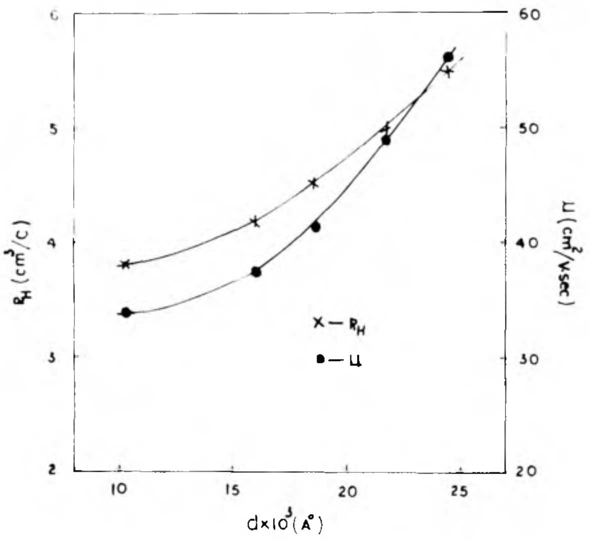

FIG 3.6

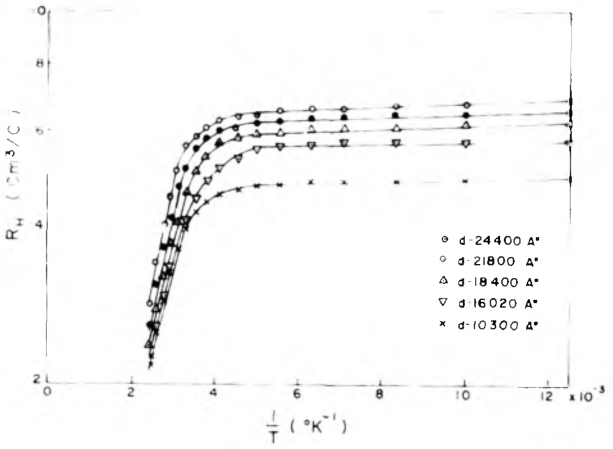

FIG 3.7

temperature region. This effect is much more predominant in thicker films. Further the slopes of log ρ vs 1/T graphs for different film thicknesses changes gradually below 270°K but between 270 to 400°K became steeper. Thus suggesting the approach of intrinsic region. These variations are however linear in the 270 to 400°K temperature region.

Activation energy from the linear portion of log ρ vs 1/T was evaluated from the relation

$$\rho = \rho_0 \exp(\Delta E/2kT)$$

and was found to be between 0.11 to 0.14 eV. However, thinner films had slightly higher value. This was also found to be true for other sets of films prepared under the same experimental and evaporation condition. All the films (1000 to 2500 A°) were semiconducting since they had lower resistivity at higher temperature.

(iii) <u>Hall constant (R_H)</u>

The above parameter was found to be independent of the magnetic field (2000 to 8000 Gauss) and impressed current (0.25 mA to 1.5 mA) but slightly dependent on film thickness as shown in Fig. 3.6. Thicker films had higher Hall constant. Hall constant was also a strong function of temperature and

film thickness as shown in Fig. 3.7 (semi-log scale). It is seen that R_H increased considerably with decrease of temperature in the higher temperature region but tendency to saturate in the lower temperature region. Further, log R_H vs 1/T graph was linear and the slopes were more or less constant as found in the case of log ρ vs 1/T graphs.

The activation energy evaluated from this agrees well with that evaluated by the thermal measurement. Since the films were semiconducting in nature, it was possible to ascertain the nature of the films and from the sign of the Hall voltage all the films were found to be p-type, suggesting that the predominant carriers were holes. This was also true for films of different film thicknesses and for films prepared in different sets of evaporations.

(iv) <u>Carrier concentration (n)</u>

The concentration of carriers namely holes was calculated from relation $n = \gamma/R_H.e$, where $\gamma = 1.93$ reason for this will be explained later on. The typical variation of log n vs 1/T for different film thicknesses is shown in Fig. 3.8. It is seen that in lower temperature range the (n) remains more or less constant for a particular film through it varies from film to film. This suggests that under lower temperature region the number of holes available for conduction remains almost the same for any particular film and

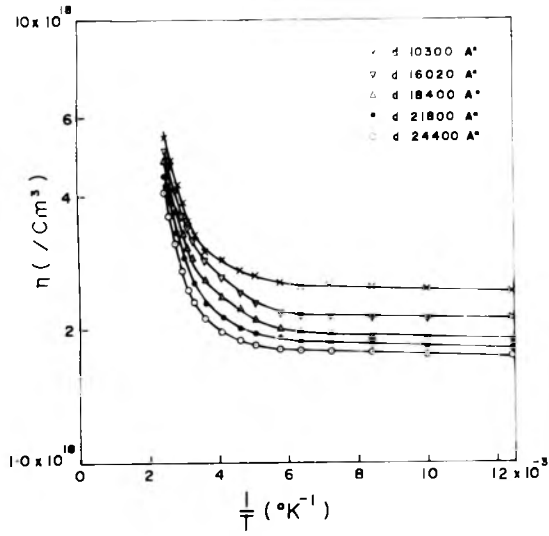

Fig 3.8

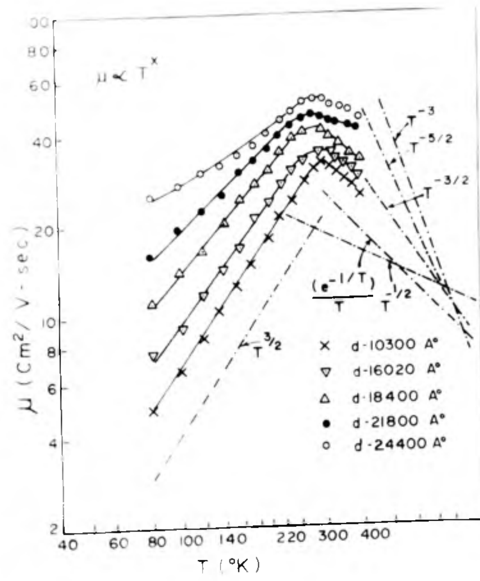

Fig 3.9

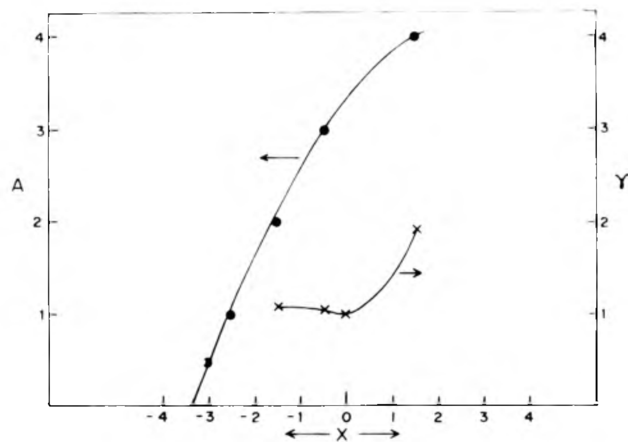

Fig 3.10

are more or less insensitive to temperature variations. On the other hand in the higher temperature region the increase in number of carriers for conduction is very high and thus with rise of temperature it increases exponentially.

(v) Mobility (μ)

The above parameter was evaluated from the relation $\mu = R_H/\rho$. It was found to be dependent on film thickness as well as temperature. A typical variation of μ with d is also shown in Fig. 3.6. It is interesting to see that thicker films had higher carrier mobilities. This suggests a possible improvement in the crystallinity of MnTe films. Fig. 3.9 (log-log scale) shows the variation of μ with temperature for different film thicknesses. All the graphs showed a characteristic peak values of mobility around temperature $T_p \approx 315^{o}K$. The mobilities increased with rise of temperature and after attaining a peak value at T_p it again decreased. This was found to be true for all the films studied by us. Further the graphs showed definite slopes in two temperature regions above and below T_p and the relation between μ and temperature could be expressed approximately by $\mu \propto T^X$ (mobility law) where magnitude and sign of X depend not only on the temperature region but also to some extent on film thickness. In the most cases below T_p region the magnitude of X was found to be 1.5 except for thicker

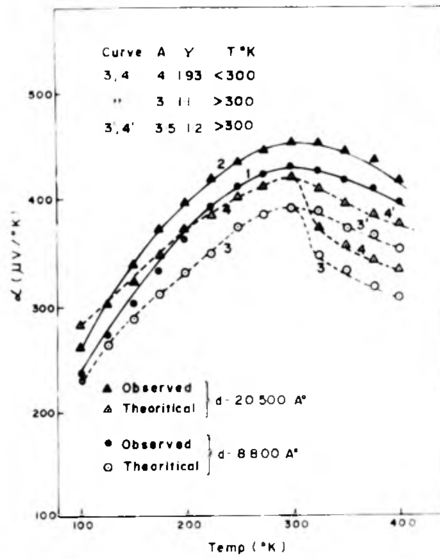

FIG 3.11

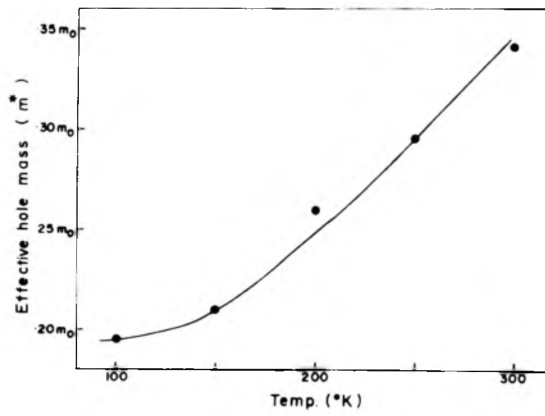

FIG 3.12

films it tends to be one. This followed approximately $\mu \propto T^{3/2}$ law. However, in higher temperature region all the graphs tend to follow $\mu \propto T^{-X}$ where X varied from 0.2 to 0.5. Most of these films followed $\mu \propto T^{-1/2}$ law.

The values of different electrical parameters at room temperature for MnTe films are shown in table 3.2.

(vi) Thermoelectric power (α)

Thermal emf were measured for different film thicknesses by differential method. The variation of (α) with temperature is shown in Fig. 3.11 for two thicknesses. It is interesting to note that (α) increases initially with increase of temperature, attains a peak at T_p ($\approx 315^{\circ}K$) and then decreased with further increase of temperature. The nature of the graphs is similar to that of μ – T plot. Thicker films had slightly higher (α) as compared to thinner ones. The thermoelectric test also showed the films to be of p-type. Also shown are the two curves 1' and 2' corresponding to the theoretical α value evaluated by using the relation

$$\alpha = \frac{k}{e}\left[A + \ln \frac{2(2\pi m^*_h kT)^{3/2}}{h^3} \cdot \frac{R_H \cdot e}{\gamma}\right]$$

assuming the magnitude of effective hole mass (m^*_h) to be

TABLE-3.2

MnTe

$T_s = 350^oC$

S. No.	Thickness d(A°)	R_H cm^3/C	$\rho \times 10^{-2}$ ohm. cm.	μ $cm^2/V.sec.$	$n \times 10^{18}$ cm^{-3}
1.	10300	3.85	12.2	31.6	3.08
2.	16020	4.15	11.6	36.0	2.93
3.	18400	4.50	11.0	41.0	2.64
4.	21800	5.05	10.4	48.0	2.33
5.	24400	5.50	9.8	56.5	2.18

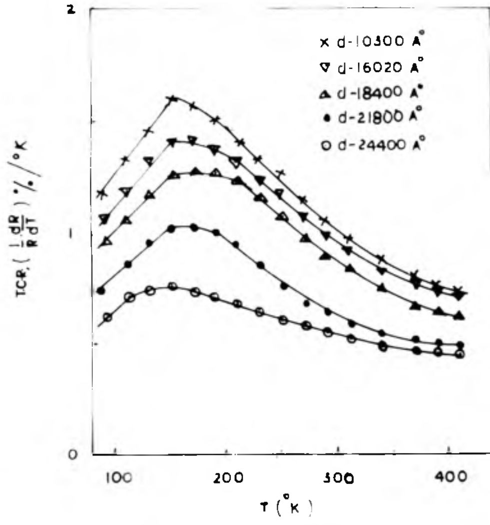

FIG. 3.13

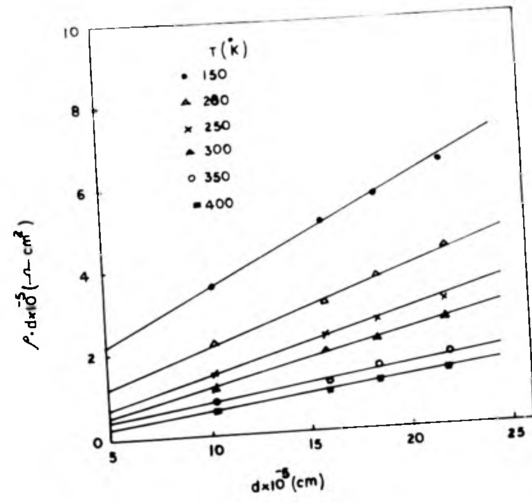

FIG 3.14

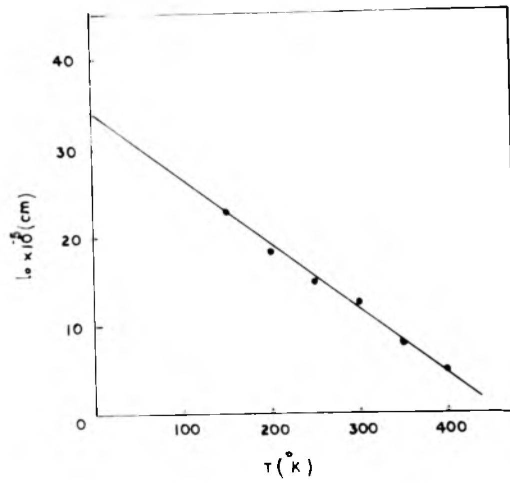

FIG 3.15

independent of temperature and γ = 1.93 and A = 4 below T_p while above T_p the value of A and γ was assumed to be 3 and 1.1 respectively.

(vii) Temperature coefficient of resistance (TCR)

The variation of TCR $= \frac{1}{R}\frac{dR}{dT}$ with temperature is shown in Fig. 3.13. It was negative for all films. It is also seen from these curves that TCR initially increased with increasing temperature and after attaining a peak at about 150°K it had a tendency to decrease fast at first and then gradually. In general, TCR was thickness dependent, thinner films having higher TCR.

(viii) Mean free path (l_o)

It is possible to estimate l_o of the charge carriers from the slopes and intercept of plot of ρd vs d as suggested by Mayer (1959). Fig. 3.14 shows ρd vs d plot for different film thicknesses at different temperatures, from which mean free path corresponding to particular temperature was evaluated. The corresponding values of l_o obtained for different temperatures are shown in Fig. 3.15. The extrapolation of graph to 0°K gave l_o as 32×10^{-5} cm.

FIG 3.16

FIG 3.17

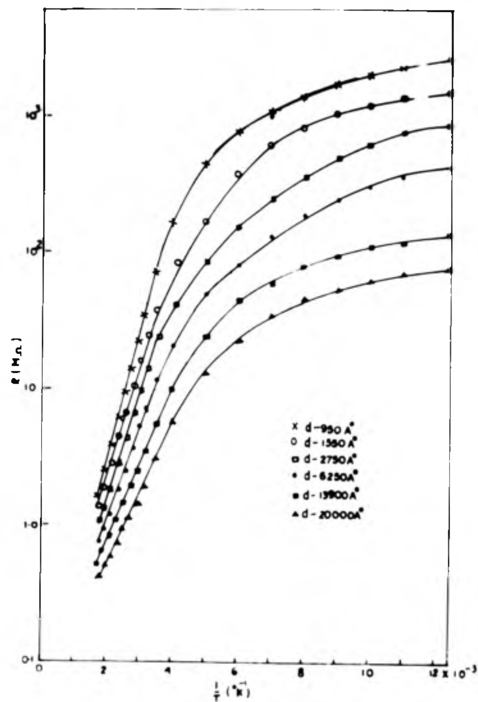

FIG. 3.18

(b) MnSe

(C) RESULTS

(i) Structure

X-Ray powder pattern of bulk MnSe had cubic structure (a_0 = 5.45 A^o) Fig. (3.16). The deposits formed at substrate temperature $\sim$ 350°C were crystalline in nature and yielded the diffraction pattern (Fig. 3.17) similar to bulk MnSe.

Electrical parameters

The electrical parameters were measured between the temperature range from 78°K to 550°K by using suitable cryostat described in Chapter I in vacuo since these samples had high resistance values only a few parameters could be measured with further facilities available here.

(ii) Resistivity (ρ) and activation energy (ΔE)

The variation of resistance with temperature and thickness is shown in Fig. 3.18 (log R vs 1/T). It is found that resistance is dependent on film thickness. Thicker films had higher resistance. The resistance of all films decreased with increasing temperature and hence these were semiconducting in nature. The variation of ρ with d is shown in Fig. 3.19. Films of lower thickness had slightly higher values.

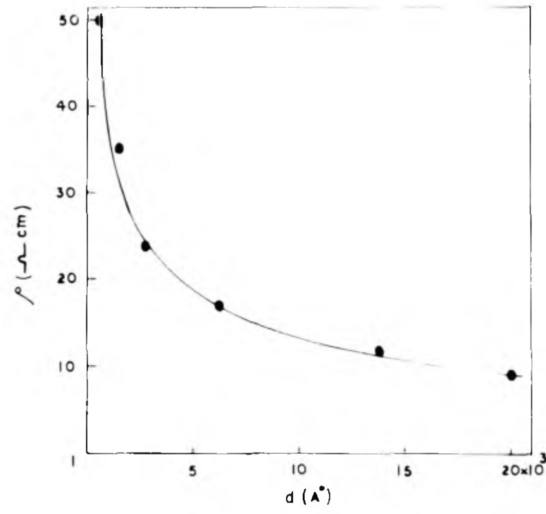

Fig 3.19

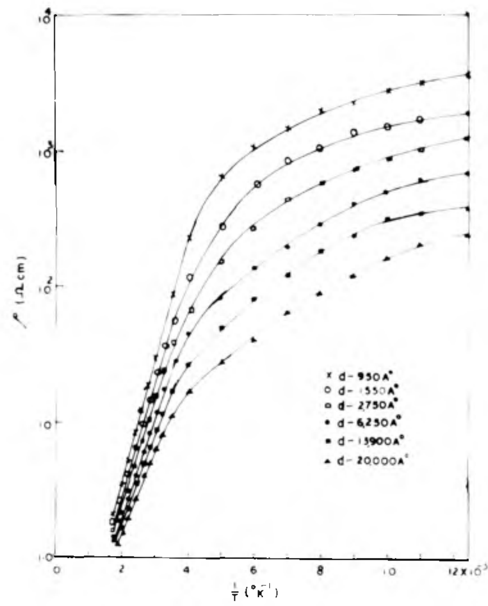

Fig 3.20

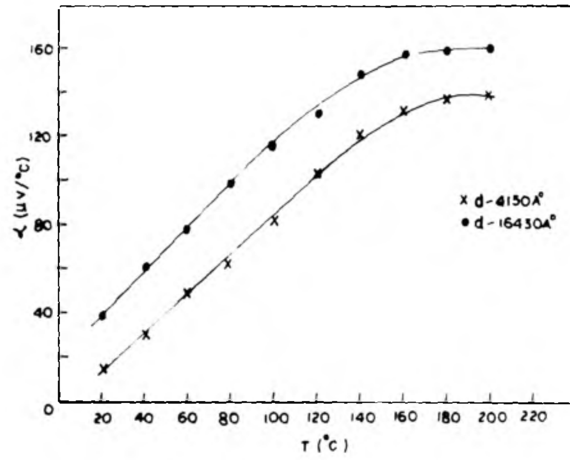

Fig 3.21

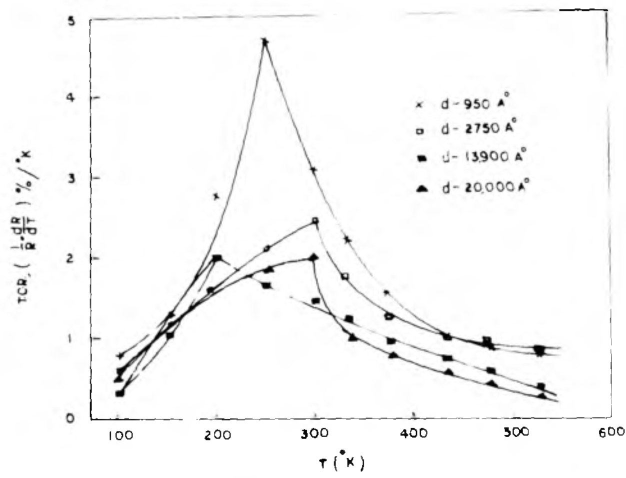

Fig 3.22

Activation energy was estimated from the linear portion of the graph (log ρ vs 1/T) Fig. 3.20). It is seen from the table 3.3 the ΔE varied from 0.57 to 0.27 eV in the temperature range 300 to 550°K. But in the range from 250°K to 120°K it varied between .045 eV to .039 eV. However at still lower temperature region (80°K to 125°K) the energy varied from .023 eV to .015 eV.

(iii) Thermoelectric power (α)

Thermoelectric power was measured for different film thicknesses (Fig. 3.21). It also increased with increasing temperature upto 180°C and then attained saturation for a further increase of temperature. It was also found to be thickness dependent. The thicker films are having higher values of α.

(iv) Temperature coefficient of resistance $= \frac{1}{R} \cdot \frac{dR}{dT}$

TCR variation with temperature and thickness is shown in Fig. 3.22. It was negative throughout the temperature range. For all ranges of thickness it increases with increasing temperature and attained a peak at about 250°K and then decreases further with the increase of temperature upto 550°K. It is interesting to see that the peaks are shifted with the film thickness.

TABLE-3.3

MnSe

T_s - 350°C

Variation of ΔE with 'd'

S. No.	Thickness d(A°)	Temp. range (550°K to 300°K) ΔE (eV)	Temp. range (275°K to 125°K) ΔE (eV)	Temp. range (125 to 80°K) ΔE (eV)
1.	950	0.57	0.045	0.023
2.	1550	0.52	0.043	0.021
3.	2750	0.47	0.040	0.020
4.	6250	0.41	0.038	0.018
5.	13900	0.35	0.036	0.0165
6.	20000	0.27	0.034	0.015

(D) DISCUSSION

The variation of different electrical parameters of the vacuum deposited films from the bulk are due to the presence of high density of defects such as discontinuity, twinning, dislocations, stacking faults, voids, internal grain boundaries, grain growth, etc. These defects as well as incorporations of some residual or absorbed gaseous molecules depending upon the deposition condition in films can produce a high concentration of defects and lead to various types of scattering mechanisms of the charge carriers.

The above study showed that the vacuum deposits formed at substrate temperatures above 350°C consisted primarily of polycrystalline manganous telluride, whereas those formed at lower temperature consisted of tellurium thus indicating that the compositions of the deposits were substrate temperature dependent. It seemed that the vapour streams obtained from the heating of bulk manganous telluride during vacuum evaporations consisted of partially or fully dissociated products of MnTe which during their condensation on the substrates might recombine at a suitable substrate temperature. It thus appeared that at about 350°C the recombination of dissociated species to form MnTe films indeed occurred. This mode of the growth process also envisaged a possible incorporation of a little of tellurium in the host matrices of the MnTe

films and these could not be detected even by electron diffraction technique. In addition, because of the highly polycrystalline nature of the films the deposits would contain innumerable grain boundaries as well as various other defects such as dislocations, structural disorders, surface asperities, etc. all of which could not be completely removed by subsequent annealing. These would, no doubt, introduce various energy levels in the energy band gap and their overall effects would determine the Fermi level and the electrical conductivity of the deposits. Since the films were p-type, the majority charge carriers were due to the presence of acceptors levels. It is quite likely that some donors were simultaneously present and after compensation the overall effect was due to the predominance of the acceptors.

The resistivity measurements of MnTe films deposited at 350°C showed that these were semiconducting in nature throughout the temperature range from 78 to 400°K. Zanmarchi (1967) also observed similar behaviour for MnTe single crystal between 80 to 375°K. Several other workers (Palmer, 1954; Valev et al, 1960; Seuter, 1967) however reported that bulk MnTe crystals were metallic below 320°K but semiconducting above it. It has also been reported that Neel temperature of MnTe was about 320°K. The resistivity changes at low temperatures range (78 to 270°K) were not much, but above it, the variation were quite significant and was linear at the

higher temperature range. When log ρ vs 1/T was plotted nearly constant conductivity at lower temperature region was obtained, thus suggesting that all free carriers are more or less frozen out. The acceptor centres are a practically therefore in non-ionized state. As the temperature rises the degree of ionisation of acceptor centres will increase with corresponding increase in carrier concentration thus resulting in a decrease of the resistivity. Some free carriers may also be available for conduction. Since 'ρ' is also dependent on 'n' and mobilities, a decrease in 'ρ' will suggest an increase in n or μ (or l) or both. But our experimental result (Fig. 3.8) shows that 'n' increases with the decrease of the film thickness and hence the lowering of 'ρ' will be due to significant lowering of μ or l. This is no doubt the case since there will be number of defects in thin films such as grain boundaries, etc. which will considerably effect μ or l

The activation energy estimated from the linear variation of log ρ vs 1/T slightly varied with thickness (0.14 eV to 0.11 eV) higher thickness have lower values. The slight decrease of activation energy with the increase of film thickness may be interpreted in terms of the mean atomic spacing which decrease with the increase of film thickness. Again the defects like stacking faults, grain boundaries

occurring in films deposited at higher temperature may also cause the slight decrease in the activation energy. The magnitude of Hall coefficient was found to be close to bulk (2.6 cm^3/C) as reported by Palmer (1954). The R_H was however found to vary slightly from 3.85 to 5.5 cm^3/C for film thickness varying from 10300 A^o to 24400 A^o. A slight variation in R_H appears to be related to defects density. It has already been shown that the carrier concentrations decrease slightly with increase of film thickness. This suggests that thicker films have effectively less number of carriers, and thicker species are relatively more ordered. It also means that R_H is also dependent on the perfection of the films. In general, higher the purity of the sample, smaller is the number of carrier concentration and hence lower the value of ($R_H = \gamma/n.e$).

Mobility variations with temperature as well as film thickness and also their gradual increase have already been mentioned earlier. This may be ascribed to the grain growth and their uniformity with the increase of substrate temperature thickness by the surface diffusion. It will also anneal out some of the defects and imperfections such as stacking faults, dislocations, etc. These effects will no doubt contribute to the increase in the mobility of the charge carriers. However, there will always be some defects such as

grain boundaries in films. The change in mobilities is fundamentally related to the modes of scattering of the charge carriers. These scattering can be due to several causes and predominance one over the other will depend on the temperature range. These are (i) lattice scattering due to phonons or optical mode, (ii) impurity ion scattering neutral impurities scattering, (iii) dislocation scattering, (iv) grain boundaries, etc. mentioned in Chapter I. In addition to these there are other modes of scattering which also dominate the transport properties. The surface scattering can also be due to the reduction in size compared to the mean free path of charge carriers affect or due to the morphological character roughness of the films. All these factors will considerably affect the mean free path of the charge carriers and hence their mobility. It has already been mentioned (Chapter I) that different modes of scattering follow different mobilities laws which can be used to explain the relation $\mu \alpha T^X$. The value of the exponent X determines the mode of scattering. Often in scattering process more than one process takes place. Hence the magnitude and sign of 'X' generally determine the primary modes of scattering (Table 1.1).

In the case of MnTe films it has been observed that mobilities gradually increased and attained a peak value and

then falls. This has been true for all films. This suggests that the modes of scattering were different below and above the mobility peak temperature (T_p) = 315°K. It can further be seen that below T_p all films more or less follow $\mu \; \alpha \; T^{3/2}$ law which suggest that scattering of charge carriers was due to ionised impurities. But above T_p region mobilities follow approximately $T^{-1/2}$ law suggesting that scattering was due to the piezoelectric mode. The above conclusion is valid in general. Since X deviates slightly from ideal case from 3/2 to -1/2 below and above T_p, these suggest that not only these modes but also there are other mechanisms of scattering present. Since in thicker films grain boundary scattering became important factor, it appears that this also contributes to affect the mobilities of the charge carriers.

According to Petritz (1956), the grain boundary scattering followed ($e^{-1/T}$) law it will tend to shift the slope from positive to negative side in log μ vs log T (graph). From above it may be concluded that $T^{3/2}$ will gradually change to a negative slope. It also appears that the effect of other modes of scattering (corresponding to $T^{-3/2}$, $T^{-5/2}$, T^{-3} laws) were absent or insignificant since in that case the graphs would have steeper negative slopes. The above considerations qualitatively explain the shape of the curves and the peak in mobility was primarily due to the shift from

$T^{3/2}$ law to $T^{-1/2}$ law around 315°K.

Thermoelectric power also showed a continuous increase with increasing temperature with a peak.

It is interesting to note that it also showed peaks were at the same T_p as for mobility. Since both the parameters are dependent on the scattering process, it is reasonable to assume that the same scattering modes as in mobility would be operating in this case also. This parameter can be calculated from the relation

$$\alpha = \frac{k}{e}\left[A + \ln \frac{2(2\pi m_h^* kT)^{3/2}}{nh^3}\right]$$

$$= \frac{k}{e}\left[A + \ln \frac{2(2\pi m_h^* kT)^{3/2}}{h^3} \cdot \frac{R_H . e}{\gamma}\right]$$

where A and γ are constants characteristics of the scattering mode and other symbols have the usual meaning. The magnitudes of A and γ for different modes of scattering are also included in the table 1.1. Since A and γ (related to α) and X (related to μ) are determined by the modes of scattering of the carriers a correlation had been sought by plotting these against X for different scattering processes and are shown in Fig. 3.10. These graphs show that the

transition from one mode to other is smooth and hence it would not be unreasonable to assume that at intermediate values of A and γ for that included in Table 1.1 mixed scatterings might be operating.

Calculations of α were made for two modes of scattering viz. ionised impurity and piezoelectric scatterings using appropriate values of A and γ below and above T_p for two film thicknesses assuming only a single scattering process operating in each region and these are shown by dashed curves 3 and 4 (cf Fig. 3.11). The magnitude of m_h* for 300°K was assumed to be 0.33 m_o and constant for all temperature. The agreement between the observed and calculated ones (Goswami and Mandale, 1978) below T_p region is quite reasonable. In the higher temperature range however there is a sharp deviation in the shape of the curve. Since the exponent of the T varied slightly from idealised $T^{-1/2}$ law, a new value of X ($\simeq$ -0.4) was assumed and corresponding values of A and γ were taken from the graphs and α was then further calculated. These are shown by the curve 3' and 4'. With this change the shape of the curves improved but it was not sufficient enough to fit in with experimental values.

It is conceivable that at the higher temperature range the effects of various factors viz. (a) multi-modes of scattering, (b) presence of mixed carriers, (c) temperature

dependence of m_h^*, (d) surface scattering, and (e) magnon drag, etc. may be important. The contribution of factor (a) and (b) are more or less taken into account by taking appropriate value of X. m_h^* has been regarded as temperature independent. It has recently been shown that m_h^* of doped MnTe crystals as calculated from α increased considerably with the rise of temperature. We also made some calculations of effective mass from the observed α assuming A and γ were 4 and 1.93 respectively for temperature T_p and its variation (Fig. 3.12) suggests that m_h^* was not temperature independent. These new values of m_h^* are no doubt artificial. Whether in reality m_h^* should be so much temperature sensitive can only be decided by suitably designed experiments. If, however, it is so, then a suitable m_h^* value for higher temperature would cause an improvement of the graphs.

MnTe crystals are also known to be antiferromagnetic below Neel temperature (320°K) and paramagnetic above it. It is quite likely that the vacuum deposited MnTe films had similar characteristics. Since T_N and the T_p are in the same region, it is reasonable to assume that the MnTe films would also be paramagnetic above T_p region. Consequently the magnon drag which are normally predominant in the paramagnetic region would also be present in these films and hence affect the thermoelectric power.

Recently Petritz (1956) showed that the scattering of the charge carriers followed the relation

$$\mu = \frac{M}{NkT} \exp\left(\frac{\phi}{kT}\right)$$

From the variation of mobility with temperature the barrier height (ϕ) across the grain boundaries was evaluated. Ludeke (1971) calculated ϕ by using the same method but assuming mobility followed the relation $\mu \alpha\ e^{-\phi/kT}$ instead of the original relation. The mobility increased with 1/T below T_p and ϕ obtained varied from .018 eV to .012 eV for different film thicknesses. However, evaluation of ϕ by Petritz formula is rather complicated. It is also possible to evaluate the Fermi energy level from the carrier concentration and observed thermoelectric power by using two separate relations viz.

(a) $$\ln \frac{n}{N} = \frac{E_F}{kT} \quad \text{where } N = \frac{2(2\pi m^* kT)^{3/2}}{h^3}$$

(b) $$\alpha = \frac{k}{e}\left(A + \frac{E_F}{kT}\right)$$

where A is the constant and its magnitude depends upon the scattering mechanism. In this case A = 4 since ionised impurity scattering mechanism was predominant below T_p. It

was found that though Fermi energy level increased with increasing temperature for both the cases. Further, E_F varied from -ve to the value, which was very much different from the values obtained by the use of formula 31a. These descripancies between the two sets of values could not be explained.

From the results of resistivity, thermoelectric power, etc. of vacuum deposited MnSe films, it is seen that there is considerable difference between bulk and corresponding properties in thin films state. Since these films are having very high resistivity, the Hall voltage could not be measured and hence the Hall constant, mobility, carrier concentration. In the absence of these data it is not possible to suggest the mechanism of scattering. Since MnSe and MnTe are the chalcogenides of Mn and both are semiconductors, it can be conjuctured that the scattering modes would possibly be the same. These films were found to be semiconducting in nature as observed for bulk. The high resistivity of films may be attributed to the large number of defects such as dislocations microtwins, etc. as reported by many workers (Pashley, et al, 1959; Phillips, 1960). The small grain size and absorption of gases will also produce high concentration of defects and scattering centres may also increase the resistivity of films.

The activation energy observed in case of films was found to be varied from 0.57 eV to 0.27 eV in the temperature range from 300 to 550°K as film thickness varied from 950 A^{o} to 20,000 A^{o}. It is very close to bulk value (.6 eV) as reported by Makovestskii and Sirota (1965). From the table 3.3, it is seen that the degree of ionisation increases with increasing temperature i.e. low value of activation at lower temperature region may be due to presence of some unionised impurities.

Thermoelectric power measurements showed that these films were p-type and also thickness dependent. The increase of α with temperature and film thickness is similar to MnTe films.

CHAPTER-III

REFERENCES

Devyakora et al, (1964), Fiz. Tverdogo Tela, 6, 1813.

Fredrick, R.E. and Manser, C.R. (1959), Chemical Abstract, 53, 167161.

Goswami, A. and Mandale, A.B. (1978), Jap. J. Appl. Phys., 17, 473.

Jones, E.D. (1966), Phys. Letters, 19, 106.

Ludeke, R. (1971), J. Vac. Sci. Technol., 8, 203.

Makovestskii, G.I. and Sirota, N.N. (1965), Dokl. Akad. Nayk. Belonisik, 9(1), 15.

Palmer, W. (1954), J. Appl. Phys., 25, 125.

Pashley, D.W. et al (1959), J. Inst. Met., 87, 419.

Petritz, R.L. (1956), Phys. Rev., 104, 1508.

Phillips, V.A. (1960), Phil. Mag., 5, 571.

Rustamove, A.G. et al (1970), Neorg. Mater., 6, 1339.

Seuter, A.M.J.H. (1967), Nat. Rech. Sci., 157, 459.

Squire, C.F. (1939), Phys. Rev., 56, 922, 960.

Uchida, E. and Kondo, H. (1953), Busstiron Kenkya, 59, 88.

Uchida, E. et al (1956), J. Phys. Soc. Japan, 11.

Valev, L.M. et al (1960), Dokl. Akad. Nauk., 22(11), 13.

Wasscher, J.D. (1967), Colloq. Int. Centre Nat. Rech. Sci., 157, 465.

Wasscher, J.D. and Hass, C. (1964), Phys. Letters, 8(5), 302.

Yadaka, H. et al (1962), J. Phys. Soc. Japan, 17(5), 875.

Zvyagin, A.I. et al (1971), Ser. Fiz., 35(6), 1190.

Zanmarchi, G., (1967), J. Phys. Chem. Solids, 28, 2123.

Zvyagin, A.I. et al (1969), Soviet Phys-Solid State, 11, 2759.

CHAPTER-IV

MERCURY TELLURIDE

CHAPTER-IV

MERCURY TELLURIDE

(A) INTRODUCTION

Tellurides and selenides of mercury have drawn considerable attention in recent times because these show high mobility as well as very low activation energy. The electron mobility of HgTe at $0^{o}K$ was reported to be as high as 480000 $cm^2/V.sec$. At liquid nitrogen temperature these compounds exhibit large magnetoresistance, Hall effect and resistance effects. These are very stable, have high output Hall voltage and also flexibility. These compounds show good magneto-thermal effects like Nernst Ettinghasen effects, the carbino-magneto-resistance, seebeck effect, photo-conductor, optical absorption, photoelectron emission and photovoltatic effect.

As a result of these properties, there is a high possibility for its use in various electronic circuits, optical devices such as Hall generator, isolator, circulator, magnetometer, phase detector, frequency spectrum analyser and infrared detectors.

Zachariasen first (1925, 1926) investigated the structures of HgSe and HgTe and reported that these two

compounds crystallised with zinc-blende type of structure. The lattice constant of the crystalline films of HgTe and HgSe were determined by Zorll (1954) (6.429 ± 0.0064 and 6.074 ± 0.006 values respectively).

Goswami and Barua (1970) prepared telluride and selenide films of mercury from vapour phase on single crystals and also on amorphous substrate and studied their structural properties by electron diffraction techniques. They reported that these deposits having cubic structure grew epitaxially on single crystals specimens even at room temperature with appropriate orientations depending on the substrate temperature.

Elpate'veskya and Regel (1956) made the Hall emf detector from HgTe, HgSe and their solid solution and used for the measurements of magnetic field between 100 to 20,000 gauss. These compounds showed carrier mobilities as high as 3000 cm^2/V.sec. at room temperature. Minden (1958) observed that HgTe had energy gap about 0.1 eV and mobility 25000 cm^2/V.sec. and also electrical properties were close to that of Ge. The thermomagnetic properties of HgTe were also studied by Rodot and Rodot (1959) and observed high mobility. Black et al (1958) measured the Hall constant and resistivity of single crystal HgTe as a function of temperature and magnetic field. It was found that above 250°K the HgTe was

intrinsic and had ΔE as .02 eV. They also reported that $\frac{u_n}{u_p}$ = 10 and u_n was 16000 $cm^2/V.sec$. Harman and others (1958) prepared a pure and nonstoichiometric HgTe which had $\frac{u_h}{u_n}$ = 0.01 and having activation energy of about 0.02 eV. Rodot and Rodot (1960) measured the magnetoresistance of single crystals HgTe and HgSe and found that accoustic phonon scattering mechanism was predominant in both the cases. The optical and electrical properties of pure HgTe were studied by Quillet et al (1962) and estimated the carrier concentration which was about $6x10^{16}$ and $9.5x10^{15}$ cm^{-3} at 7^oK and 20^oK respectively. R_H was found to be independent of magnetic field. It was also noticed that in the infrared region square of absorptivity (h^2) is proportional to the incident radiation energy ($h\gamma$). The mobility, Hall constant and thermoelectric power of stoichiometric compound HgTe single crystals (n or p type) were measured as a function of temperature by Osnach (1965). He found that Hall coefficient increased from 1.53 to 40 when excess of Hg varied from 0 to ~5%. Similar changes in the mobility from 135 to 54000 $cm^2/V.sec$. were also observed by him.

The effect of annealing at different temperatures on electrical parameters of HgTe with the excess of Hg were

studied by Sharavskii and Khabarova (1964). They found that there was gradual change in R_H, σ and μ in samples annealed at 50°C. Thermoelectric power, Hall coefficient and mobility of HgTe measured by Dziub and others (1964) in the intrinsic region and explained them from the parabolic band model. Optical scattering mechanism was found to be predominant. Giriat et al (1964) reported thermoelectric power to be about 120 uv/^{o}K, R_H = 1 cm^3/c and the value of m^* = 0.30 m_o for HgTe. Kolosov and Sharavskii (1965) studied the dependence of R_H and σ on magnetic field (4-20 K. gauss) in the temperature range from 294°K to 77°K for HgTe (p-type). Hall constant was found to be independent of the magnetic field but σ as well as magnetoresistance decreased with increase of magnetic field. Rodot et al (1963) estimated the (n) from R_H as a function of temperature and observed that $nT^{3/2}$ was not exponential of 1/T. At low temperature HgTe behaved like semimetal. Effective electron mass was estimated to be 1.1x10^{-3} m_o (at the base of conduction band) and hole mass 0.60 m_o (of d states in valence band).

Kot and Maronchuk (1963) observed that above 100°C there was an increase in conductivity and change in sign of α. This parameter was thickness dependent. ΔE was found to be about 0.03 eV at room temperature. The dependence of Hall coefficient on temperature (80-300°K) and pressure (1 to 500

Atm. pressure) of HgTe bulk was studied by Porowski and Zakrzewski (1965). At higher temperature R_H followed $T^{-3/2}$ law but not so at low temperatures.

The transport coefficient in weak transverse magnetic field, in the temperature range of 100 to 300°K was measured by Wagini and Reiss (1966). The results were compared with theoretical calculation by assuming different scattering accoustic optical phonons and ionised impurities near intrinsic region. They suggested the predominance of the optical phonon scattering mechanism. Magnetoresistance, Hall voltage and resistance were measured by Harman et al (1967) at 4.2°K. Three carrier band models one having two sets of electrons and other one set of holes was observed. The Hall mobility was observed about 40,000 cm^2/V.sec. at 4.2°K for bulk HgTe.

Ivanov and others (1967) observed similar metallic nature of HgTe and explained it from the three band model. Aliev et al (1971) investigated that the carrier concentration dependence of α, magneto thermal emf in strong magnetic field in HgTe (n-type). They showed that there was a contribution to the thermoelectric power due to the heavy holes at high temperature and low electron concentration. Ivanov et al (1971) investigated the optical absorption and reflection magneto plasma reflection at various temperatures

on HgTe (p and n-type). The effective masses of electrons, their relaxation time, Fermi energy and energy gap were estimated. The dependence of R_H, of single crystal HgTe on magnetic field was investigated by Zakrezevski and others (1972) at 4.2°K, 77°K and 300°K. The results are explained with assumption that the transport phenomena are caused not only by electron-holes but also by addition of low mobility carriers. The additional low mobility carriers are assigned to an impurity band. Rode and Willey (1973) reported that for the zero gap semimetals like α-Sn, HgSe and HgTe, that the piezoelectric deformation potential scattering by accoustic phonons, polar optical model of scattering and coulombs scattering were predominant. Optical constant for HgTe and CdTe were studied by Odarich (1973) in the intrinsic absorption range. It was observed that in HgTe the band edge portion (1.2 eV) agrees with the theoretical value of spin-orbit splitting of valence band at point (ΔE = 1.13 eV). Dziuba (1974) measured the Hall coefficient and conductivity of undoped HgTe in the temperature range from 4.2 to 300°K and in the magnetic field $\leq$ 300 K.G. The results are explained by using a three carrier model of conductance have conduction band states, valence band states and impurity states. Mycielski (1974) measured absorption reflection, magneto absorption and magneto reflection in the air (2-60 μ) of HgTe and studied the optical properties of zero and small gap

semiconductors like HgTe and deduced the effective mass carrier, energy gap and relaxation time. Okazaki and Shogenji (1975) observed that for annealed films the mobility increased to a very high value (about 33000 $cm^2/V.sec.$) but the magnetoresistance decreased. Accoustic scattering mechanism was predominant near about room temperature. Ivanov et al (1975) showed that the conductivity R_H and magnetic susceptibility of these compounds depended on temperature. Lambus et al (1975) studied the electrical properties of HgSe and HgTe in the temperature range from 1.5 to 350^oK and reported that the inverted two-band model was not valid for the solid solution. Nishizawa and others (1976) found that R_H was magnetic field dependent and it was interpreted on the assumption of two sets of electrons with different mobilities. Effective hole was mass observed to be about 0.53 m_o at 300^oK and independent of temperature and hole concentration.

A few measurements were also made for thin films. Elpat'evskaya (1958) prepared thin films of HgSe and HgTe in both opaque and translucent forms. They observed that for the opaque films μ_e was found to be about an order of magnitude higher than the other. Goswami and Deokar (1970) observed that R_H, σ and μ increased with the increase of substrate temperature for polycrystalline as well as single crystal films (deposited on mica). These values were much

higher for single crystal films and also found to be thickness dependent. Barua and Barua (1974) studied the electrical properties such as activation energy, seebeck coefficient, TCR, R_H, u_H of film HgTe (d = 500 A^o to 25000 A^o) in the temperature range 265^oK to 400^oK. They reported that seebeck coefficient was 300 uv/^oK and it increased with decreasing film thickness. Activation energies are found to be independent of film thickness.

It is thus seen that although considerable amount of work has been done on the bulk single crystal of HgTe but very little systematic work has been carried out on the thin films. Hence a detailed study of different electrical properties especially at low temperature and their dependence on temperature was investigated.

(B) EXPERIMENTAL

(a) Preparation of mercury telluride

The bulk mercury telluride was prepared by the direct reaction of mercury (A.R. grade, doubly distilled) and tellurium (specpure 99.999%). The constituent elements were taken in stoichiometric proportion (1:1) in a silica tube and sealed in vacuo (10^{-5} mm of Hg). The sealed tube containing the mixture was slowly heated in an electric furnace to 480^oC and kept at this temperature for about three hours so that

fig 4.1

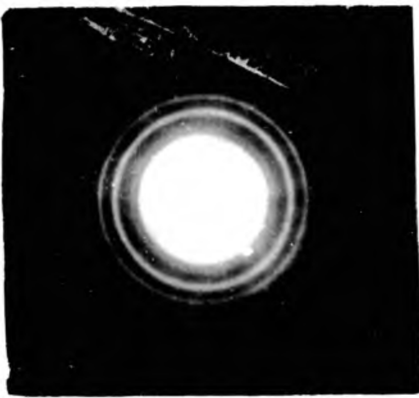

fig 4.2

fig 4.3

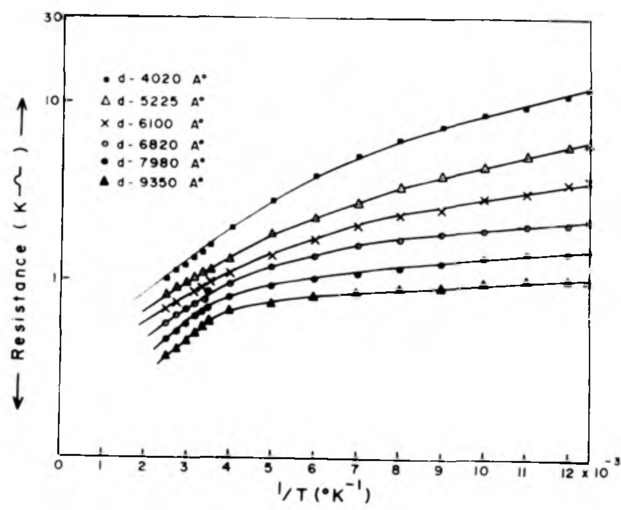

fig 4.4

reaction between tellurium and mercury was easily controlled. The temperature of the furnace was then raised step by step (at the rate of about $100^{o}C/h$) and finally to about $700^{o}C$ to get the homogeneous product (liquid) of HgTe (mp $\approx 670^{o}C$) and kept at this temperature for a period of 8 hours. The furnace temperature was then lowered to about $300^{o}C$ and then the tube was suddenly quenched in cold water.

(b) Film preparation

Mercury telluride films were prepared by the vacuum deposition of bulk HgTe from a molybdenum boat which was earlier flashed in vacuo. Films were deposited on precleaned glass substrates keeping the substrate temperature at about $120^{o}C$. Before measuring the electrical parameters, all films were annealed at the same temperature in high vacuo (3×10^{-5} torr) for two hours. HgTe films thus prepared had a thickness range of 4000 to 10000 A^{o}. Thickness of the films was measured by the multiple beam interference method.

(B) RESULTS

(i) Structure

The bulk material HgTe was polycrystalline in nature as confirmed from the X-ray powder analysis (table 4.1). The disorption of various reflections and their d-values agreed with the normal HgTe ($a = 6.45\ A^{o}$) having a zinc-blend type

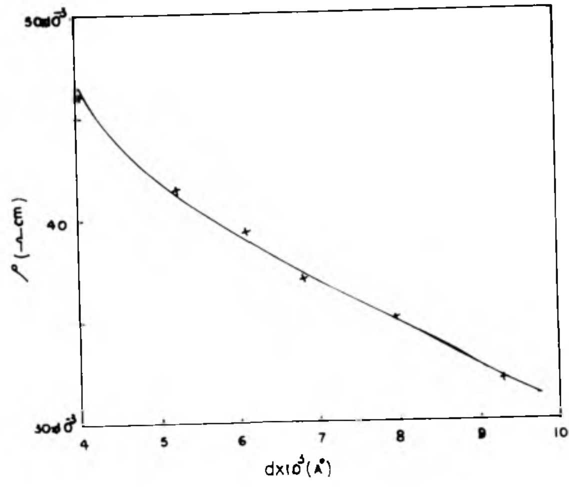

fig 4 5

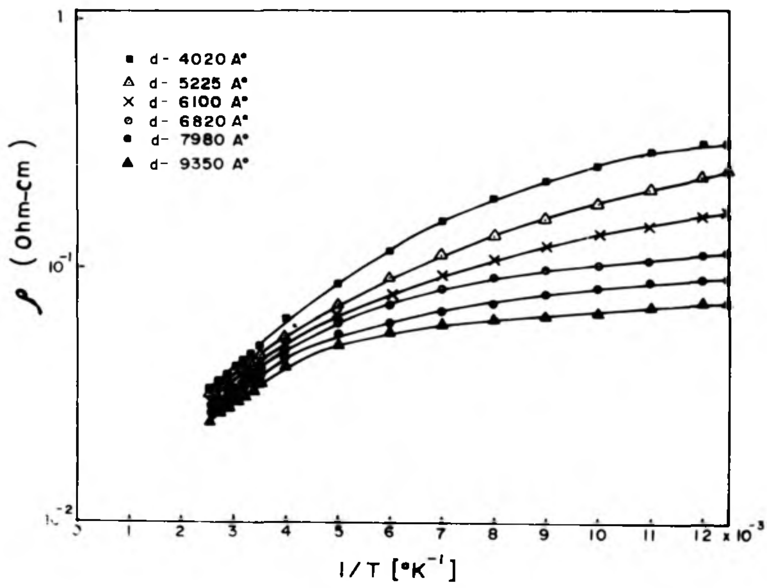

fig 4 6

structure (Fig. 4.1).

Electron diffraction studies of HgTe films deposited at 120°C on NaCl polycrystalline substrate also had lattice parameter (table 4.2) conforming to bulk HgTe (Fig. 4.2). The deposits formed on glass substrate showed patterns (Fig. 4.3). It is ssen that the deposits developed a 1-d{111} orientation conforming to the observation of Goswami and Barua (1970).

(ii) Resistance, resistivity and activation energy

The variation of resistance with temperature for films of various thicknesses (4000 to 10000 A^{o}) formed at 120°C is shown in Fig. 4.4. R vs 1/T in semilog scale. It is seen that with the increase of temperature from 78°K, the resistance for all films initially decreased slowly later on, it was rather steep, thus suggesting the approach to the intrinsic region (300°K to 420°K). The decrease of resistance with the increase of temperature suggests that the films are semiconducting in nature. The variation of resistivity with film thickness (d) is shown in Fig. 4.5. It was found that resistivity of these films decreased with increasing film thickness. The variation of resistivity with temperature is also shown in Fig. 4.6. The trend for the variation of with temperature and thickness is similar to the resistance variation.

TABLE-4.1

HgTe

(Fig. 4.1)

Intensity I/I_o	d(A^o)	hkl
w	3.77	111
vw	3.23	200
ms	2.31	220
ms	1.97	311
w	1.63	400
m	1.49	331
ms	1.33	422
m	1.25	-
w	1.15	-
m	1.10	-
m	1.03	620
w	0.99	533

$a_o = 6.45\ A^o$

w - weak
vw - very weak
ms - medium strong
m - medium
s - strong

TABLE-4.2

$HgTe$

(Fig. 4.2)

Intensity I/I_o	$d(A^o)$	hkl
w	3.16	-
w	3.22	200
w	2.72	-
s	2.28	220
ms	1.92	311
w	1.58	400
w	1.47	331
w	1.27	440

$a_o = 6.45\ A^o$

w - weak
s - strong
ms - medium strong

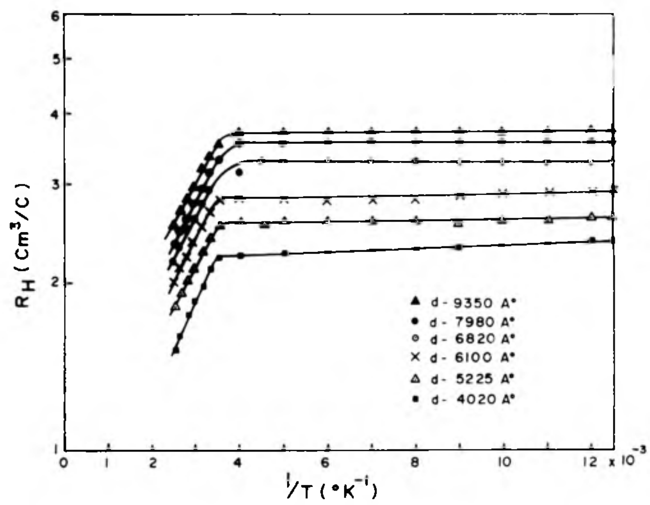

fig 4·7

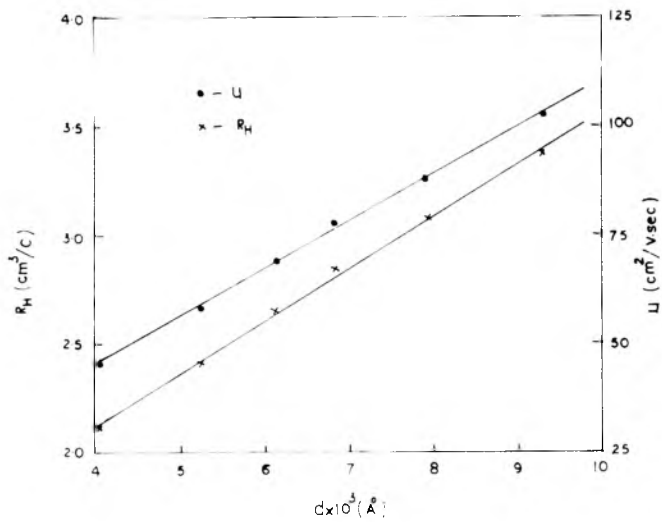

fig 4·8

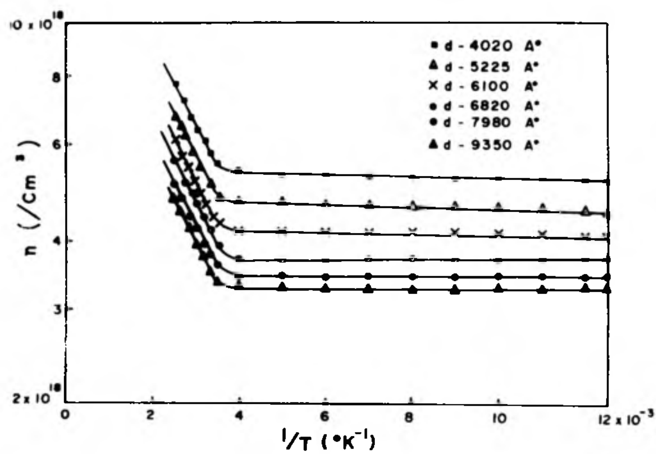

fig 4·9

(iii) Hall constant (R_H) and carrier concentration (n)

The Hall voltage measurements for all films showed that these were p-type. The variation of Hall constant with temperature is as shown in Fig. 4.7. It is seen that R_H was almost constant in the low temperature region (78 to 280°K) but decreased sharply at higher temperature range (300-420°K). Further, R_H was found to be thickness dependent, thinner films having lower value of R_H (Fig. 4.8). It should be mentioned here that R_H was independent of the magnetic field (2000 to 8000 gauss) and current 0.25 mA to 2.5 mA between 78-420°K.

The carrier concentration was evaluated from the relation $n = \gamma / R_H e$ (γ = 1.93). The variations of (n) with temperature and thickness is shown in Fig. 4.9. (n) was more or less constant in the low temperature region (78 to 280°K) while after 280°K it increased with temperature. It is interesting to see that thicker films had lower carrier concentration as compared to the thinner ones. This suggests that thicker films and comparatively less defect density than the thinner ones. Activation energy calculated from this (log n vs 1/T) agreed well with the resistivity values.

(iv) Mobility (μ)

The variation of mobility with film thickness is shown

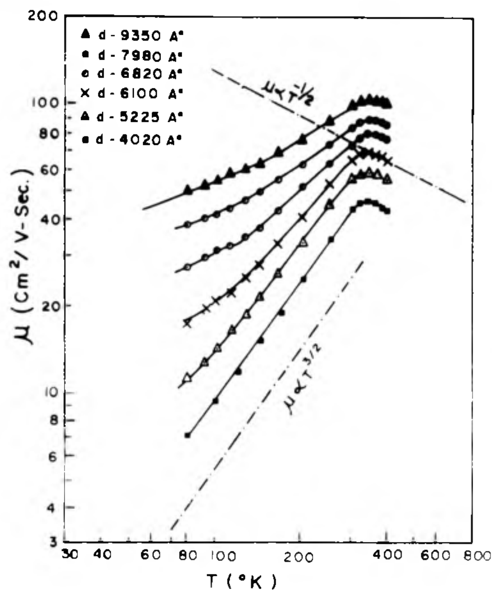

Fig 4.10

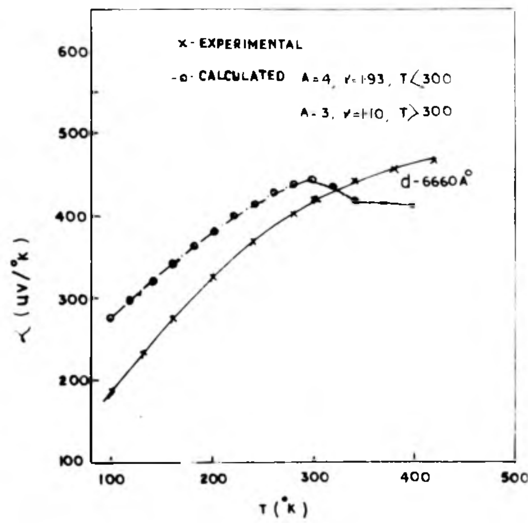

Fig 4.11

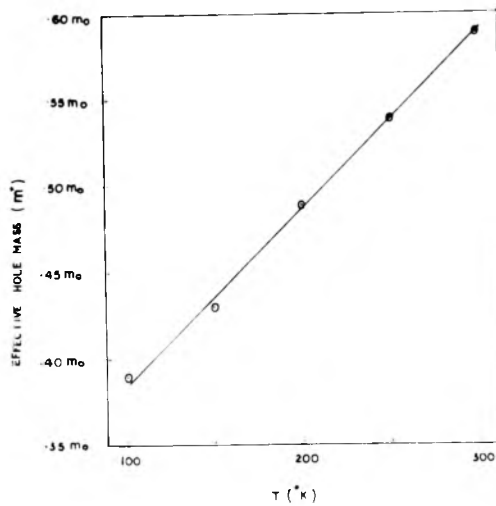

Fig 4.12

in Fig. 4.8. It is seen that films with higher thickness had higher mobilities. The temperature dependence of mobility is shown in Fig. 4.10 (log-log scale). Mobility increased with the rise of the temperature between the range 78 to $310^{o}K$ and then decreased with the further increase of temperature (310 to $420^{o}K$) thus showing a peak in mobility curves at about $310^{o}K$. In lower temperature region mobility followed $\mu \propto T^{x}$ law where x varied between 1.5 to 1.0 depending on film thickness. However, thinner films followed exactly $\mu \propto T^{3/2}$ law. In the higher temperature region mobility followed the $\mu \propto T^{-x}$ where x varied between 0.2 to 0.5.

Table 4.3 shows the values of different electrical parameters of HgTe films measured at room temperature.

(v) Thermoelectric power (α_s)

Thermoelectric power of mercury telluride film was measured by differential method. This measurement suggests that these films are p-type. The variation of thermoelectric power with temperature is shown in Fig. 4.11 and was found to be increasing gradually with increase of temperature.

Theoretical calculation of α was made by using the relation (31a) where A and γ are the constants characteristic of the scattering mode. The magnitude of A

TABLE-4.3

$HgTe$

$T_s = 120^{o}C$

S. No.	Thickness d (A^o)	R_H cm^3/c	$\rho \times 10^{-3}$ ohm. cm.	μ $cm^2/V.sec.$	$n \times 10^{18}$ cm^{-3}
1.	4020	2.12	46.0	45.6	5.70
2.	5225	2.40	41.5	57.8	5.05
3.	6100	2.65	39.0	68.5	4.55
4.	6820	2.85	37.0	78.5	4.16
5.	7980	3.10	35.0	88.5	3.90
6.	9350	3.35	32.0	103.0	3.68

and γ were estimated from the slopes of temperature dependent mobility graphs (Fig. 4.10). The mobility graph roughly corresponds to the ionised impurity scattering mechanism ($T^{3/2}$ law), in the lower temperature region (78 to 320°K) and at higher temperature i.e. above T_p (320°K) mechanism was due to piezoelectric scattering. Since A and γ (related to α) and X (related to λl) are determined by the modes of scattering of the carriers, values of these are taken from the table 1.1. Again in this relation the effective hole mass (0.53 m_o at 300°K) was assumed independent of temperature range (78 to 420°K). Now there are two types of scattering mechanisms below T_p and above T_p. So for the calculation of α appropriate values of A, γ were taken from table 1.1 and these are equal to 4 and 1.93 respectively below T_p and above T_p. A = 3 and γ = 1.10. The dotted line in Fig. 4.11 shows the theoretical curve of α.

i) <u>Effective hole mass (m^*_h)</u>

The magnitude of m^*_h was taken to be 0.53 m_o at 300°K for our theoretical calculation of thermoelectric power and regarded as temperature independent. So some calculations of effective mass were made from the observed α values assuming A and γ were 4 and 1.93 respectively in the temperature range of 78 to 300°K i.e. below T_p. Its variation with temperature is shown in Fig. 4.12. It suggests that m^*_h

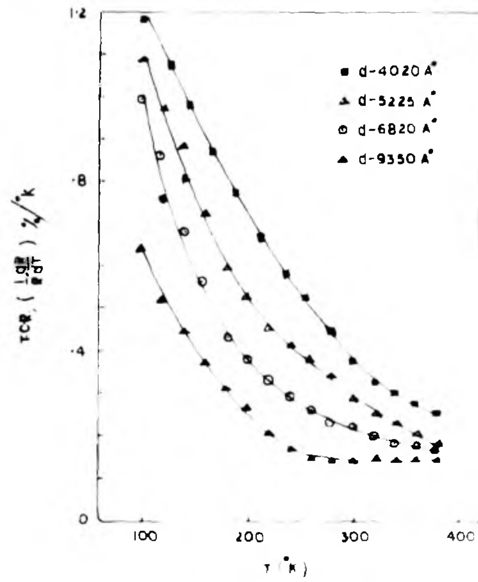

fig 4.13

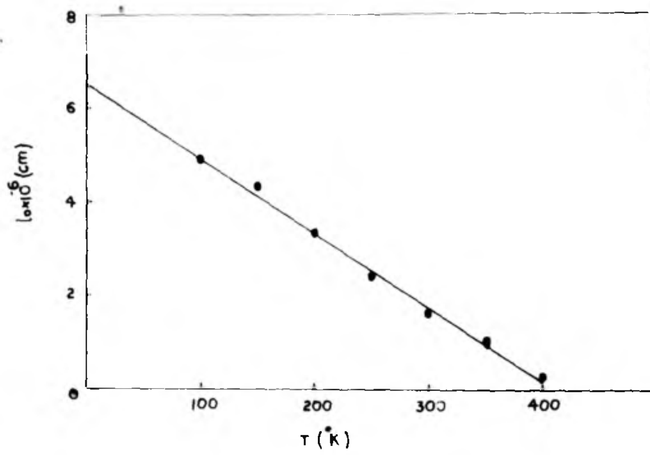

fig 4.14

was not temperature independent.

(vii) Temperature coefficient of resistance (TCR)

It was estimated by using the relation $\frac{1}{R}\frac{dR}{dT}$ and was negative for all films and also thickness dependent. The variation of TCR with temperature is shown in Fig. 4.13. It is seen that the values were higher at low temperatures as compared to those at higher temperatures. Further, thicker films had slightly lower TCR.

(viii) The Mean free path (l_o)

This parameter was evaluated from the ρ d vs d method. It is found that it increases with decrease of temperature and increasing film thickness. The variation of l_o with temperature is shown in Fig. 4.14. The value of l_o obtained at 0^oK was about 6.5×10^{-5} cm.

(D) DISCUSSION

The structure studies of HgTe films clearly indicate that all the films developed 1-d {111} orientation without any phase change. Further these deposits increased crystal size with increase of film thickness as shown by sharp diffraction pattern.

The electrical studies of the different parameters

namely ρ, R_H, μ and α differ considerably from those of the bulk material. These variations may be adduced to the presence of innumerable imperfections such as dislocations, grain boundaries, misfits of atoms, misalignment of crystallites, stress, etc. The vacuum deposited films with appropriate annealing in vacuo these defects can only be partially removed. The presence of these defects will no doubt produce impurity centres in the energy band gap even though starting material was highly pure. With increasing thickness some of the defects such as voids, discontinuity, etc. will be partially removed thus decreasing the effective defect concentration. Hence also the carrier concentration. Consequently, thicker films will show lower (n) with thinner ones. This is also coloborated with decrease of carrier concentration with increasing film thickness. Even though all the films developed the same 1-d{111} orientation showed that electrical parameters slightly differ from thickness to thickness. Since perfection of ordering may change with thickness, cause the charge parameters. Same thing is true for all films studied between the thickness range from 4000 to 10000 A°. Since the structure of thin films also conformed to bulk HgTe, the semiconducting behaviour of films cannot be attributed to the change of structure or to the crystalline size or preferred orientation. All films, however, showed p-type characteristics. In a recent paper by Goswami

and Ojha (1975) have showed that bulk Bi which is semimetallic in nature also behave in the film state as semiconductor. The semiconducting behaviour of HgTe films may arise from the following causes.

(a) The presence of potential barriers in the discontinuous films having island structure when conduction under an electrical field can take place by direct tunnelling or through substrate as proposed by Minn (1960), Neugebauer et al (1963).

(b) The quantum size effect (QSE) where the film thickness is comparable to the de Broglie waves (Ogrin et al, 1966; Sandomirskii, 1967). The theoretical treatment for such cases has been given by Sandomirskii (1967).

The former mechanism presumes an island structure and discontinuity of these films. Since the semiconducting behaviour even for the thick films ($\gtrsim$10000 A°) observed where island structure will no longer be present it seems that the former mechanism may not be valid for including inducing semiconducting properties. Semimetallic nature of HgTe and HgSe were, no doubt, due to the overlapping conduction and valence bands. However, due to quantum size effect these two bands may split into sub-bands of low film thickness. If the thickness is substantially small, the small gaps may be formed

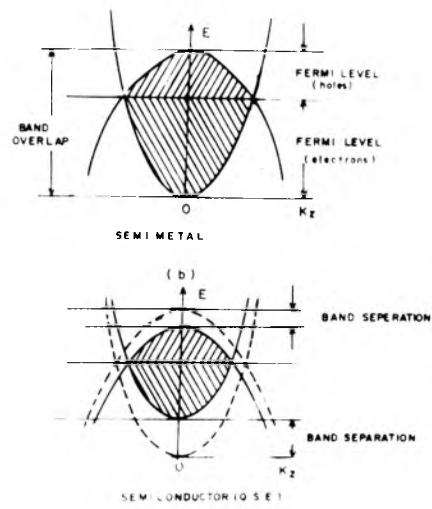

FIG 4 15

and a semi-metal becomes a semiconductor (Fig. 4.15 Sandomirskii model 1967). This effect depends on the film thickness. Hence a material can change from the degenerate to the non-degenerate state. The above presumption involves a comparatively small thickness of the material (Hoffman et al, 1971) had shown that even for thickness as high as 5000 A^{o}, QSE is observed for Bi films. It is likely that the same may be true in the present case also.

The mobility of these films was very much less as compared to the bulk values as reported by several workers. The variation of μ with temperature was observed to be similar to that for the manganous telluride films i.e. it increased with the increase of temperature from 78 to $310^{o}K$ and attaining a peak at $310^{o}K$ and decreases further with increase of temperature. The mobility variation followed $\mu \alpha T^{X}$ law where X varied from 1.5 to 1 which depends on film thickness below peak and above it follows the $\mu \alpha T^{-X}$ law where X = -1/2. It shows that the predominance of ionised impurity scattering and piezoelectric scattering mechanism below and above it respectively. The decrease in above peak can be due to various causes such as presence of mixed carriers, temperature dependence of m^{*}_{h} surface scattering and grain boundaries, etc.

Since the experimental μ—T curves do not fit in

exactly with ion peak and piezoelectric scattering mode it seems that some other mode of scattering might have also been present though to a less extent.

It is also seen that the thermoelectric power also increases continuously with the increase of temperature. This may be due to several factors such as mobility increases with area temperature, the decrease of n increase in effective mass (m^*_h), etc.

Attempt has been made for theoretical calculation of α by assuming ionised impurity scattering and piezoelectric scattering below and above 310°K respectively. It was found that there was good agreement in shapes of the experimental and theoretical curves upto 300°K. However, above it the theoretical graph shows a decreasing while experimental showed continuous increase. The reason is not yet clear. However, one possibility may be that m^*_h is also temperature dependent though our assumption has been quite opposite.

If m^*_h has also been evaluated from the experimental value of α at different temperatures by using the relation 31a where most of the other factors are known. It can be seen that m^*_h showed an increase with the rise of temperature, suggesting that the temperature behaviour of m^*_h. Whether the above calculation is justified is still a matter of conjecture.

CHAPTER-IV

REFERENCES

Aliev, T.A. et al (1971), Fiz. Tekh. Poluprov., 5(2), 325.

Barua, D.C. and Barua, K. (1974), Indian J. Phys., 48(4), 332.

Black, J. Et al (1958), J. Electrochem. Soc., 105, 723.

Deokar, V.D. and Goswami, A. (1970), Indian J. Pure and Appl. Phys., 8, 93.

Dziuba, E.Z. (1974), Phys. Stat. Solidi, B, 62(1), 307.

Elpat'evskaya, O.D. (1958), Zhur. Tekh. Fiz., 28, 2669.

Elpat'evskaya, O.D. and Regel, A.R. (1956), Zhur. Tekh. Fiz., 26, 2432.

Giriat et al (1964), Brit. J. Appl. Phys., 15, 151.

Goswami, A. and Barua, K.C. (1970), Jap. J. Appl. Phys., 9, 705.

Goswami, A. and Ojha, S.M. (1975), Indian J. Phys., 49, 847.

Harman, T.C. et al (1958), J. Phys. Chem. Solids, 7, 228.

Harman, T.C. et al (1967), J. Phys. Chem. Solids, 28(10), 1995.

Hoffmann, R.A. and Frankal, D.R. (1971), Phys. Rev., B, 3(b), 1825.

Ivanov, V.I. et al (1967), Fiz. Tekh. Poluprov., 1(2), 289.

Ivanov, V.I. et al (1971), Zh. Fiz. E. Abstr. No. 7E, 1054.

Ivanov, V.I. et al (1975), Fiz. Tverdogo Tela, 17(8), 2509.

Kolosov, E.E. and Sharavskii, P.V. (1965), Zh. Fiz. E. Abstr. No. 12E, 782.

Kot, M.V. and Maronchuk, Yu. E. (1963), Zh. Fiz., Abstr. No. 4E, 450.

Lambus, B.A. et al (1975), J. Phys. Chem. Solids, 36(11), 1193.

Minden, H.T. (1958), Sylvania Technologist, 11, 13.

Minn, S.S. (1960), J. Rech. Centre Natl. Rech. Sci. Lab., Bellevue, Paris, 51, 131.

Mycielskii, A. (1974), Postey Fiz., 25(1), 55.

Nishizawa, J. et al (1976), J. Phys. Chem. Solids, 37(1), 33.

Neugebauer, C.A. and Webb, M.B. (1963), J. Appl. Phys., 33, 74.

Odarich, V.A. (1973), Vkr. Fiz. Zh., 18(4), 656.

Ogrin, Yu. F. et al (1966), Zh. Eksparimi Theor. Fiz. Pisma V Redaktsiga, 3(3), 114.

Osnach, L.A. (1965), Zh. Fiz. E., Abstr. No. 11E, 577.

Okazaki, T. and Shogenji, K.C., (1975), J. Phys. Chem. Solids, 36(5), 439.

Porowski, S. and Zakrezewski, T. (1965), Phys. Stat. Solidi, 11, K-39.

Quillet, A. et al (1962), Proc. Intern. Conf. Phys. Semiconductor Exeter England, p.711.

Rodot, M. and Rodot, H. (1959), Compt. Rend., 248, 937.

Rodot, M. and Rodot, H. (1960), Compt. Rend., 250, 1447.

Rodot, M. et al (1963), Compt. Rend., 256(26), 5535.

Rode, D.L. and Willey, J.D. (1973), Phys. Status Solidi, B56(2), 699.

Sandomirskii, V.B. (1967), JETP (Solid State) Tranl., 25, 107.

Sharavskii, P.V. and Khabarova, V.A. (1964), Zh. Fiz., 3E, 454.

Wagini, H. and Reiss, B. (1966), Phys. Stat. Solidi, 15(2), 457.

Zachariasen, W.H. (1925), Nork. geol. tidssk, 8, 302,(1926) Zeits, Phys. Chem., 124, 436.

Zakrezewski, T. et al (1972), Phys. Stat. Solidi, B52(2), 665.

Zorll, U. (1954), Z. Phys., 138, 167.

CHAPTER-V

TIN TELLURIDE AND TIN SELENIDE

CHAPTER-V

TIN TELLURIDE AND TIN SELENIDE

(A) INTRODUCTION

The chalcogenide compounds of tin are found to have good electronic properties and some of them are used in devices, especially in film transistors, photoconductors, etc. Because of their sensitivitiness to temperature variation, these are also used as thermistors, in oscillators, liquid level meters, high frequency power meters and in space research.

The X-ray diffraction study of SnSe bulk was made by Palatnik and Levitin (1954) and they showed that it had an orthorhombic structure (a = 4.19 A^{o}, b = 4.46 A^{o} and c = 11.57 A^{o}) whereas SnTe and a NaCl type structure (a_o = 6.32 A^{o}) as confirmed by Hashimoto and Hirakawa (1956). Badachhape and Goswami (1964) made an electron diffraction study on chalcogenide films of tin deposited at different substrate temperatures varying from room temperature to about 300°K. They observed that these films developed different structures with the substrate temperatures. Thus SnS films had the normal orthorhombic structure (a_o = 4.33 A^{o}, b_o = 11.18 A^{o}, c_o = 3.98 A^{o}) from room temperature to about 200°C but at

higher temperatures say at $300^{o}C$, they observed a new cubic phase (a = 5.16 A^{o}) and also on some additional phase correspondant to the h.c.p. structure (a = 3.63 A^{o}, c = 6.00 A^{o}). The growth characteristics of SnTe films on substrates like rocksalt, mica at different substrate temperatures were studied by Goswami and Jog (1969). They observed that these deposits (a_o = 6.37 A^{o}) grow epitaxially with parallel orientation at high temperature $>$ $200^{o}C$ and developed different orientations depending on substrate surface. Freik (1970) observed a similar structure of SnTe deposited at higher substrate temperature (300 to $500^{o}K$).

Electrical parameters such as resistivity, Hall coefficient and thermoelectric power of bulk SnTe, in the temperature range from 100 to $1000^{o}C$ were studied by Hashimoto and Hirakawa (1956). It was found that TCR and R_H were positive and thermoelectric power was rather low (α = 26 $\mu V/^{o}K$) and it changed its sign at about $250^{o}C$. These appeared to be semimetallic. Hashimoto (1957) also studied the electrical properties of SnTe, SnSe and InBi at the low temperature region (30-$100^{o}K$) and observed that both ρ and R_H remain constant below $30^{o}K$ and increased smoothly with temperature. The variations of ρ and R_H were $2x10^{-3}$ to $9x10^{-2}$ ohm cm and $9x10^{-3}$ to $2x10^{-2}$ cm^3/C in these temperature ranges respectively. However, these values for SnSe were reaching maximum at $0^{o}K$ ($4x10^{-2}$ ohm, 20 cm^3/C).

Allgaier and Scheic (1961) also observed the similar behaviour. Sagar and Miller (1962), from the measurement of R_H, n and α in the temperature range of 4.2 to 800°K, explained the band structure of SnTe (p-type). It was found that R_H varied from 0.003 to 0.03 cm^3/C in these temperature ranges. The thermoelectric power got maximum in the temperature range between 77°K to 450°K but for pure samples α decreased with increasing temperature from 77° to 200°K with 5 ± $\mu V/^{\circ}C$. The carrier concentration varied from 3.5 to 10^{20} cm^{-3} in the above temperature range. These results could not be fitted on the basis of either a double valence band model or overlapping of valence and conduction band. Strauss et al (1963) prepared a semiconducting SnTe compound by reducing the concentration of Sn vacancies under the pressure about 15 k-bars. The compound had carrier concentration (3.6 to 7.3)$\times 10^{19}$ cm^{-3}. The variations of α and μ with 'n' were also measured. Moldovanova and others (1964) however showed the semimetallic character of SnTe which could be changed to semiconducting by purifying Te and Se and outgasing them before making the bulk compound. Galvanomagnetic properties of SnTe were studied by Allgaier (1966) and suggested that it was not a semiconductor but a degenerate semiconductor. Andrew and Regel (1967) observed the $R_H \simeq 1\times 10^{-4}$ cm^3/C and suggested that it was metallic in character rather than a semiconductor. According to him, neither the band model of free electron nor

the scheme of intrinsic semiconductor was adequate to interpret the experimental data.

Zemel and others (1965) studied the optical and electrical parameters of SnTe films in the 2-15 μ region and in the temperature range from 77°K to 300°K and also measured the optical dielectric constant and energy gap as a function of temperature and observed that the carrier mobility of bulk crystal was inversely proportional to carrier concentration while the conductivity was independent of it in the above temperature range. Mobility was found to be about 200 $cm^2/V.sec.$ for bulk. The thin layers (500 to 80000 A°) of SnTe deposited at the rate of 4 A°/sec by flash evaporation at various substrate temperatures (20–400°C) in high vacuum (10^{-6} mm of Hg) on amorphous substrate were studied for their electrical parameters such as ρ, R_H and μ in the temperature range from 77 to 400°K by Pierre (1967). He could also prepare samples with high mobilities and small carrier concentration under some special condition. Goswami and Jog (1969) measured the 'ρ' and 'α' for SnTe and SnSe vacuum deposited films in the temperature range from 25 to 300°C. They found that SnTe was metallic in character whilst SnSe films were semiconductor type. Thermoelectric power of SnTe was about 22 uv/°K and 160 uv/°K for SnSe films. These SnSe films have high resistivity. The band structure and activation

energy were explained from the spin-orbit interaction of SnTe films by Tsang and Cohen (1969). They suggested the intervalley deformation potential was due to electron phonon. Superconductivity observed in SnTe films have also been explained from the deformation potential. The transport properties of thin SnTe films on heated NaCl substrate in the temperature range from 77 to 273°K and effect of evaporation time on film properties were studied by Yusuke and Zemel (1969). It was found that the thinnest film (400 Å) had mean free path somewhat greater than the half film thickness and mobilities at room temperature and 77°K agreed with the bulk data. Optical data partially confirm the conclusion on the presence of large inhomogeneity in films. The optical and electrical properties of SnTe films deposited at 4.2 to 300°K were investigated by Brown et al (1970). They observed that resistivity dropped abruptly by 4 times or more in magnitude at 180°K and suggested that originally these films were amorphous and of superconducting. The origin of temperature dependence of conductivity and valence band level at the gap discussed in details by Tsang and Cohen (1971). E_g generally varied between 0.33 to 0.28 eV in the temperature range from 80 to 400°K on "L" point of Brillion zone.

Energy band structure of SnTe obtained by pseudo-potential calculations and analysed in terms of Jones Zone scheme by Onodera (1972) results in the band gap of 2.2 eV

on {311} zone plane. Gaiduchok et al (1972) investigated resistivity Hall constant and Seebeck effect of SnTe film ranging from 0.2 to 0.6 μ thickness evaporated in vacuo at 470-500°K on glass substrate. It was found that with increasing Te in films, ρ , R_H and α decrease simultaneously and its magnitude increased with increasing temperature at $\leqslant$ 470°K.

A change in sign of TCR and α appeared in weakly doped SnTe films prepared from SnTe or Sn and Te (stoichiometric mixtures). For undoped films as well as those films with excess of Sn, the scattering due to lattice vibrations was predominant at T $>$ 450°K. However, at low temperature the role of scattering due to defects present increased. A considerable change in R_H with temperature is in equal agreement with two band model of valence band. By measuring the absorption spectra, the optical properties of single crystals SnSe and SnS were studied by Takashi et al (1972). For p-type sample, absorption bands were found that at energy gaps at 0.5 eV and 0.7 eV for E$//$ b on C and .52 and .74 eV for E $//$ a at liquid nitrogen temperature and room temperature respectively. The effect of substrate temperature on crystal size SnTe films was studied by Gaiduchok et al (1972). The crystal size was found to increase from 40 to 1000 A^{o} with the varying substrate temperature from 300°K to 500°K. Todoroki

and others (1975) showed the Hall constant and α are dependent on carrier concentration of a p-type polycrystalline thin films. These films, however, exhibited a maximum R_H at about 450^oK and α had a maximum at a hole density ranging from $3x10^{20}$ - $5x10^{20}$ cm^{-3}. These anomalies are interpreted in terms of second valence band theory. Akyoshi (1976) studied the magnetoresistance in epitaxial p-SnTe films at 77^oK in fields upto 6000 gauss. It was found that it depends on field and 'n' and magnetoresistance was linear against square of field.

From the above survey it appears that the different workers have been reported different type of behaviour of both bulk as well as films of SnTe. Some of these results are contradictory. Therefore a detailed investigation on the electrical properties of these films was made.

(B) EXPERIMENTAL

(i) Preparation of SnTe and SnSe

The tin telluride (SnTe) was prepared by mixing Tin (99.9% pure, Johnson Mathey and Co.) and Te (spec-pure, 99.999% pure) were taken in atomic proportion (1:1) in a silica tube which was initially cleaned with nitric acid, then with distilled water and finally with distilled alcohol. The silica tube was sealed in the vacuum of the order of about

10^{-5} mm of Hg. The vacuum sealed silica tube thus was then inserted in a vertical electric furnace the temperature of the electrical furnace was raised in stages upto 500°C and kept it at about 4 hours to till the tellurium melted completely and then the temperature of the furnace was raised upto 900°C and kept the mixture at this temperature for 6 hours. The final product was slowly cooled to room temperature and bulk material was removed. In a similar way the bulk SnSe was prepared.

(ii) Preparation of films

From the bulk compound, thin films were made on precleaned glass substrate through an appropriate mask at room temperature through the conical tungsten filament in a high vacuum of an order of 3×10^{-5} mm of Hg. All the films before doing the electrical measurement were annealed at 150°C for 2 1/2 hours in the same vacuo.

Tin selenide films were made on the glass substrate at 150°C and then these were annealed at 150°C for two hours in high vacuum. Film thickness of these films was measured by the usual methods described in Chapter-II.

FIG. 5·1

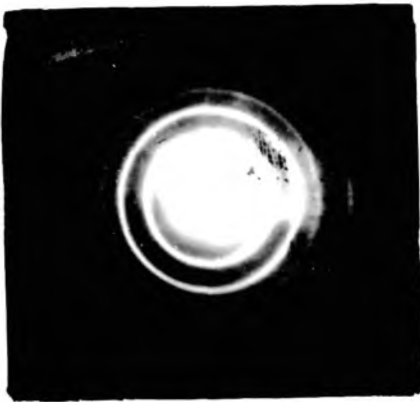

FIG. 5·2

FIG. 5·3

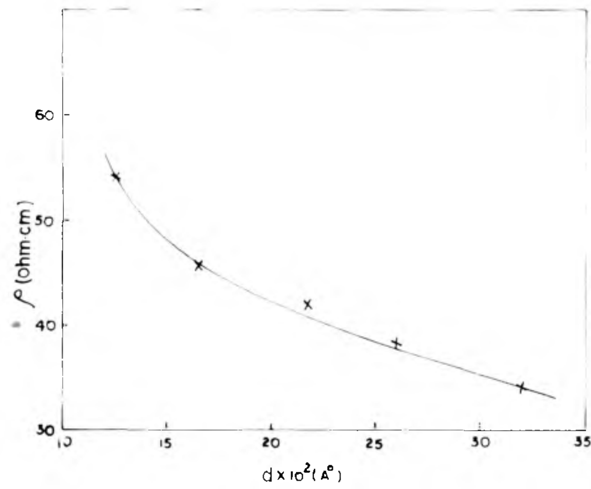

FIG. 5·4

(a) SnTe

(C) RESULTS

(i) Structure

Bulk tin telluride when investigated by X-ray powder method yielded pattern shown in Fig. 5.1. The measurement of d values of different rings suggest that the compound had NaCl type structure (Fig. 5.2) (a_0 = 6.31 A^0) as reported by Goswami and Jog (1966). An electron diffraction pattern was also taken for thin film of SnTe deposited on glass substrate at room temperature and annealed at 150^{0}C for two hours in high vacuo. This also conformed the above structure as shown in Fig. 5.3).

(ii) Resistivity

Fig. 5.4 shows the variation of resistivity with thickness for SnTe films deposited on glass. The resistivity increased continuously as the thickness decreased i.e. thinner films having higher resistivity.

Fig. 5.5 shows the temperature variation of resistivity. Resistivity was almost constant at lower temperature but increased sharply at higher temperatures thus showing a semi-metallic character for all thicknesses.

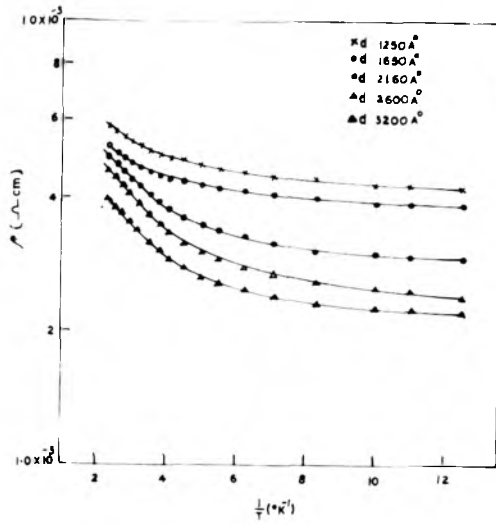

Fig 5.5

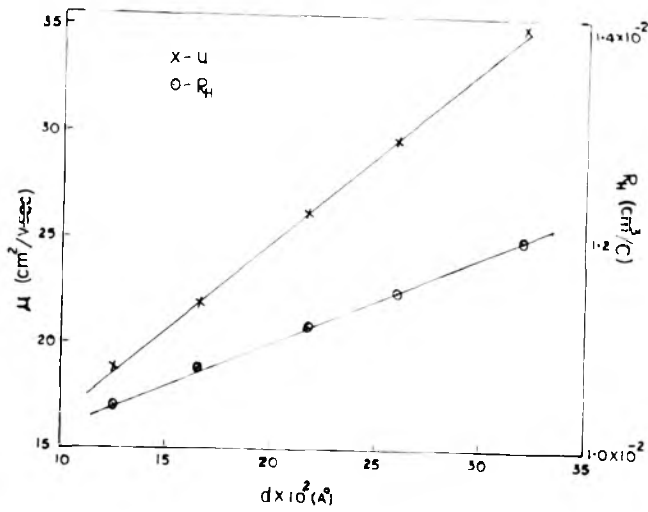

Fig 5.6

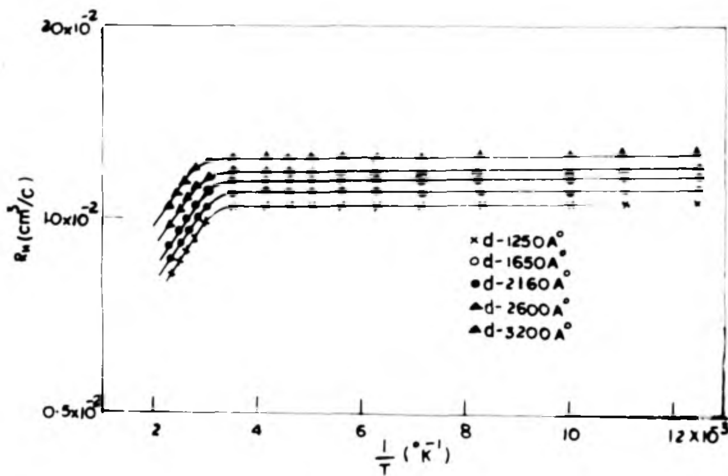

Fig 5.7

(iii) Hall coefficient and carrier concentration

R_H was found to be thickness dependent, thinner films were having lower R_H (Fig. 5.6). It may be mentioned here that R_H was independent of magnetic field (2000-8000 gauss) and current 0.5 mA to 2.5 mA both at room temperature and also at liquid nitrogen temperature. R_H like ρ was almost constant at low temperature but decreased sharply at higher temperature (Fig. 5.7). The thickness variation did not have any effect on the trend of R_H vs 1/T curves. Hall effect measurements showed films may be p-type.

The carrier concentration though constant in the low temperature region (78 to 280°K) increased with the further rise of temperature (Fig. 5.8). It may be noted that (n) at a particular temperature was also thickness dependent similar to R_H, thinner films having higher carrier concentration than thicker one.

(iv) Mobility and potential barrier height

Mobility was estimated from the relation $|R_H|\sigma = \mu$ It increased with increasing film thickness (Fig. 5.6) as also observed for other materials.

Fig. 5.9 showed the variation of mobility with temperature. It increased with decreasing temperature. This

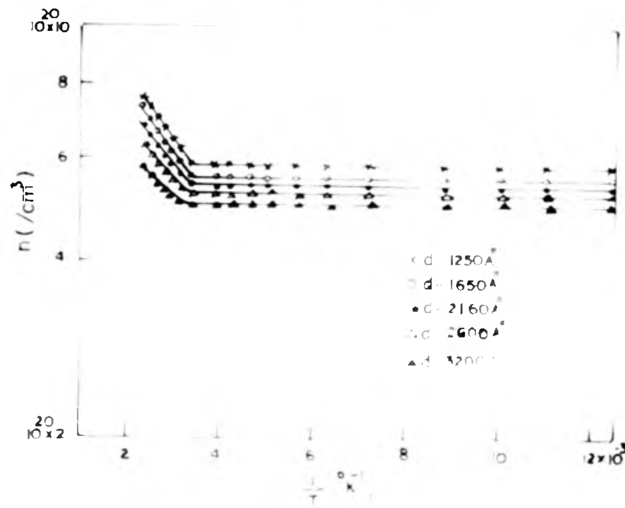

Fig. 5.8

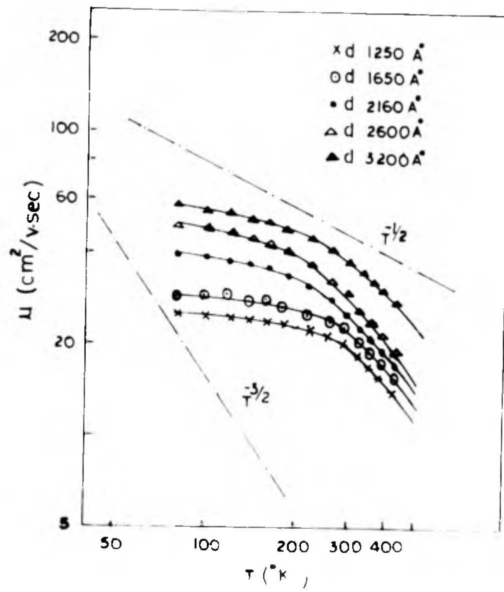

Fig. 5.9

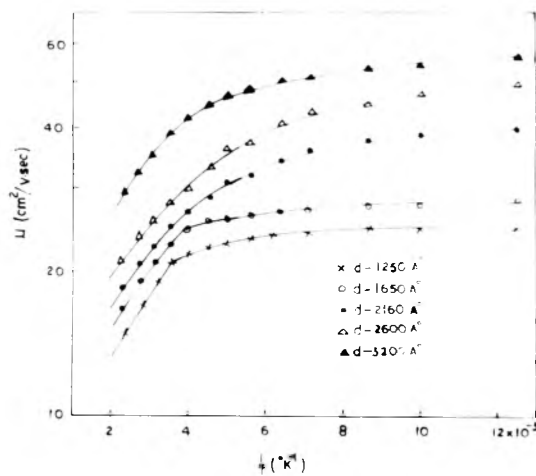

Fig. 5.10

shows that at the higher temperature region (300–400°K it followed $\mu \alpha T^{-3/2}$ law but in lower temperature region (78 to 300°K) $\mu \alpha T^{-x}$ (x = 0.2 to 0.5) depended on the film thickness.

Potential barrier height (Ø) estimated from the slope of log μ vs 1/T as shown in Fig. 5.10. It was found to be thickness dependent and varied from 0.06 eV to 0.04 eV for thinner to thicker films.

Table 5.1 shows the variation of R_H, ρ, μ and n with film thickness for SnTe films.

(v) Thermoelectric power (α)

Thermoelectric power was measured by differential method in the temperature range from 78° to 400°K. Fig. 5.11 showed the variation of α with temperature. It increases with increasing temperature and also thicker films have higher magnitude of thermoelectric power.

(vi) Fermi energy level (ΔE_F)

The resistance of all films increases with increasing temperature i.e. these are semi-metallic in character. So Fermi energy level evaluated from the observed thermoelectric power by using the semi-metallic relation between Fermi energy and α.

TABLE-5.1

SnTe

T_s = room temperature

S.No.	Thickness d(A°)	$R_H \times 10^{-2}$ cm^3/c	$\rho \times 10^{-4}$ ohm.cm.	μ $cm^2/V.sec.$	$n \times 10^{20}$ cm^{-3}
1.	1250	1.035	53.50	18.8	5.81
2.	1650	1.082	45.70	24.6	5.65
3.	2360	1.121	42.30	26.7	5.58
4.	2600	1.150	39.00	29.6	5.43
5.	3200	1.195	34.00	35.2	5.24

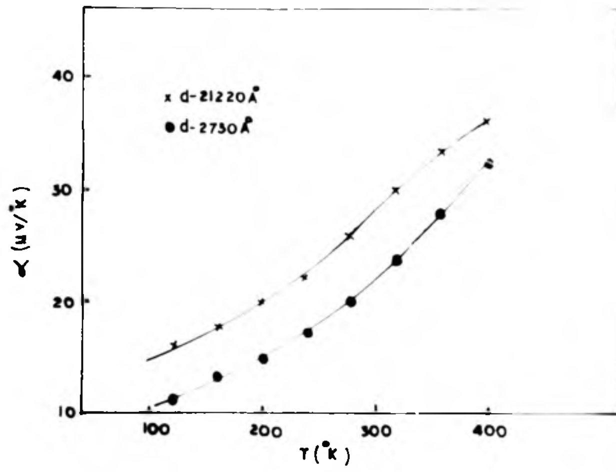

Fig. 5.11

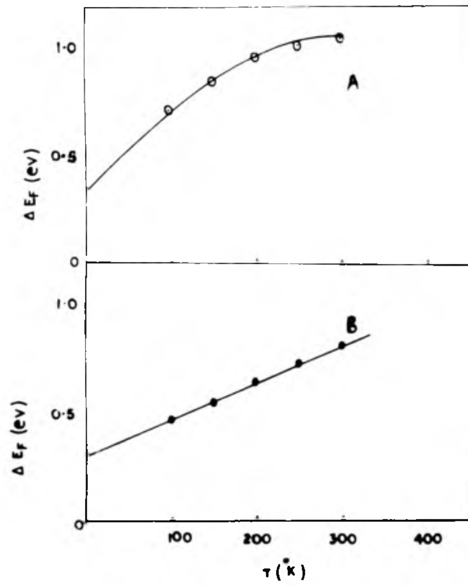

Fig. 5.12

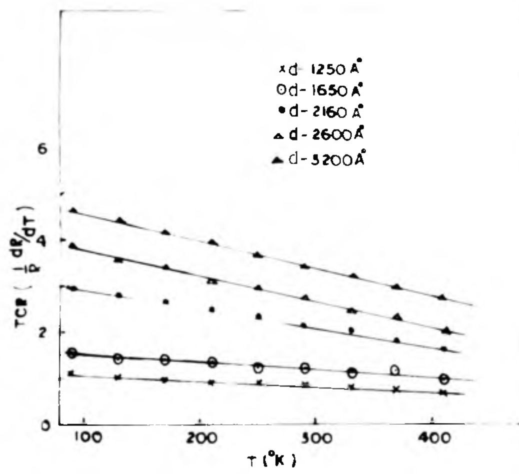

Fig. 5.13

$$\alpha_p = \frac{\pi^2 K^2 T}{eE_F} \quad .. \quad (1)$$

It was found that it increases with increasing temperature as shown in Fig. 5.12. But according to variation of carrier concentration with temperature especially at low temperature region (78 to 300°K) it suggests degenerate type semiconductor. Fermi energy also calculated from α by using degenerate semiconductor formula

$$\alpha_p = \frac{\pi^2 K}{e} \left(\frac{kT}{E_F}\right)\left(\frac{1}{2} - \frac{1}{3} S\right) \quad .. \quad (2)$$

$\tau = aE^{-S}$, here $S = -\frac{1}{2}$ for the temperature range from 78 to 300°K. It was also found that ΔE_F increases with increasing temperature as shown in Fig. 5.12.

(vii) TCR

It is positive throughout the temperature range. It increases with decreasing temperature. Fig. 5.13 shows the variation of TCR with temperature. Thinner films are having higher TCR.

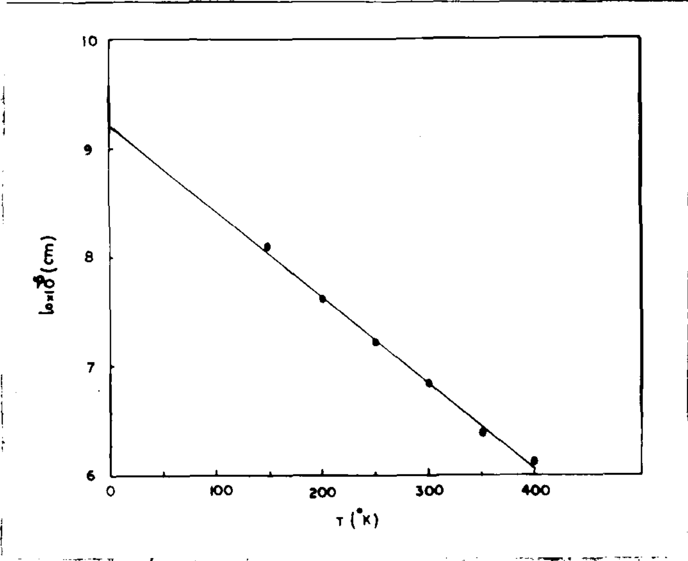

FIG. 5.14

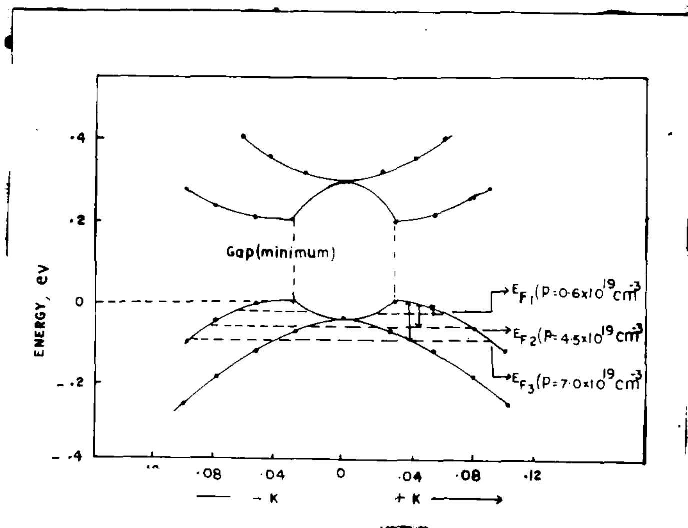

FIG. 5.15

Fig 5·16

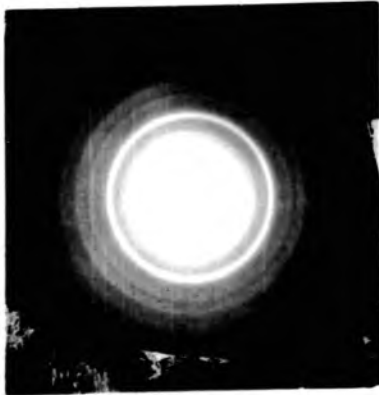

Fig 5·17

Fig 5·18

(viii) Mean free path

It was estimated by usual method, was found to decrease with increasing temperature and its variation with temperature is shown in Fig. 5.14. The value of l_o at 0^oK obtained by extrapolating was about 9.2×10^{-5} cms.

(b) SnSe

(C) RESULTS

(i) Structure

The X-ray powder pattern (Fig. 5.16) of the compound showed that all the reflections were due to SnSe only (Fig. 5.17). The electron diffraction pattern for SnSe films, on glass at 150^oC and then annealed at same temperature.

It is clear from the analysis of the X-ray and electron diffraction patterns that in both the cases the compound is only SnSe orthorhombic (a_o= 4.19, b_o = 4.46 A^o and c_o = 11.57 A^o).

Electron diffraction patterns on glass at higher substrate temperature yielded patterns (Fig. 5.18) showing characteristic of one degree orientation of SnSe deposits crystals.

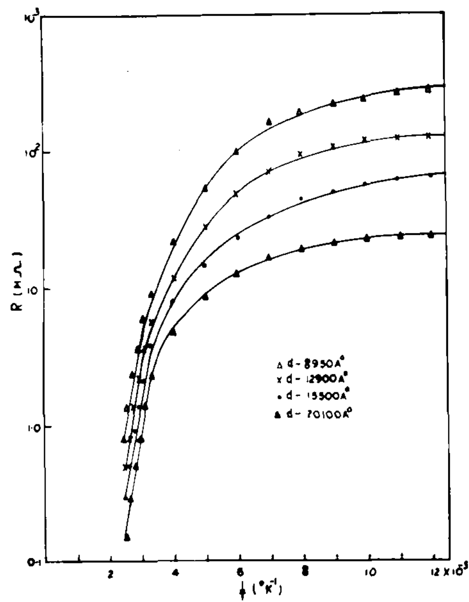

FIG. 5.19

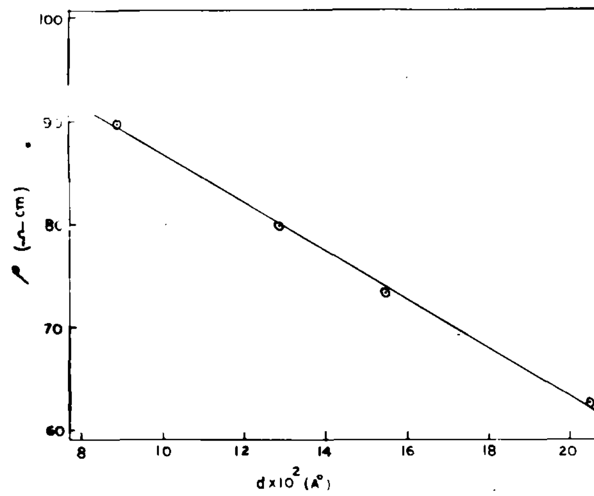

FIG. 5.20

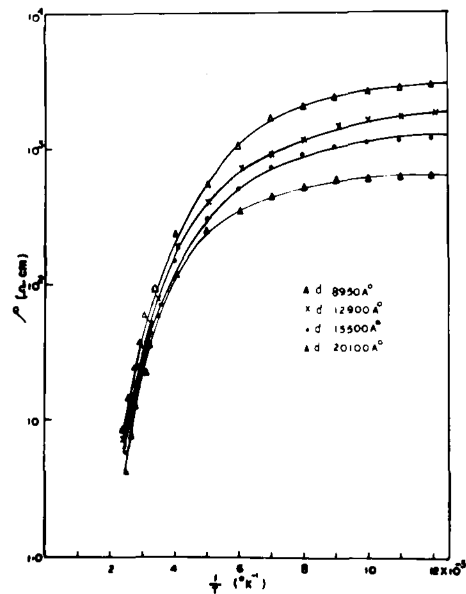

FIG. 5.21

(ii) Resistance, resistivity and activation energy

Fig. 5.19 showed the variation of R with temperature. It seems that in the lower temperature region the change in R with T is very low as compared with higher temperature. It decreases with increasing temperature i.e. all films are semiconducting in nature. Fig. 5.20 shows the variation of with thickness (d), lower thickness having higher resistivity.

Activation energy

The activation energy estimated from the linear variation log ρ vs 1/T. It is also thickness dependent. Thinner films are having slightly higher ΔE. Table 5.2 shows the variation of ΔE with different temperatures and film thickness.

(iii) Thermoelectric power

Thermoelectric power measured by differential method. Its variation with temperature as shown Fig. 5.21. It also increased with temperature and was found to be thickness dependent. The thicker films are having higher value of α. These measurements showed that all the films were p-type semiconductors.

TABLE-5.2

T_s = 150 $^{\circ}$C

SnSe

Variation of 'ΔE' with 'd'

S.No.	Thickness d(A$^{\circ}$)	Temp. range (400 to 300°K) ΔE (eV)	Temp. range (250-150°K) ΔE (eV)	Temp. range (120-80°K) ΔE (eV)
1.	8950	0.570	0.100	0.010
2.	12900	0.550	0.088	0.007
3.	15500	0.535	0.077	0.006
4.	20100	0.520	0.068	0.005

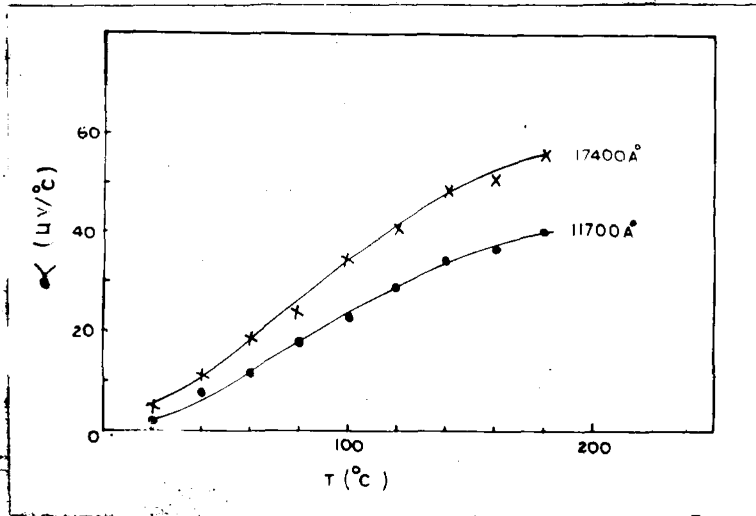

FIG. 5·22

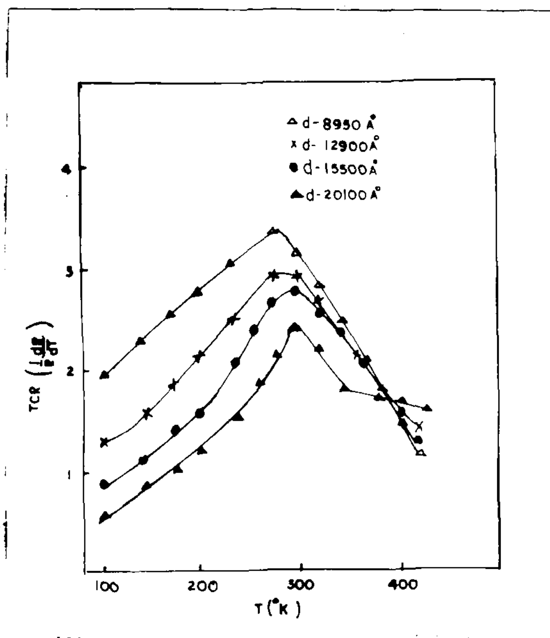

FIG. 5·23

(iv) $TCR = \frac{1}{R} \frac{dR}{dT}$

Fig. 5.22 shows the variation of TCR with temperature. TCR is negative for all films. It is increasing with increasing temperature upto $300^{o}K$ and then decreased with further increase of temperature. It was also found to be thickness dependent. Thinner films are having higher values of TCR.

(D) DISCUSSION

The electrical parameters of the vacuum deposited SnTe films were studied in details and these were found to be similar to those of the bulk. The resistance of these films increased with increasing temperature i.e. TCR was positive thus suggesting the semimetallic nature of them as observed by Hashimoto and Hirakawa (1956) for bulk and Goswami and Jog (1969) for thin films. The magnitude of 'ρ' was found to be of the order of 10^{-4} ohm cm which is also close to the bulk values reported by several investigators (Hashimoto, 1957; Allgaier and Scheic, 1961).

These films were p-type as found in our investigation thus suggesting an acceptor type of charge carriers possibly associated with defects, imperfection grain boundaries and other types of defects invariably present in thin films. The

Hall constant (R_H = $1x10^{-2}$ to $1.2x10^{-2}$ cm^3/c) and carrier concentration (n = 5.8 to $5.3x10^{20}$ cm^{-3}) at room temperature did not significantly even with film thickness (d = 1250 A^o to 3200 A^o). The little variation of R_H with film thickness may partly be attributed to a better ordering and crystallinity of the thickness etc. The observed R_H was found to be slightly higher than the values (10^{-3} cm^3/C) reported by Sagar and Millar (1962). R_H decreased with increasing temperature in the temperature range (300 to 400^oK) as generally observed for semiconducting films but in the lower temperature region (78 to 300^oK) it remained practically constant attaining saturation unlike other semiconducting films which now show general tendency to increase without attaining any saturation. The low magnitude of R_H and n and its temperature independence behaviour in the low temperature region along with very high concentration of carriers (n = $10^{20}/cm^3$) suggest the degeneracy state beading to form degenerated semiconductors or semimetals. Since the characteristic of other parameters with temperature or film thickness were similar to semimetal like HgSe films (Goswami and Ojha, 1975). It appears that SnTe in film state is also of the same type rather than semiconducting. It is interesting to note that even for the bulk SnTe, Allgaier (1966) also found similar semimetallic behaviour.

The mobility variation with temperature (Fig. 5.9) of

these films is rather typical as compared to the other chalcogenides films studied so far, i.e. it increased with the decreasing temperature. The mobility followed the $\mu \alpha T^{-3/2}$ relation in the higher temperature region (300 to 400°K). Gaidushok (1972) observed the same nature above 450°K. However, in the lower temperature region the SnTe film followed the $\mu \alpha T^{-X}$ law where X = 0.2 to 0.5 depending on film thickness. Even though X slightly varies with film thickness, it can be said that piezoelectric scattering was more predominent at least for thicker films at lower temperature region. However, at higher temperatures all films followed -3/2 law thus suggesting the predominance of lattice scattering.

The variation of thermoelectric power with temperature (Fig. 5.11) shows the general increase of α following a relation similar to that of semiconducting material as mentioned in case of HgTe and MnTe. Since these films are not semiconducting in nature, the relation (31a) cannot be used for a theoretical calculation of α. Both these equations involve the estimation of E_F for which no data are as yet available. Consequently, it is not possible to compare the shape of α-T graphs without that of theoretically evaluated one. On the other hand, assuming the validity of the above equations even for films it is possible to estimate E_F from the experimental α. The variation of E_F thus evaluated

assuming both metallic and degenerate nature with temperature is shown in Fig. 5.12. Though the graphs are similar in nature, the magnitudes of α differ significantly in the two cases. It is not, however, easy to determine unambiguously its exact nature, except that the films were more likely to be semi-metallic since resistivity etc. lend support ot it. The mean free path (l_0) for SnTe films observed was of the order of 10^{-5} cm. Similar value has also been reported for bulk by Yusuke and Zemel (1969).

The above consideration, however, suggests that the vacuum deposited SnTe films, were semi-metallic in nature. This property has to be considered from the band structure of SnTe. As yet not much work has been carried out on the energy band model of bulk SnTe crystal. According to recent work Tsang et al (1971) the band studies of SnTe seem quite complex but a simplified picture as envisaged by them is shown in Fig. 5.15. The above diagram however is presumed to be valid for 0^oK and E_F changed with carrier concentration. However, with the increase of temperature the band shape may slightly change. Presuming the similarity of band structure we can consider the effect of film thickness rather than carrier concentration on it.

According to Tsung and others, these sub-bands are present in both the valence and the conduction bands. Since

the bulk SnTe are also p-type and shows the semi-metallic behaviour, it is presumed that the carrier must be situated in the valence sub-bands which determined the Fermi energy level. According to this, hole mass may vary depending on the situation in the valence band thus giving rise to light holes with small effective mass and heavy holes with higher ones.

Assuming metallic (semi-metallic behaviour) and also of similar band structure for SnTe films it will be seen that E_F position will depend upon charge carrier concentration. From Fig. 5.10 it seems that α is lower for thinner films. This means that the calculated E_F will be larger for thin films than thicker films. Hence E_F position for thinner films will be at higher level than that of thicker ones.

The vacuum deposited tin-selenide (SnSe) films had very high resistance (MΩ). So Hall voltage could not be measured by D.C. method and hence the mobility and the type of scattering mechanism could not at all be evaluated. Similar to bulk material, these films are also semiconducting in nature. It is seen from the variation of log R vs 1/T the change of R with temperature is small in the lower temperature region but as the temperature increases the fall of R with temperature is rapid. This may be due to the most of the carriers in the lower temperature region were frozen out at the centres

containing large number of impurities. The rapid fall of R in the higher temperature range (300 to 400°K) indicated that all the films became intrinsic in character. The variation of activation energies for different temperature regions of SnSe films is shown in table-5.2. From this we conclude that the degree of ionisation of the charged carriers increases as the temperature increases from 78 to 400°K. The magnitude of thermoelectric power observed in case of film was slightly lower than the bulk. This may be due to the films were having large number of impurities associated at the time of deposition.

CHAPTER-V

REFERENCES

Akyoshi, N. (1976), J. Appl. Soc. Japan, 38(4), 1276.

Allgaier, R.S. and Scheic, P.O. (1961), Bull. Amer., 6, 636.

Allgaier, R.S. (1966), Phys. Rev., 152(2), 808.

Andrev, A.A. and Regel, A.R. (1967), Fiz. Tekh. Poluprov. 1(12), 1832.

Badachhape, S.B. and Goswami, A. (1964), Indian J. Pure and Appl. Phys., 2, 250.

Brown, R.W. et al (1970), Thin Solid Films, 5(3), 157.

Freik, D.M. et al (1971), Kristallografiya, 16(2), 459.

Goswami, A. and Jog, R.H. (1969), Indian J. Pure and Appl. Phys., 7(4), 273.

Goswami, A. and Jog, R.H. (1969), Indian J. Physics, 43(10), 563.

Goswami, A. and Ojha, S.M. (1975), Indian J. Pure and Appl. Phys., 13, 721.

Gaiduchok, G.M. et al (1972), Izv. Vyssh. Vcheb Zeved Fiz., 15(6), 137.

Hashimoto, K. (1957), J. Phys. Soc. Japan, 12, 1423.

Hashimoto, K. and Hirakawa, K. (1956), J. Phys. Soc. Japan, 11, 716.

Moldovanova, M. et al (1964), Soviet Phys-Solid State, 6(12), 2979.

Onodera, Y. (1972), Solid State Commun., 11(10), 1397.

Palatnik, L.S. and Levitin, V.V. (1954), Doklady Akad. Nauk. SSSR, 96, 975.

Pierre, B. (1967), C.R. Acad. Sci. Paris Ser. AB265 B(15), 819.

Sagar, A. and Miller, R.C. (1962), Proc. Inter. Conf. Phys. Semiconductor, 653.

Strauss, A.J. et al (1963), Appl. Phys. Letters, 4(5), 931

Tsang, Y.W. and Cohen, M.L. (1971), Phys. Rev. B(3), 3(4) 1254. Phys. Rev. (1969), 180(3) 823.

Takashi et al (1972), Sci. Light, 12(3), 132.

Todoroki et al (1975), Shinka, 17(2), 438.

Yusukeota and Zemel, J.M. (1969), J. Vac. Sci. Technol., 6(4), 558.

Zemel, N.J. and Jensen, D.J. (1965), Phys. Rev., 140(A), 330.

CHAPTER-VI

LEAD TELLURIDE AND LEAD SELENIDE

CHAPTER-VI

LEAD TELLURIDE AND LEAD SELENIDE

(A) INTRODUCTION

Among the various IV-VI compounds lead chalcogenides have been subjected to intense investigations since these show interesting properties with regard to photoelectric, photoconducting, thermoelectric, optical and semiconducting behaviour. These have high thermal e.m.f., good rectification and also transistor action, and are also used as thermoelectric generators in electro-optical devices like multicolour sensors, solar absorber, etc.

The structural properties of lead-chalcogenides have been studied by several workers both by electron as well as X-ray diffraction techniques. Makino (1964) studied the electron diffraction pattern of single crystal films of PbTe on mica and the lattice constant was observed to be the same as that of bulk. The structure of single crystal film of PbTe on different single crystal substrates and mica was studied by Voronina and Semiletove (1964) by electron diffraction. A detailed study of the epitaxial growth of PbSe (above 150°C) on different faces of rocksalt and cleavage faces of mica has been done by Goswami and Koli (1972). It

was observed that these deposits developed parallel orienta-tions on different faces of rocksalt and also on mica often along with an h.c.p. phase corresponding to the cubic phase.

A number of workers have published data on the measure-ment of galvanomagnetic properties of lead chalcogenides in bulk forms. Detailed studies on the electrical properties were made by Eisenmann (1940), Hinterberger (1942). They also showed that these materials could exist in either n-type or p-type form and one form could be changed to the other by a suitable treatment of the material. Deyatkova (1952) from the measurements of conductivity and Hall effect of PbSe in the temperature range from 20 to 550°C reported that instead of mobility following $\mu \propto AT^{-3/2}$, it followed $\mu \propto AT^{-3}$ Various electrical parameters of single crystals of PbS, PbTe, PbSe were studied in detail by Putley (1952). He found that conductivity of single crystals was higher than that of polycrystalline by a factor of 5 to 100. Matsushita et al (1953) measured the thermoelectric power of PbSe with the variation of Se and observed the α was positive and at lower temperature and turned negative at higher temperature say upto 600°C. The reported value of α was 10^{-6} V/deg and 3.10^{-4} V/deg. at low temperature and at room temperature respectively. A similar study was carried out by Gauss and Hirahara (1953)

who reported that either impurity scattering mechanism ($\mu \alpha\ T^{3/2}$) or lattice vibration mechanism ($\mu \alpha\ T^{-3/2}$) was predominant. Scanlon (1953) observed a change in the carrier concentration from $4x10^{17}$ to $7x10^{18}/cm^3$ due to thermal cycling from room temperature to 1000^oC. Silverman and Levinstein (1954) showed that mobility of PbTe and PbSe were 1000 and 850 cm^2/v.sec. respectively and followed $\mu \alpha\ T^{-5/2}$ relation. Hirahara and Murchani (1952), on the other hand, observed that mobilities of PbSe (n and p-type) varied from 2.2 to 4.60 cm^2/v.sec. and 1.6 to 1150 cm^2/v.sec. for the temperature range between room temperature to 123^oC respectively and suggested that two types of scattering (lattice and impurity) and also temperature dependence of Fermi energy. Tsilkovski (1955) observed that the mobility followed $\mu \alpha\ T^{-2.4}$ to $\alpha\ T^{-2.6}$ at room temperature to higher temperatures.

The lead chalcogenides had the highest mobilities (140000 cm^2/v.sec. for PbS (n-type) 101000 cm^2/v.sec. for PbSe (n-type) and 228000 cm^2/v.sec. for PbTe (p-type) was first reported by Putley (1955) and he also observed that in the temperature region between 110^oK to 1000^oK these compounds followed $\mu \alpha\ T^{-5/2}$ relation. He also determined the effective masses of holes and electrons from thermoelectric measurements. The effective electron mass (m^*_e) and hole mass (m^*_h) were in the range of 0.25 m_o and 0.36 m_o at 300^oK

whereas Petritz and Scanlon (1955) estimated m^*_e and m^*_h 0.33 for PbTe from the mobility data. Smirnov (1960) from the measurement of α for PbSe in the temperature 100 to 400°K determined the effective mass and showed that it was independent of carrier concentration. Lyden (1962), however, reported that the effective mass was highly dependent on temperature (0.052 at 4°K, 0.105 at 300°K and observed optical and accoustic modes of scattering in PbTe. The thermoelectric power at 450°C for PbTe and PbSe was found to be nil. by Kolomiets and others (1957). They also made some theoretical calculations of α and μ below the temperature range 200°K and found that both depended on the carrier concentration. Mobility followed $\mu \propto T^{-3}$ for PbTe and $\mu \propto T^{-3/2}$ for PbSe. Jones (1960) measured the R_H and σ at the H_e temperature and found that R_H was constant below 100°K and 'n' varied between 3 to $15 \times 10^{16}/cm^3$. Thermal and galvanomagnetic properties of PbSe with different concentrations of impurities (electrons or holes) was measured by Smirnov (1961) and reported α = 420 uv/°K at 400°K. He also observed a change in the effective masses with temperature and suggested that accoustic mode of scattering mechanism was dominant. Stavitskya et al (1966) from the measurement of α, σ and R_H (in the magnetic field 10 K.G.) and in the temperature range from 300 to 950°K, showed that mobility followed $\mu \propto T^{-3.5}$ and $m^* \propto T^{.6 \text{ to } .8}$. Optical and thermal energy gaps in PbTe was

estimated by Tauber and others (1966) and reported 0.36 eV and .19 eV respectively in the intrinsic temperature range between 500°K to 900°K. The non parabolic shape of the conduction band was explained by Zhitriskya (1966). A second band theory of lead chalcogenides was explained by Chernik (1968). Activation energy and carrier concentration were found to be .33 eV and 10^{20} cm^{-3} respectively. Dubrovskya (1970) obtained the (n) variation as $8x10^{19}$, $2x10^{19}$, $6x10^{19} cm^{-3}$ for PbTe PbSe and PbS respectively and also he found that (n) $\alpha\ a_o^2$ (Static dielectric constant). Ravich (1970) observed that thermoelectric and thermomagnetic effects were influenced by collision between carriers. Budzhak et al (1974) concluded that acoustic phonon scattering mechanism was predominant at high temperature. Bauer (1976) from different electrical parameters concluded the existence of deep impurity levels in the band structure.

Even though exhaustive investigations have been made on bulk compounds, comparatively little work has been done on the vacuum deposition of films. Some of the reported results are summarised below. Chasmar and Putley (1951) studied the photoconducting layers of PbS and PbTe and reported that $\frac{u_e}{u_h} = 4$ and $\Delta E = 0.62$ eV. The effect of O_2 pressure on the photoelectric and electric properties of PbS group were

studied by Kolomiel and Lanichev (1958). Both optical and electrical parameters of these films at various temperatures were studied by Smith (1951). Optical and activation energy estimated were 1.4, 1.05 and 0.9 eV and .4, .62 eV for PbS, PbSe, PbTe respectively. However, thermal activation energy was found to be 0.37 eV, .26 eV and .29 eV for PbS, PbSe and PbTe respectively by Scanlon (1958). Effective electron masses estimated were 0.20 m_o, 0.12 m_o and 0.1 m_o respectively. Gobrecht et al (1965) found that polycrystalline films of PbSe exhibited a T^X law (X = 1.5 to 2.0) variation for the hole mobility. But the hole mobility in epitaxial films followed a T^{-X} variation of higher temperature and approached saturation at low temperatures. This behaviour was interpreted in terms of scattering by dislocations rather than point defects. Zemel (1965) showed the dependence of magnetic resistance on magnetic field strengthen. Deokar and Goswami (1966) observed a significant increase of Hall constant with the increase of substrate temperature and film thickness for PbTe films. From the resistivity measurements, the activation energy was estimated and found that its dependence on the film thickness. Similar results were also reported by Goswami and Koli (1966). Spinulesch and others (1968) found the resistivity and activation energy of film varied from 1.5 to 2 Ω cm and 0.345 eV to 0.630 eV for the temperature range from 290° to 550°K for p-type PbTe formed at room temperature. The films

formed at higher substrate temperatures say 250 to 350°C were found to be n-type and their mobility was about 20 $cm^2/v.sec$. Watanabe (1971) reported the activation energy to be about 1.35 eV and the conductivity of the PbTe films being influenced by oxygen. The electrical properties as a function of temperature and strain were studied by Todoroki and others (1975) for PbTe films. It was found that transition from n to p-type occurred at the substrate temperature at about 270°K.

It can easily be seen from the above survey that though a lot of work has been carried out on bulk lead chalcogenide only a little investigation has been made on thin films especially on the scattering mechanism. Further there is lot of discrepancy between results of different workers. The present work has been undertaken with a view to carry out a systematic study of the semiconducting properties on vacuum deposited films of these compounds especially about the scattering mechanisms.

(B) EXPERIMENTAL

(i) Preparation of lead telluride

Bulk lead telluride was prepared by melting the two consistent elements in atomic proportion (1:1) in a silica tube

The lead used (99.99% pure, Johnson Mathey and Co.) and tellurium (specpure 99.999%) was used. Then the tube was evacuated till the vacuum was of the order of $\simeq 10^{-5}$ mm of Hg and then sealed. It was then heated to about 450°C in an electric furnace for two hours and then temperature was raised to 600°C and kept at this temperature for about 2 hours. When the furnace attained a temperature of about 1150°C and the sample was kept at this temperature for six hours. After the completion of reaction of lead and telluride the temperature of the furnace was lowered slowly to 600°C and the tube was quenched in cold water. The final product was then used as bulk material.

Lead selenide

Lead selenide was prepared by melting lead (99.99% pure) and Se (spec. pure) in 1:1 proportion in a similar way as that of lead telluride.

(ii) Preparation of films

The thin films of lead telluride were prepared on glass substrate at room temperature by using appropriate mask, through a conical silica boat which was covered by tungsten filaments in high vacuum (10^{-5} torr). All the films were annealed at 200°C for two hours in the same vacuum. All the

Fig 6·1

Fig. 6·2

Fig 6·3

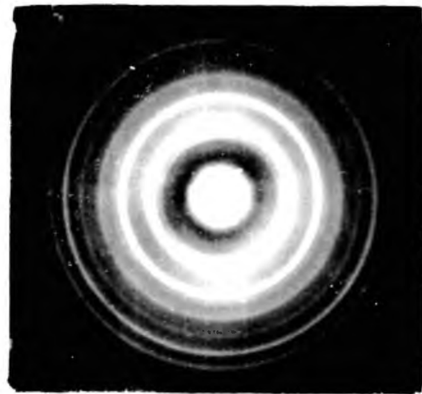

Fig 6·4

films before going to measurements of electrical parameter were stabilised by thermal cycling of heating and cooling cycles from room temperature to 120°C in vacuo (10^{-3} mm of Hg).

Lead selenide films

These films were prepared on glass substrate at room temperature similar to PbTe films. However, these films were annealed at 300°C for two hours in high vacuo ($3x10^{-5}$ torr). before the measurements of the electrical parameters, the films were stabilised by heating cooling from room temperature to 150°C in vacuo.

(C) RESULTS

(i) Structure

The structure of bulk lead telluride and lead selenides was studied by X-ray powder method. Both the compounds have the cubic structure (Fig. 6.1, 6.2).

An electron diffraction pattern was also studied for the PbTe and PbSe films deposited at room temperature. Both types of films had the NaCl type of structure (Fig. 6.3, 6.4) as reported by Goswami and Koli (1972).

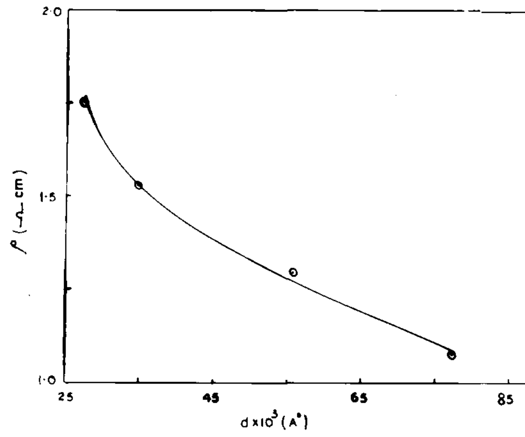

FIG. 6·5

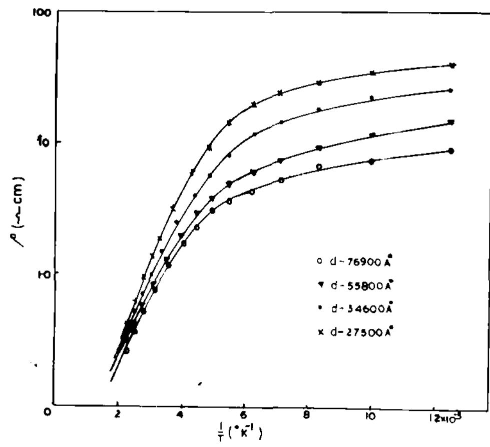

FIG. 6·6

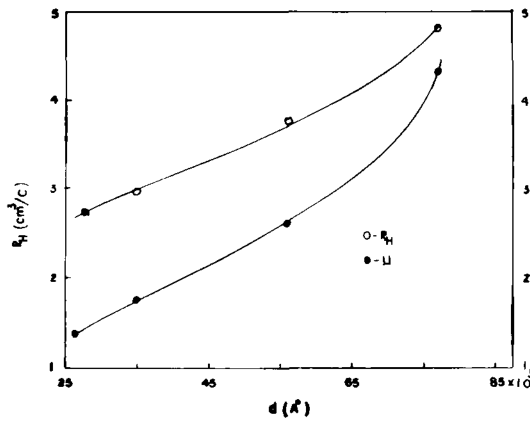

FIG. 6·7

(a) PbTe

(ii) Resistivity and activation energy

The thickness dependence of resistance and resistivity was similar to that observed for the films of other compounds investigated. The resistivity decreased with the increasing film thickness (Fig. 6.5). The variation of resistivity with temperature and thickness is shown in Fig. 6.6. It was found that it decreased with increasing temperature. Thus suggesting that all the films were semiconducting in nature. In the low temperature region (78 to 270°K) it attained more or less a constant value after which it started decreasing rapidly. It was found that these resistivities were more sensitive to temperature at the higher temperature range (300–400°C).

Activation energy was estimated from the linear portion of log ρ vs 1/T and was found to be thickness dependent. These varied from 0.25 eV to 0.35 eV for the thickness range between 27000 A^{o} to 77000 A^{o}. However, ΔE at lower temperature was very low.

(iii) Hall coefficient and carrier concentration

Hall coefficient was also found to be thickness dependent, increasing with increasing film thickness (Fig. 6.7).

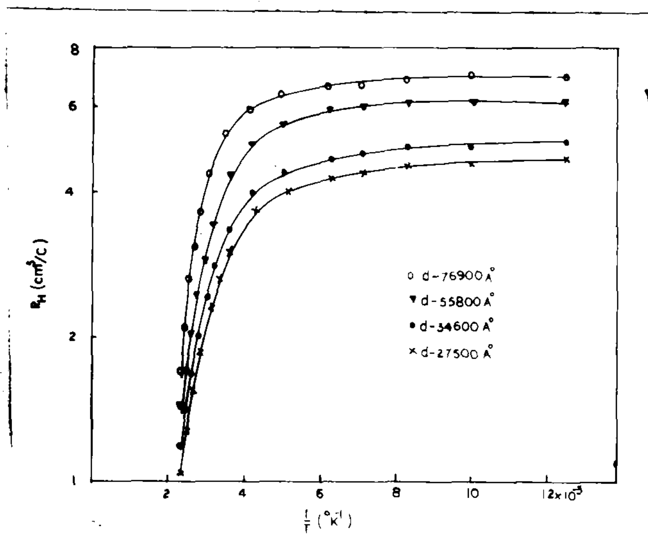

FIG. 6.8

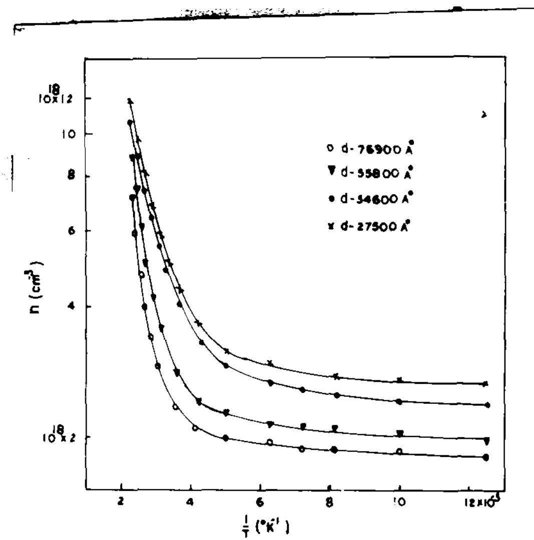

FIG. 6.9

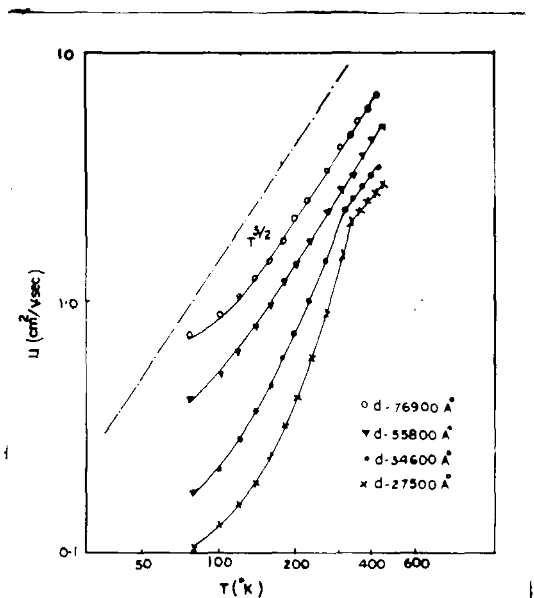

FIG. 6.10

R_H similar to that of other films previously studied was found to be independent of current (0.25 to 2.5 mA) and magnetic field 2000 to 8000 gauss. The measurements showed that these films were p-type. Hall coefficient when measured as a function of temperature (Fig. 6.8) was found to be constant in the low temperature region (78° to 300^oK) and then it decreased sharply with further rise of temperature. The activation energy estimated from linear variation of R_H vs 1/T agreed well with resistivity measurements. The carrier concentration calculated from the relation $n = \gamma/R_He$ (γ = 1.93) and its variation with temperature and thickness is shown in Fig. 6.9. It was nearly constant at low temperature range for all films and then increased with the increasing temperature. The thinner films had more carrier concentration than thickness films.

(iv) Mobility (μ) & potential barrier height (ϕ)

The mobility was calculated from the relation $\mu = |R_H| \sigma$ for different film thicknesses and its variation with thickness is shown in Fig. 6.7 . It is seen that similar to R_H it increased with increasing film thickness. It may be mentioned here that μ was rather low as compared to the bulk. Mobility variations with temperature and thickness are shown in Fig. 6.10. It increased with increasing temperature from 78° to 4000^oK. Similar trend was observed for all films. It also

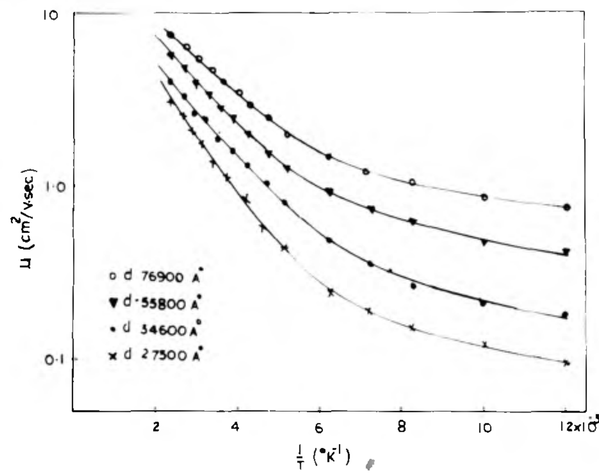

Fig 6.11

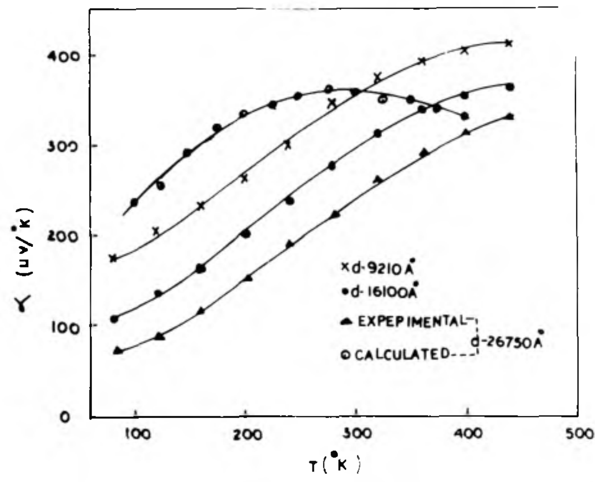

Fig 6.12

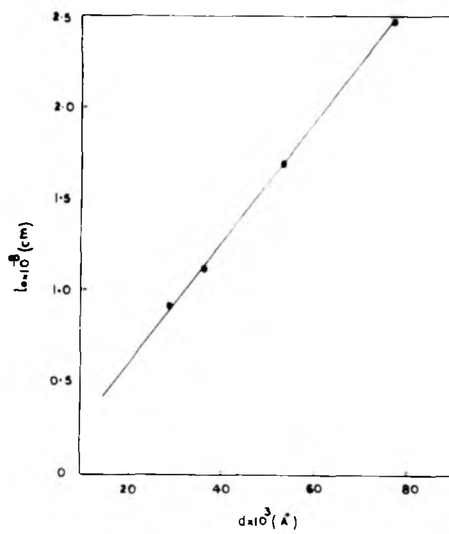

Fig 6.13

followed the relation μ α T^X where X = 1.5 to 2.2 depending on film thickness. The potential barrier height (ØY) across the grain boundaries was also calculated from Petritz relation. The variation of log μ vs 1/T is shown in Fig. 6.11 and Ø was evaluated from the slope. It varied from 0.065 eV to 0.12 eV for the thickness range.

The values of different electrical parameters of lead telluride films are shown in Table-6.1.

(v) Thermoelectric power

Thermoelectric power of different thicknesses of lead telluride films were measured by the differential method. Thermal e.m.f. measurements of all films showed that these films were p-type. Similar results were observed with the Hall effect measurements also. Fig. 6.12 shows the temperature variation of thermoelectric power. It is seen that for all the films it increases with increasing temperature but at higher temperature the rate of increasing with temperature is rather slow as compared with lower temperature. It is also interesting to see that it also depended upon film thickness. However, thinner films are having higher value of α. All three solid lines indicate the experimental variation of α with temperature. Thermoelectric power was also calculated theoretically from the relation(31a). The magnitude of A and Y

TABLE-6.1

PbTe

T_s = room temperature

S. No.	Thickness d(A^o)	R_H cm^3/c	ρ ohm. cm.	μ $cm^2/V.sec.$	$n \times 10^{18}$ cm^{-3}
1.	27500	2.75	1.75	1.57	4.40
2.	34600	2.95	1.53	1.93	4.05
3.	55800	3.94	1.35	2.98	3.03
4.	76900	4.70	1.08	4.40	2.56

are constants characteristic of the scattering mechanisms are obtained from the curve of mobility temperature variation (log-log scale) and from the Table-1.1 in the manner described for MnTe and HgTe films. Corresponding values for A = 4 and γ = 1.93 were assumed and α was calculated by assuming effective hole mass (0.33 m_o) independent of temperature. Theoretical curve is shown in Fig. 6.12. It is seen that calculated values are higher in lower temperature region (78 to 280°K) than the experimental ones but at higher temperature instead of α theoretical increasing it decreases with increase of temperature.

(vi) Mean free path (l_o)

It is also possible to calculate the mean free path from the mobility by using an expression based on Lorentz-Sommerfeld theory, viz.

$$\mu_o = \frac{l_o}{225\sqrt{2\pi m^*_h kT}} \quad cm^2/V.sec.$$

$$l_o = 3.5\,\alpha \times 10^{-10}\,\mu_o\sqrt{T}\,\sqrt{m^*_h}$$

Here we assumed the m^*_h about 0.33 m_o and to be independent of temperatures. The variation of mean free path with thickness (d) is shown in Fig. 6.13. It was found that the

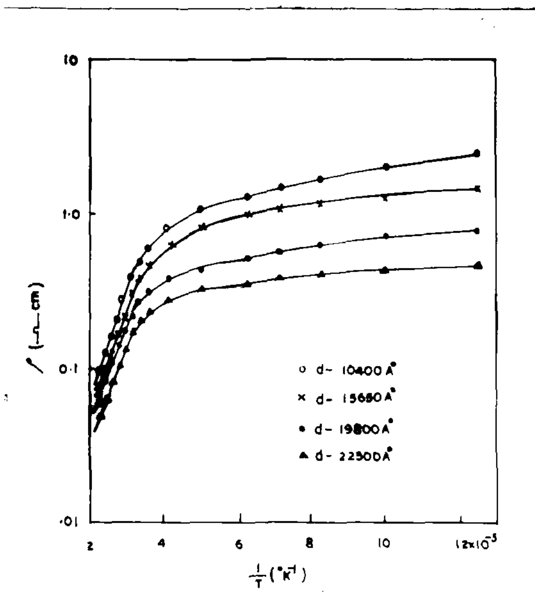

FIG. 6.14

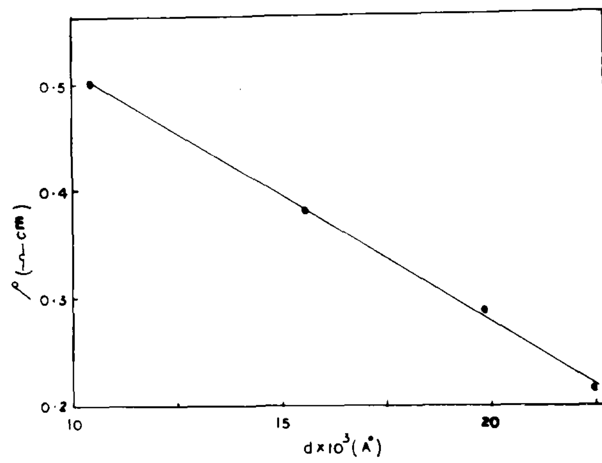

FIG. 6.15

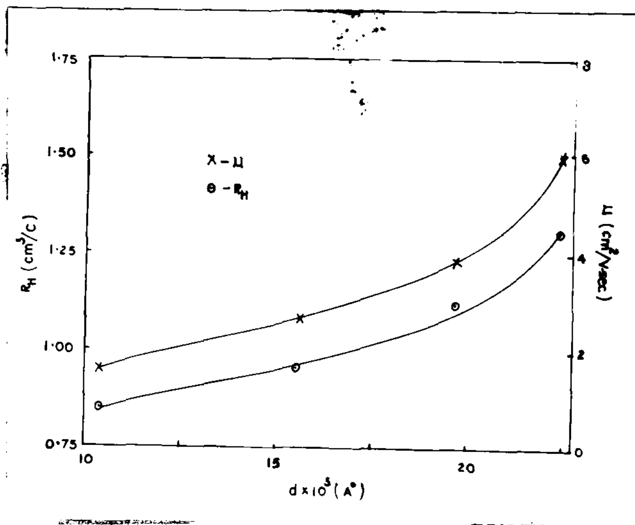

FIG. 6.16

mean free path increases with increasing film thickness and order of was about 10^{-8} cm.

(b) PbSe

(C) RESULTS

(i) Resistivity & activation energy

The temperature and thickness variation of resistivity is shown in Fig. 6.14. Resistivity decreases with increasing temperature but sharp decrease was observed between 250 to 400°K. This shows that semiconducting behaviour of the films. Fig. 6.15 shows that resistivity increased continuously as the thickness decreased. The activation energy was evaluated in the usual way and found that it varied from 0.34 eV to 0.27 eV and depend on film thickness from lower to higher film thickness.

(ii) Hall constant and carrier concentration

Hall effect measurements showed the films were p-type. R_H was independent of both current and magnetic field. However, it was found to be thickness dependent (Fig. 6.16) i.e. thinner films are having lower R_H. The variation of R_H with different temperatures is shown in Fig. 6.17. It increased with decreasing temperature. However, sharp decrease

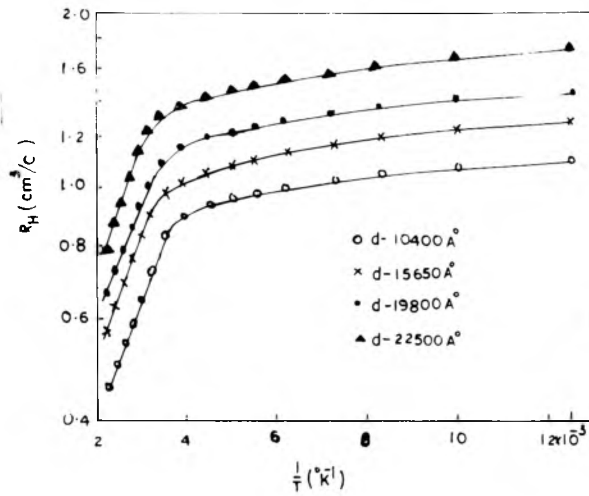

Fig. 6.17

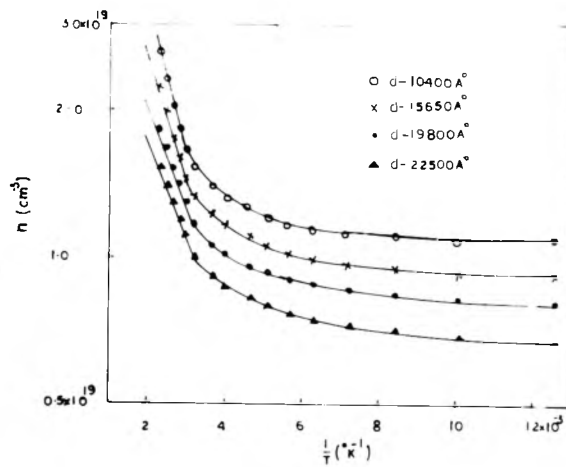

Fig 6.18

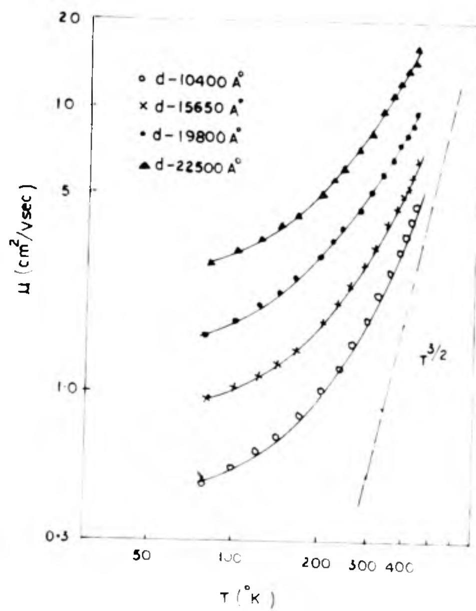

Fig 6.19

was observed in the temperature range of 280 to 400°K. Again for thinner films it remained more or less constant at the lower temperature range 78 to 280°K and then decreased i.e. thickness variation effect was observed on the trend of R_H vs 1/T curve.

However, the carrier concentration variation with temperature (Fig. 6.18) showed for thicker films it increased with decreasing temperature but for thinner films it remained constant. Like R_H similar variations at higher temperature region were observed in carrier concentration, but thinner films had higher values of (n). Activation energy calculated from the linear variation of log n vs 1/T tallied with resistivity values.

(iii) Mobility & potential barrier height

Mobility like R_H was also found to be function of film thickness (Fig. 6.14). It is interesting to see that mobility increases with increasing temperature (Fig. 6.19). The slope of the curves (log μ vs log T) was found to be approximately 1.5 for all films. Thus it follows the relation $\mu \propto T^{3/2}$. The dotted line in Fig. 6.19 shows theoretical curve for a hypothetical film obeying the above relation.

The potential barrier height (ϕ) was evaluated from the curves log μ vs 1/T (Fig. 6.20). It was found to be

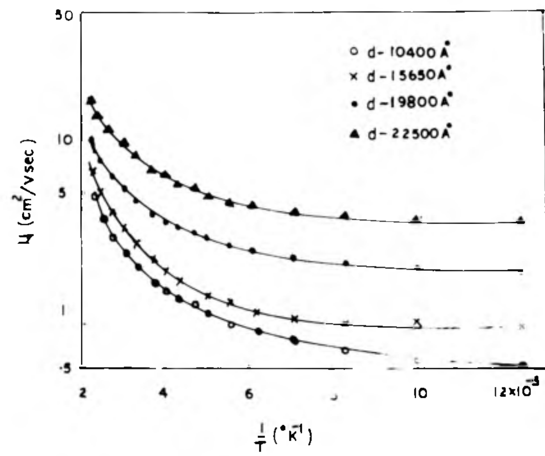

Fig 6.20

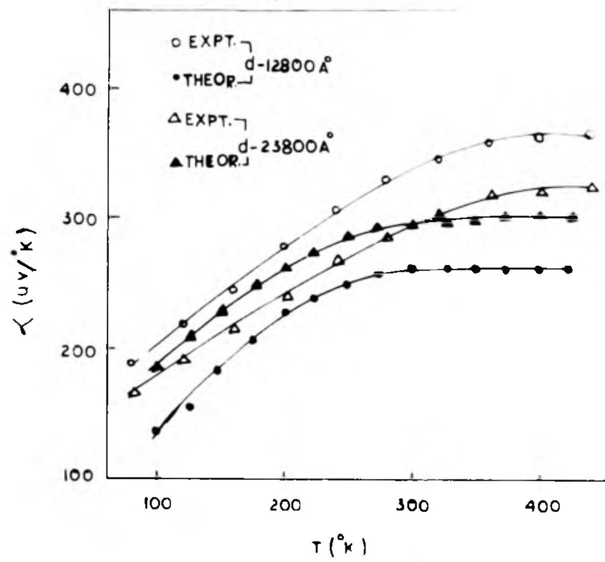

Fig 6.21

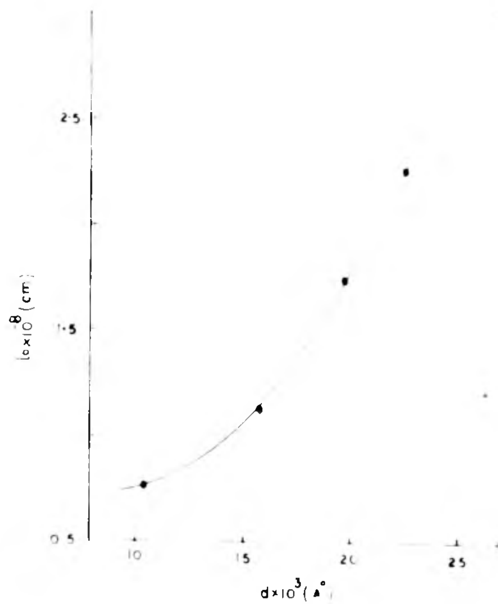

Fig 6.22

thickness dependence and varied from the 0.052 to 0.102 eV. Like other chalcogenide films thinner films are having, however, higher values of ϕ.

The values of different electrical parameters of lead selenide films are shown in Table-6.2.

(iv) Thermoelectric power

Thermal e.m.f. of these films were measured by differential method for two different film thicknesses. These measurements show that all the films are p-type. The variation of thermoelectric power with temperature is shown in Fig. 6.21. It is seen that thermoelectric power initially increased with the increasing temperature and at higher temperature it became more or less constant, the thinner films having slightly higher values of α than thicker ones. From the mobility temperature variation curve it was found that the scattering mechanism was due to impurity ions ($\mu \propto T^X$ where X varied from 1.2 to 2.2). The values of A = 4 and γ = 1.93 were chosen from the graph and table (cf 1.1). Again assumed the effective hole mass (0.36 m_o) was constant throughout the temperature range. By using the relation 31a theoretical values of α estimated as shown in Fig. 6.21. Theoretical values of α were also found to be thickness dependent but lower thickness had less α than thicker ones. However, the experimental values

TABLE-6.2

PbSe

T_s = room temperature

S.No.	Thickness d(A°)	R_H cm^3/c	ρ ohm.cm.	μ cm^2/V.sec.	nx10^{18} cm^{-3}
1.	10400	0.84	0.50	1.68	14.28
2.	15650	0.97	0.36	2.53	12.35
3.	19800	1.12	0.29	3.86	10.80
4.	22500	1.32	0.22	6.00	9.18

of α were having higher values than the theoretical values. The variation of α with temperature in the low temperature region (78 to $300^{o}K$) agreed nicely with experimental values. However, at higher temperature these values were slightly less than experimentals.

(v) Mean free path

By using the relation 39 it was estimated from mobility. Here $m^* = 0.36\ m_o$ at $300^{o}K$ was used. The variation of l_o with thickness (d) is shown in Fig. 6.22. It increases from 1 to 2.5×10^{-8} cm for the thickness range of 10,000 A^{o} to 22500 A^{o}.

(D) DISCUSSION

The above study clearly showed that both vacuum deposited films of PbTe and PbSe were p-type semiconductors. These characteristics might be due to the presence of excess of Te and Se species in PbTe and PbSe films respectively. These would create an acceptor level close to the valence band.

The dependence of different electrical parameters such as ρ, R_H, μ etc. on film thickness was similar to that observed for films of other semiconducting films such as MnTe, HgTe, etc. which had already been studied. The activation energy observed in PbTe and PbSe films was close to the values reported for bulk material by several workers (Tauber and

others, 1966; Charnic, 1968; Scanlon, 1958). However, in the lower temperature region, ΔE was less (by an order of two) than that for the higher temperature (0.25 to 0.35 eV). This suggests that a large number of acceptor impurities remained unionised at the low temperature region.

The typical variations of R_H with temperature (cf Fig. 6.8) also show that R_H was more or less constant at low temperature region for PbTe films for PbSe films were also similar except that these values are slightly increases in the lower temperature region. The mobility for both films were much less as compared to the bulk as reported by Putley 1955. This clearly indicates that the predominance of scattering of the changed carriers. This is also confirmed from the high carrier concentration ($n = 10^{19}$ cm^{-3}). The mobility however increased with increasing temperature for all films and followed $\mu \propto T^X$ law where X varied from 1.5 to 2.3, but thinner films conformed to ideal $T^{3/2}$ law. It is interesting to note that for all temperature ranges studied, continuously increased with T. This suggests that, lattice scattering conforming to $T^{-1/2}$ law was not present or even if it was present its contribution was insignificant. Gobrecht et al (1965) also reported a similar variation of T^X where X varied from 3/2 to 2 for PbTe films. The scattering mechanism was due to impurity ions as reported by many investigators

which are given in introduction of this chapter. The mobility is generally given by the relation,

$$\frac{1}{\mu_{obs}} = \frac{1}{\mu_{imp}} + \frac{1}{\mu_{latt}} + \frac{1}{\mu_{surface}} + \frac{1}{\mu_{poly}}$$

where

μ_{imp} = due to ionised impurity scattering

μ_{latt} = due to lattice scattering

$\mu_{surface}$ = due to surface mobility

μ_{poly} = due to polycrystalline nature of the films

The scattering processes followed the different mobilities laws as mentioned in Chapter I. Since in the present case the relation conformed to the impurity scattering, it appears that the effect of others was not significant.

It has been observed that the thermoelectric power, in throughout the temperature region and for all film thicknesses was positive. It increased gradually with the rise of temperature (78 to 320°K) but at higher temperature region the slope changed and the increase was much less with temperature. Calculations were also made for the variation of α with T assuming constant m^{*}_{h} and observed R_{H} at different temperatures by using the relation (31b). The graphs showed the downward trend slightly above 300°K for PbTe even though

there was no appreciable lattice scattering. The experimental results, however, did not exhibit any downward trend. This discrepancy appears to be due to lower magnitude of R_H and consequently higher concentration of n at higher temperature. Less R_H will automatically result in lowering the value of α (equation 31b). Recently Johnson (1962, 1964) and Smirnov (1961) have suggested that m^*_h of PbTe was not constant but was shown to increase with temperature. In general, this is in conformity with the prediction for MnTe and other films (cf Chapters III, IV). Thus as m^*_h of PbTe increases with temperature, there will be an effective rise in α even though R_H is less which is in conformity with our observation. In the case of PbSe films, the calculated theoretical graph shows a saturation with a very small downward trend whereas the observed α shows slightl increasing tendency. It seems that the increase of m^*_h in this case might be comparatively small.

CHAPTER-VI

REFERENCES

Bauer, G. et al (1976), J. Appl. Phys., 47(4), 1721.

Blomqvist, C.E. and Nikson, P.O. (1968), Phys. Rev., 174(3), 849.

Budzhak, Y.S. et al (1974), Fiz. Elektron, 8, 8.

Chasmar, M.P. and Putley, E.M. (1951), "Semiconducting Material" p.208.

Chernik, I.A. (1968), Fiz. Tekh. Poluprov, 2(8), 1173.

Deokar, V.D. and Goswami, A. (1966), Proc. Intern. Symp. on Basic Problems in Thin Film Physkcs, Clausthal, Vandenhock and Ruprecht, Gottingen, 653.

Devyatkova, E.D. (1952), Doklady Akad. Nauk. SSSR, 84, 687.

Dubrovskya, I.N. (1970), Fiz. Tekh. Poluprov, 4(11), 2201.

Eisenmann, L. (1940), Am. Physik., 38, 14.

Gauss and Hirahara, E. (1953), Bussievon Kenkya, 59, 168.

Gobrecht, H. et al (1965), Z. Physik., 187, 232.

Goswami, A. and Koli, S.S. (1966), Proc. of Int. Symp. on "Basic Problems in Thin Films Physics" Clausthal-Gottingen, Germany, p.646.

Goswami, A. and Koli, S.S. (1972), Indian J. Pure and Appl. Phys., 10, 629.

Hinterberger, H. (1942), Z. Phys., 119, 1.

Hirahara, E. and Murckani, M. (1954), J. Phys. Soc. Japan, 9, 67.

Jones, R.H. (1960), Proc. Phys. Soc., 76, 783.

Johnson, G.W. (1962), J. Electronics and Control, 12, 421.

Johnson, G.W. (1964), J. Electronics and Control, 16(5), 495.

Kolomiel, B.J. and Lanichev, V.M. (1958), Soviet Phys-Tekh. Phys., 3, 1266.

Kolomiets, M.V. et al (1957), Soviet Phys-Tekh. Phys., 2, 59.

Lyden, A.H. (1962), Tekh. Servo. AD 274, 131.

Makino, Y. (1964), J. Phys. Soc. Japan, 19, 580.

Matsushita, B. et al (1953), Bull. Fac. Engr., 3, 37.

Putley, E.H. (1952), Proc. Phys. Soc., 65B, 388.

Putley, E.H. (1955), Proc. Phys. Soc., 68B, 22.

Petritz, R.L. and Scanlon, W.W. (1955), Phys. Rev., 97, 1620.

Ravich, Yu. I. (1970), Fiz. Tverdogo Tela, 12(3), 971.

Scanlon, W.W. (1953), Phys. Rev., 92, 1573.

Silverman, S.J. and Levinstein, H. (1954), Phys. Rev., 94, 871.

Shogenji, K. and Uchiyama, S. (1977), Phys. Rev., 94, 871.

Smirnov, I.A. et al (1960), Fiz. Teverdogo Tela, 2, 1092.

Smirnov, I.A. et al (1961), Proc. Inter. Conf. Semiconductor, Phys. Prague 645.

Smit, R.A. (1951) "Semiconducting Materials" 198.

Spinulesch et al (1968), Phys. Stat Solidi, 26(1), 439.

Stavitskya, T.S. et al (1966) Izv. Akad. Nauk. SSSR, Neorg. Mater., 2(12), 4855.

Tauber, R.N. et al (1966) J. Appl. Phys., 37(13), 4855.

Todoroki et al (1975) Jap. J. Appl. Phys., 14(21), 466.

Tsictikovskii, I.M. (1955), Doklady Akad. Nauk. SSSR 102, 737.

Voronina, I.P. and Semiletov, S.A. (1964), Fiz. Tevrdogo Tela, 6(5), 540.

Watanabe, H. (1971) Rep. Res. Inst. Eleco. Commun., 23(1), 39.

Zemel, N.J. et al (1965), Phys. Rev., 140(A), 330.

Zhitriskya, M. (1966), Fiz. Tverdogo Tela, 8(1), 295.

CHAPTER-VII

GALLIUM TELLURIDE, GALLIUM SELENIDE AND INDIUM OXIDE

CHAPTER-VII

GALLIUM TELLURIDE, GALLIUM SELENIDE AND INDIUM OXIDE

(1) GALLIUM TELLURIDE AND GALLIUM SELENIDE

(A) INTRODUCTION

Telluride and selenides of gallium formed different types of compounds such as MX, MX_2 and M_2X_3 where M and X stand respectively for Ga and Te or Se. Some of these compounds have been reported to have good semiconducting properties.

Structural studies of these compounds have been carried out by several workers. The bulks crystals Ga_2Te_3 and Ga_2Se_3 have cubic structures with lattice parameters 5.86±5 A° and 5.429 A° respectively (Hahn and Klinger, 1949) and super structure to be zinc blend form for Ga_2Se_3 (Hahn, 1952). Anderevski et al (1962) studied the structure of Ga_2Se_3, Ga_2Te_3 and In_2Se_3 films and concluded that these compounds had varying structures depending on the substrate temperature. An electron diffraction study was made on the films of Ga-Te system by Semiletov and Vlasov (1963) and they observed several phases such as GaTe (a_o = 4.06 A°) and second phase (a_o = 10.32 A°) having composition intermediate between GaTe and Ga_2Te_3.

The optical and electrical properties of Ga_2Te_3 in the wavelength between 0.8 to 3.2 μ and temperature range from 20 to 790^oC were measured by Harbeke and Lamtz (1957). These compounds were found to be semiconducting and had activation energies of $\approx$ 1.55 eV and 1.00 eV was measured by electrical and optical method respectively. Kauer and Rabenau (1958) observed that activation energies of Ga_2Se_3 and Ga_2Te_3 were 1.9 eV and 1.0 eV respectively. However, the activation energy observed by Harbeke and Lamtz (1961) in case of Ga_2Te_3 was rather less and varied between 1.55 eV to 1.35 eV. Mobility and optical energy gap were estimated as 2.0 $cm^2/V.sec.$ and 1.1 eV at 300^oK respectively. Photoelectric and also electrical parameters of single crystal of the Ga-Te system were measured in the temperature range from -180^oC to 350^oC by Gramotski and Mushinskii (1964) and observed maximum photosensitivity at about 760 mμ for Ga_2Te_3. Similar studies were also made on Ga-Te system over a wide range of temperature by Velikanov et al (1969).

Koshkin et al (1971) studied the galvanomagnetic properties and thermoelectric power of Ga_2Te_3 and In_2Te_3 as a function of the excess of Ga and In contents and concluded that these impurities like Zn and Cu have no effect on these parameters. But Gramatskii and Mushinskii (1970), from the measurements of physical and galvanomagnetic properties of GaTe and

Ga_2Te_3 doped with impurities such as Cu, Ag, Au found a significant rise in ICR, thermo e.m.f. and conductivity in both pure and doped Ga_2Te_3. The ratio between the electron and hole mobilities in pure Ga_2Te_3 was observed 2 and increased with level of dopings. However, according to Koshikin et al (1971) there was neither a significant change in 'σ' nor in 'n' of Ga_2Te_3 and In_2O_3 doped with 1% excess atoms of Zn or CuO. This was assumed to be due to non-interaction of localised impurities with lattice atoms. Optical absorption and photo-conductivity of Ga_2Se_3 crystals studied in the temperature range from -77 to 293^oK by Mushinskii and Pavlenko (1971) suggested two types of recombination levels occurring in Ga_2Se_3. The reflection spectra of α-Ga_2Te_3 crystals with sphalerite structure (a_o = 5.43 A^o) and other properties were studied by Karaman et al (1972). Life time of optical phonon was estimated to be about 2.04x10^{-2} sec. IR and Raman spectra of semiconductors In_2O_3 and Ga_2Se_3 were studied by Finkaman et al (1975). Some work also has been done by a few workers on films of these compounds. Woolley and Pamplin (1961) measured the thermal conductivity, conductivity and Hall constant of Ga_2Te_3 and Ga_2Se_3 films in the temperature range from liquid air temperature to 900°C. Activation energy estimated from the plot of $R_HT^{3/2}$ vs 1/T at 500°C and 900°C was 1.0 and 2.0 eV respectively.

From the above survey it is apparent that a very few studies have been made on thin film of Ga_2Se_3 and Ga_2Te_3. Only recently Goswami and Goswami (1977) made a study on the epitaxial growth of Ga_2Se_3 and Ga_2Te_3 on different faces of rocksalt and observed that these films had cubic structures (a_o = 5.42 A^o, Ga_2Se_3, a_o = 5.88 Ga_2Te_3) and grew epitaxially at appropriate substrate temperatures (t_s). Ga_2Te_3 at higher temperatures often developed a new hcp phase (a = 4.16 A^o, c = 6.79 A^o). In the following, therefore, a detailed study has been made on the semiconducting properties of vacuum deposited thin films.

(B) EXPERIMENTAL

(i) Preparation of gallium telluride (Ga_2Te_3)

Gallium telluride was prepared from the reaction of constituent elements, Ga (99.99%) and Te (spec pure, 99.999%) were taken in stoichiometric proportion (2:3) in a silica tube which was then sealed under vacuum (10^{-5} mm of Hg). The tube along with its contents was then placed in an electrical furnace in an inclined position. The temperature of the furnace was slowly raised to about 480°C and kept it for three hours so that molten elements could react and the reaction be completed. To get the homogeneous compound the temperature of the furnace was raised to about 900°C and kept at this

temperature for 24 hours. The temperature of the furnace was then slowly lowered to about 500°C and then silica tube was quenched in cold water and final product was removed from tube.

In the case of Ga_2Se_3 preparation almost the same procedure was adopted except that final temperature was raised to about 1200°C. The mixture was kept at this temperature for 20 hours. While cooling the tube was immersed in cold water at about 500°C.

(ii) Preparation of films

The thin films of gallium telluride was made on glass substrate at 350°C from small conical silica boat covered by tungsten filament which was initially flashed in vacuum. All the films of Ga_2Te_3 were annealed in high vacuum ($3x10^{-5}$) at the same temperature for two hours before any electrical measurements were done. The set of films of various thicknesses was made under the same condition.

Similar technique was used for making the gallium selenide (Ga_2Se_3) films on glass substrate. However, these films are annealed at 350°C for 4 hours in high vacuum ($\simeq 10^{-5}$ mm of Hg). The films were reddish in colour.

Fig 7.1

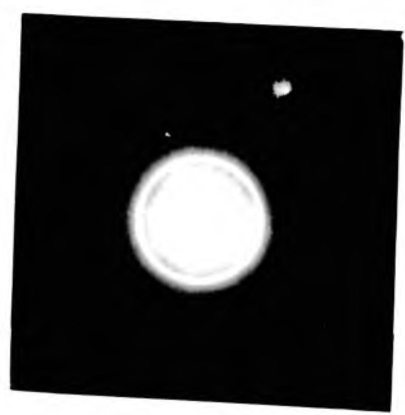

Fig 7.2

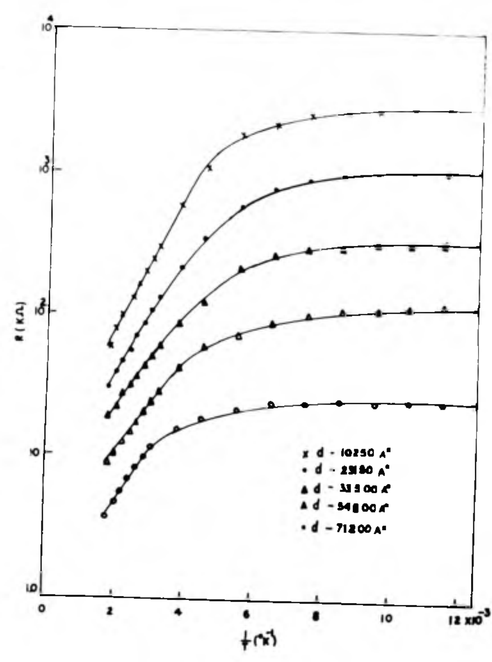

Fig 7.3

(a) Ga_2Te_3

(C) RESULTS

(i) Structure

Bulk powder of Ga_2Te_3 was studied by X-ray diffraction techniques. The measurements of X-ray powder pattern (Fig. 7.1) conformed to the cubic structure (a_o = 5.88 A°). Electron diffraction studies of films deposited below 300°C consisted of either tellurium or Te rich films. The deposition was made at 350°C and above had a cubic structure (Fig. 7.2) as reported earlier by Goswami and Goswami (1977).

(ii) Resistance, resistivity & activation energy

The resistance of annealed films was measured in vacuo and in the temperature range from 78° to 600°K. The variation of resistance with temperature is shown in Fig. 7.3 (R vs 1/T). It was found that the resistance decreased with increasing temperature but a change in resistance in the lower temperature region (78 to 300°K) was less compared to those at the higher temperature region (300 to 600°K). All the films were semi-conducting type. The variation of resistivity with thickness is shown in Fig. 7.4. It is seen that like other chalcogenides it was also a function of thickness, but these had very high

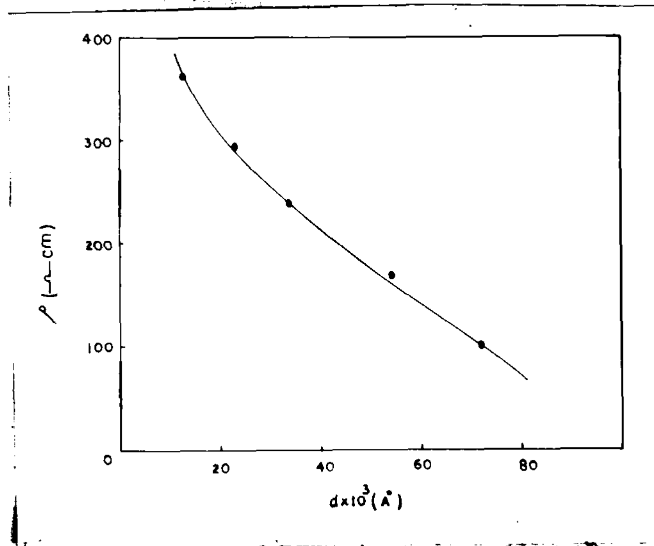

FIG. 7·4

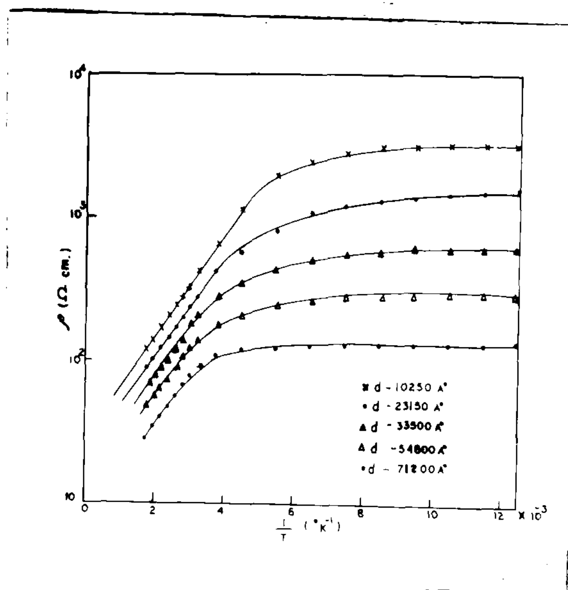

FIG. 7·5

resistivity. Its variation with temperature and thickness is shown in Fig. 7.5. It is seen that at lower temperature region (78 to 300°K) the change in resistivity with temperature was not much but this parameter decreased rapidly after 300°K when it became intrinsic.

Activation energy

The activation energy was estimated from the linear variation of log ρ vs 1/T relation for different temperatures ranges and different film thicknesses. The variation of activation energy with temperature and the thickness is given in Table-7.1. It is seen that it varied with thickness and temperature, thinner films having higher values. At lower temperature region (200-100°K) it was smaller by a factor of about 10 than that of the higher temperature region (300-500°K).

(iii) TCR

A typical variation of TCR with temperature is shown in Fig. 7.7. It increased with increasing temperature, attained a peak at 300°K and then decreased with the further increase of temperature. The peaks varied with the film thickness. It is also a function of thickness.

TABLE-7.1

$T_s = 350^{o}C$

Ga_2Te_3

Variation of 'ΔE' with 'd'

S.No.	Thickness d(A^o)	Temp. range ($600-300^{o}K$) ΔE (eV)	Temp. range ($300-200^{o}K$) ΔE (eV)	Temp. range ($200-100^{o}K$) ΔE (eV)
1.	10250	0.220	0.095	0.024
2.	23150	0.200	0.086	0.016
3.	33500	0.185	0.075	0.009
4.	54800	0.175	0.058	0.006
5.	71200	0.160	0.047	0.004

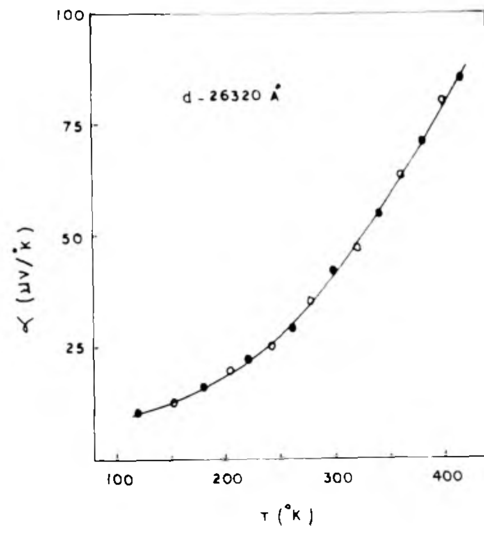

Fig 7.6

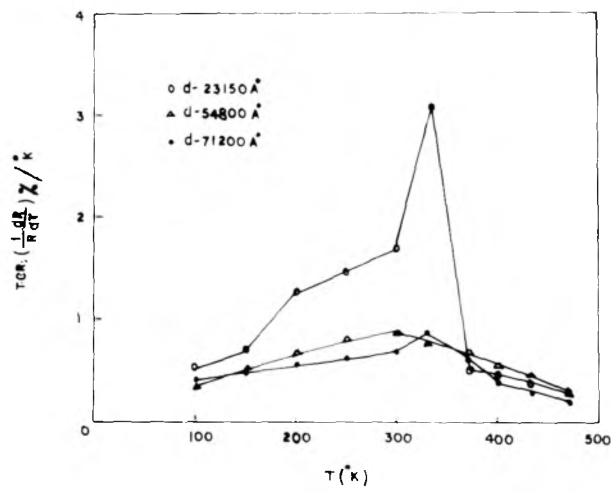

Fig 7.7

Fig 7 8

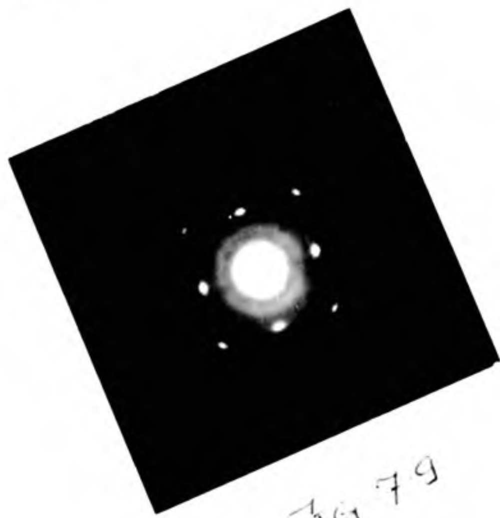

Fig 7 9

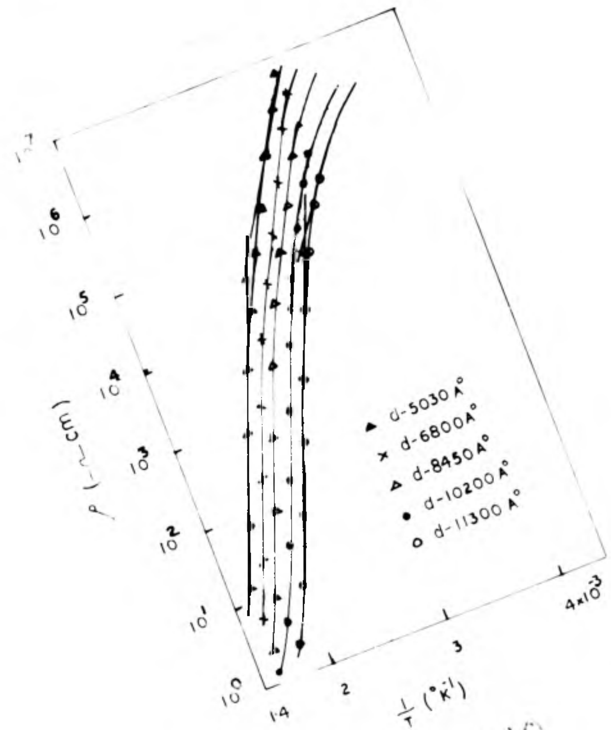

Fig 7 10

(iv) Thermoelectric power

Thermoelectric power measurement showed that all gallium telluride films were n-type and it was measured by differential method. Thermoelectric power variations with temperature is shown in Fig. 7.6. It increased continuously with the increase of temperature. But the increase in α in the temperature range from 78 to 300°K was more than that to higher temperature range (above 300°K).

(b) Ga_2Se_3

(C) RESULTS

(i) Structure

Bulk material studied by X-ray powder techniques were found to have cubic structure as shown in Fig. 7.8. Fig. 7.9. Electron diffraction study of films also confirmed the above structure earlier reported by Goswami and Goswami (1977). These films had very high resistivity and hence the electrical parameters measurements could be carried out at higher temperatures.

(ii) Resistivity and activation energy

The variation of resistivity with temperature and film

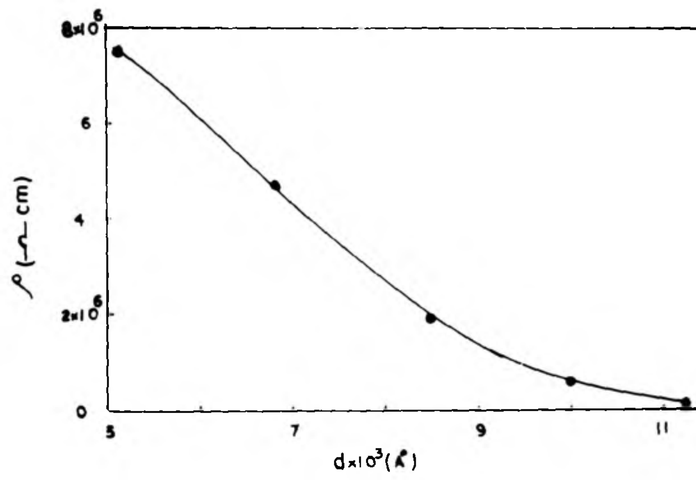

Fig 7 11

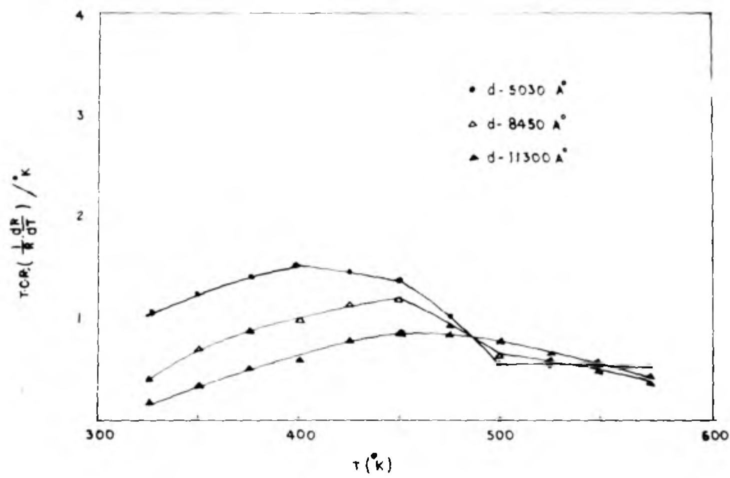

Fig 7 12

thickness is shown in Fig. 7.10. Fig. 7.11 shows the variation of ρ with thickness (d). Thinner films are having higher value of resistivity.

Activation energy

Activation energy was estimated from linear relation log ρ vs 1/T for various films deposited under the same condition. It was found to be thickness dependent. Thinner films are having higher activation energy as observed in the case of other compounds. The variation of activation energy with different thicknesses and with different temperature ranges is shown in Table-7.2. It is seen that activation energy in the temperature range 300 to 400°K is slightly less than that of higher temperature region (400-600°K).

(iii) TCR

All films had negative TCR. Its variation with temperature is shown in Fig. 7.12. It increased gradually with the increase of temperature and after attaining the peaks which shifted with thickness it decreased with further increase of temperature.

(D) DISCUSSION

Bulk Ga_2Te_3 and Ga_2Se_3 have the cubic ZnS type of structure. The above structure study of the films deposited at

TABLE-7.2

$T_s = 350^{o}C$

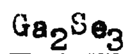

Ga_2Se_3

Variation of 'ΔE' with 'd'

S.No.	Thickness d(A^o)	Temp. range ($300-400^oK$) ΔE (eV)	Temp. range ($400-600^oK$) ΔE (eV)
1.	5030	1.25	1.87
2.	6800	1.11	1.82
3.	8450	1.00	1.78
4.	10200	0.99	1.69
5.	11300	0.96	1.60

350°C demonstrates that the deposits formed had mostly the cubic structure (Ga_2Se_3 a_o= 5.42 A^{o}, Ga_2Te_3 a_o= 5.88 A^{o}) similar to the bulk compounds. The thicker films were mostly polycrystalline in nature.

During our present study it has been observed that resistivities of these films at room temperature were of the order of $2x10^{2}$ ohm cm and $5x10^{6}$ ohm cm respectively for Ga_2Te_3 and Ga_2Se_3 films. These also had negative temperature coefficient of resistance with increase of temperature thus suggest these were semiconducting nature. Thermoelectric test showed that Ga_2Te_3 were n-type whilst Ga_2Se_3 were p-type. These observations suggested that the majority carriers in the two cases were electrons and holes respectively.

The temperature dependence of resistance as shown in log R vs 1/T graph (cf Fig. 7.3) for Ga_2Te_3 shows that these follow the linear relation at higher temperature (300 to 600°K) but tend to saturate at lower temperature. The linear slope showed the variation with the thickness. Thinner films have slightly higher slopes. Activation energy for these films varied from 0.16 eV to .22 eV which are about an order less than the bulk (1.5 eV). The low value of ΔE appears to be due to creation of donor levels close to the conduction band edge. This is also in conformity with our observation of electron diffraction patterns. These films were found to be intermixed

with some other species arising from the dissociation of Ga_2Te_3. These dissociated products would, no doubt, create new donor levels since their concentrations would be quite high. Hence with a slight thermal energy they will ionise to facilitate the electrical conduction.

At the low temperature region, thermal ionisation will be less and conduction will also be less. This resulted in the high magnitude of resistivity. When the temperature is very low the thermal ionisation will be minimum and so will be conductivity and hence materials would tend to saturate as observed in the present study.

Ga_2Se_3, on the other hand, showed more or less a linear relation for log R or ρ vs 1/T. They tend to saturate below $400^{o}K$. Since the magnitude of resistance these films was very high no measurements were possible below $300^{o}K$. It is interesting to note that ΔE measured for Ga_2Se_3 were about 1.8 eV which is in close that of bulk (1.9 eV) as reported by many investigators (Kauer and Rabena, 1958; Wooley and Pamplin, 1961). This suggests that unlike Ga_2Te_3, Ga_2Se_3 did not have sufficient defects density to lower its activation energy. This is also in conformity with the fact that Ga_2Se_3 films were having high resistivity ($10^{6}\ \Omega$ cm) compared to $10^{2}\ \Omega$ cm of Ga_2Te_3 films. Since the incorporation of defects normally increase the electrical conduction due to thermal ionisation in

films, one can conclude that Ga_2Se_3 films were composed of defects.

Since both type of films had high resistivities, no measurements could be made about R_H at different temperatures and consequently the evaluation of 'n' as well as μ. Because of the supporting evidences of variation of 'n' with temperature. The above considerations are more or less tentative. Attempts to measure α for Ga_2Te_3 have been partially successful but no such measurements were possible for Ga_2Se_3 again because of high resistance. The temperature dependence of α showed an increase with temperature as observed for other cases. However, no comparison with theoretical model could be made because of the lack of experimental data about variation of μ with temperature.

CHAPTER-VII (i)

REFERENCES

Anderevski, et al (1962), Kristallografiya (USSR), 7, 865.

Finkaman, E. et al (1975), Phys. Rev., B11(10), 2785.

Goswami, A. and Goswami, N.N. (1977), Indian J. Pure and Appl. Phys., 15, 513.

Gramatskii, V.I. and Mushinskii, V.P. (1964), Izv. Akad. Nauk. SSSR, Ser. Fiz., 28(6), 1077.

Gramatskii, V.I. and Mushinskii, V.P. (1970), Poluprov Sovedin Ikh Tvered Rastrovy, 124, 34.

Hahn, H. (1952) Angew Chem., 64, 203.

Hahn, H. and Klinger, W.Z. (1949), Z. anorg. chem., 250, 155.

Harbeke, G. and Lamtz, G. (1957), Z. Naturforsch, 11A, 1015.

Harbeke, G. and Lamtz, G. (1961), J. Electrochem. Soc. 108, 874.

Karman, M.I. et al (1972), Neorg-mater, 8(7), 1301.

Kauer, E. and Rabanau, A. (1958), Z. Naturforsch, 13a, 531.

Koshikin, V.M. et al (1971). Fiz. Tekh. Poluprov, 5(10), 1983.

Mushinskii, V.P. and Pavlenko, N.M. (1971), Fiz. Tekh. Poluprov, 5(8), 1674.

Semiletov, S.A. and Vlasov, V.A. (1963), Kristallografiya, 8(6), 877.

Velikanov, A.A. et al (1969), Tr. Inst. Met. Sverallorsk, 20, 90.

Woolley, J.C. and Pamplin, B.R. (1961), J. Electrochem. Soc., 108, 874.

(2) INDIUM OXIDE

(A) INTRODUCTION

Indium oxide films have attracted considerable attention because of their practical uses in many solid state devices. These films though supposed to have high resistance often show conduction in thin film form. Further, because of their transparency and at the same time, they are now being used as transparent electrodes or conducting coatings.

Some electron diffraction studies on vacuum deposited amorphous films on glass has been made by Sheftal and Tataninva (1965). The interatomic distances were reported to be 2.05 and 3.5 A°. Marezio (1966) observed that In_2O_3 had a cubic structure (a_o = 10.117 A°). Goswami and Kolhe (1971) investigated the structures of In_2O_3 films on different substrates and temperatures. These deposits of In_2O_3 (a_o = 10.13 A°) grew epitaxially on NaCl {100} face with {111} orientation occasionally mixed with other orientations.

The semiconducting properties of bulk indium chalcogenides were studied by Kauer and Rabenau (1958). The activation energy and band gap of In_2O_3 was found to be 1.0 eV and 2.8 eV by electrical and optical methods respectively. Weiher (1962), on the other hand, found these to be about 1.55 eV and 2.8 eV at elevated temperature and E_g was reported about 3.1 eV.

Thiel and Luckman (1928) reported the dissociation of In_2O_3 to In_2O when heated in vacuo but Khrostukhina (1962) suggested that the dissociated products were mostly InO and O_2. Remeika and Spencer (1964) prepared transparent (visible region) semiconducting single crystal of In_2O_3 and reported very low activation energy. Weiher and Ley (1966) observed several transition such as at energy gap $\approx$ 3.75 eV indirect forbidden transition at energy gap 2.61 eV and phonon transition at 0.069 eV. According to them, conduction band minimum did not coincide with that of valence band maximum. This was also confirmed by Tippins and Chase (1966) and later by Vainshtein and Fistual (1971). Dissociated products of In_2O_3 consisted of In^+, O_2^+ and In_2O^+ and some traces of InO were observed by Burns (1960). He found that there was no In_2O_3 species in the gaseous state. Dewit (1975) also measured the electrical conductivity in air upto 1400^oC and observed the activation energy about 1 eV at higher temperature which was interpreted in terms of the nonstoichiometric nature of the compound.

Thin film properties also have been studied by several workers. Holland and Siddall (1953) studied the transmittance of sputtered In_2O_3 films in the visible region. However, no study was made about their structure and composition. Rupprecht (1954) observed an increase in conductivities of

In_2O_3 films when measured in air which had been ascribed to the reduction of contact of O_2 at the surface region. The effect of strong electric field on mobility and carrier concentration of polycrystalline films was observed by Lutskii (1966) and the increase in mobility with the field was noted. Ryabova and Savitskya (1968) observed a change in resistivity from 10^{12} to $10^{2}\ \Omega$ cm by conducting from amorphous state to that of well oriented crystalline state. The optical, electrical and structural properties of sputtered In_2O_3 films were studied by Burbulevicius (1969) and showed that the above parameters changed on thermal treatment in vacuo. In recent years, sputtered films of In_2O_3 with some % of SnO_2 or CdO have been used as transparent electrodes (Fischer, 1954; Vossen, 1971; Mehta and Volgel, 1972). Molzen (1965) made sputtered film from alloy target of In + 5% Sn in presence of oxygen by R.F. sputtering technique. The films annealed at 600°C in argon showed 95% transparency (in the visible region) and had sheet resistance 2.3 $\Omega/\square$. Goswami and Goswami (1977) investigated the optical and dielectric properties of vacuum deposited indium oxide films (In-O) as well as the oxidised films (In_2O_3). Their a.c. behaviour at different temperatures and at various film thicknesses in the audio-frequency region were studied. They found that ϵ of In-O films were thickness dependent and also showed dielectric relaxation at lower frequencies due to the dipolar orientation

arising from their non-stoichiometric nature. The results have been discussed from the classical theory of dielectric polarisation.

(B) EXPERIMENTAL

(i) Film preparation

The films of In_2O_3 were prepared by the oxidation of vacuum deposited indium film in air. Indium films were deposited on glass substrate by vacuum deposition from conical basket type tungsten filament initially flashed in vacuum. The deposited indium films were then oxidised in air atmosphere at about 400^oC for 20 hours. These films were found to be transparent. Films of In_2O_3 with different thicknesses were prepared and their electrical properties were studied in the air from room temperature to 600^oK. These were then subjected to cycles of heating and cooling from room temperature to 600^oK so as to stabilise them in air. These films were then studied for their electrical properties in the usual way.

(C) RESULT

(i) Structure

Fig. 7.13 shows a typical transmission pattern obtained from the oxidised films formed on polycrystalline NaCl tablets. An analysis of this pattern showed that the films were due to

Fig 7.13

Fig 7.14

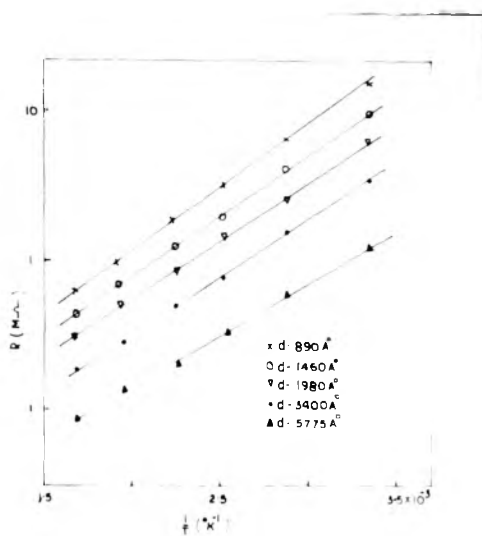

Fig 7.15

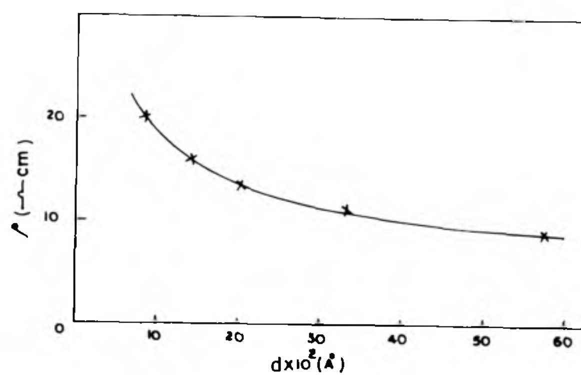

Fig 7.16

In_2O_3 having b.c.c. type of structure with a_o = 10.12 A^o. Reflection patterns (Fig. 7.14) were also taken from films deposited on glass substrate and subsequently oxidised in air at 300°C for three hours. Sharp reflections clearly showed that these films were crystalline.

(ii) Resistance , resistivity & activation energy

Before carrying out the measurements of electrical parameters the discontinuity temperature of In_2O_3 films were found out about 370°C. These films were annealed at temperature about 325°C in air for 4 hours.

The resistance for the different samples was measured with the increase of temperature from 300°K to 600°K in air the reason for which has already been given. The resistance of all films deposited were very high and was about the order of megohm. It, however, was found to decrease with the increasing temperature thus showing the semiconducting in nature. Typical curves (Fig. 7.15) show the variations of log R vs 1/T for various film thicknesses ranging from 800 A^o to 6000 A^o, thicker films, however, having lower resistance. The variation of resistivity with thickness is shown in Fig. 7.16. It was also found that ρ was dependent on film thickness as observed in other films. Similar trend was also observed in variation with temperature and film thickness (Fig. 7.17).

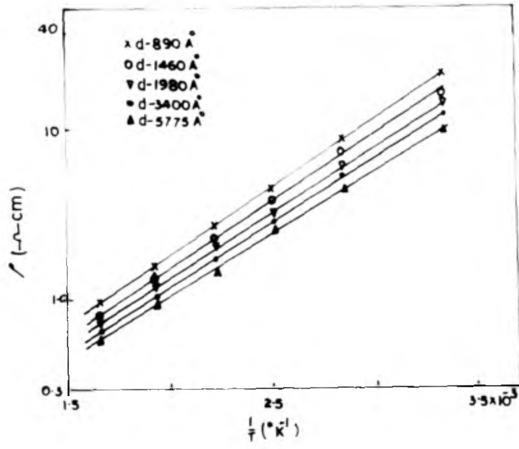

Fig 7.17

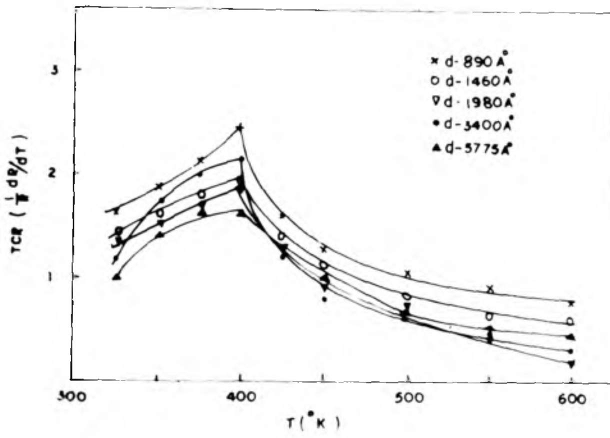

Fig 7.18

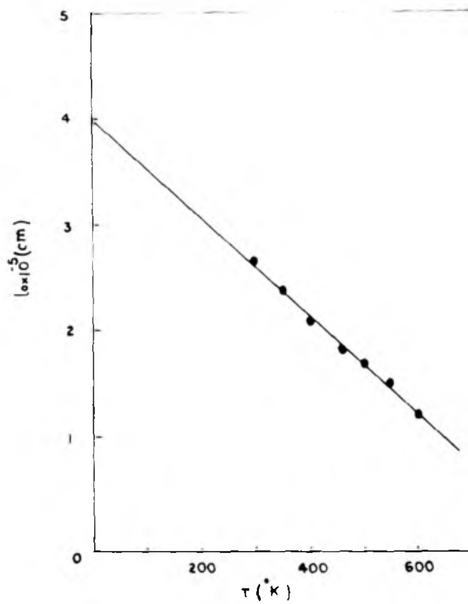

Fig 7.19

Activation energy

The activation energy for different film thicknesses was estimated from the linear variation of log ρ vs 1/T by the usual way. It varied from 0.47 eV to 0.57 eV for the thickness variation from 800 A^{o} to 6000 A^{o}. It showed that the activation energy increased slightly with decrease of the film thickness.

(iii) TCR

This parameter for In_2O_3 films was measured in the usual way described previously (Chapters III, IV). The Fig. 7.18 shows the typical curves for TCR vs temperature for In_2O_3 films. It is seen that TCR was negative and its range increased with increasing temperature upto 375°K and then decreased further with increase of temperature upto 600°K. It is interesting to see that the peaks are shifting with thickness and thicker films are having lower TCR.

(iv) Mean free path (l_o)

The mean free path for In_2O_3 films was calculated from the resistivity measurements at different temperatures for the different film thicknesses prepared under the same condition of deposition. From the Fig. 7.19 it is seen that it decreased with the increase of temperature and the value obtained from

the intercept of l_o vs T was about $4x10^{-5}$ cm to 0^oK.

Table-7.3 shows the variation of R, ρ , and ΔE with the film thickness.

(D) DISCUSSION

The electron diffraction study of the In_2O_3 films showed that these films were having b.c.c. type structure and deposits were crystalline in nature. These films had very high resistance in the range of $M\Omega$. The measurements of resistance in vacuum from room temperature to 600^oK showed a fall in resistance during the initial heating process. But during cooling the resistance variation with temperature did not follow the same path. For each and every heating cooling cycles the resistance values changed. These changes occurring during the above heating-cooling cycles in vacuum appeared to be due to the thermal dissociation of In_2O_3 to lower oxides. Gadgil and Goswami (1970) found during the recent study of Bi_2O_3 that BiO was intermediate product during both oxidation and in vacuum measurement. Such type of intermediate sub-oxide such as In-O phase may be present during the thermal evaporation of In_2O_3 or dissociation of the compound. However, when these films were in air atmosphere and measurements during heating and cooling cycles were also carried out in air, the same path was followed. The films showed semiconducting

TABLE-7.3

In_2O_3

S.No.	Thickness d(A°)	R (M Ω)	ρ (ohm.cm.)	ΔE (eV)
1.	870	13.50	20.0	0.560
2.	1460	8.50	16.0	0.530
3.	1980	5. 60	13.0	0.505
4.	3400	3.00	11.5	0.490
5.	5775	1.12	9.0	0.470

characteristic. The variation of resistance with temperature (i.e. log R vs 1/T) was linear throughout the temperature region (300° to $600^{o}K$). The slopes varied slightly with the film thickness. The magnitude of ΔE were found to vary from 0.45 eV to 0.57 eV which was less as compared to the bulk value $\simeq$ 1.0 eV reported by Dewit (1975). The low values of ΔE were no doubt due to these films having high density defects. These films were n-type i.e. the impurities were in sub-band which was very close to the conduction band. The mean free path was observed to decrease with increase of temperature and value obtained at $0^{o}K$ was about 4×10^{-5} cm.

CHAPTER-VII (ii)

REFERENCES

Burns, R.P. (1966), J. Chem. Phys., **44**, 3307.

Burbulevicius, L. (1964), Neorgmatter, **5(3)**, 551.

Dewitt, J.H.W. (1975), J. Solidstate Chem., **B(3)**, 1972.

Fischer, A. (1954), Z. Naturforchg, **99**, 508.

Gadgil, L.H. and Goswami, A. (1970), Indian J.Chem., **8**, 431.

Goswami, A. and Goswami, A.P. (1977), Pramana, **18** No.4, 335.

Goswami, A. and Kolhe, D.B. (1971), Ph.D.Thesis, University of Poona.

Holland, L. and Siddal, G. (1953), Vacuum, **3**, 375.

Kauer, E. and Rabenau, A. (1958), Z. Naturforsch, Ba 531.

Khrostukhina, N.A. (1962), Akad. Nauk SSR, 78.

Lutskii et al (1966), Vop. plenochem Elektron, 423.

Marezio, M. (1966), Acta. Cryst., **20**, 723.

Mehta, R.R. and Volgel, S.F. (1972), J. Electrochem. Soc., **119**, 752.

Molzen, W.W. (1975), J. Vac. Sci. Tech., **12(1)**, 99.

Remeika, J.P. and Spencer, E.G. (1964), J. Appl. Phys., **35(10)**, 2803.

Rupprecht, G. (1954), Z. Phys., **139**, 504.

Ryabova, L.A. and Savitskya, Y.S. (1968), Thin Solid Films, **2**, 141.

Sheftal, R.N. and Tataninva, L.I. (1965), Kristallografiya, **10(2)**, 205.

Thiel, A. and Luckamann, H. (1928), Z. anorg. chem., **172**, 353.

Tippina, H.H. and Chase, A.B. (1960), Bull. Am. Soc., **11**, 765.

Vainshtein, V.M. and Fistul, V.I. (1971), Soviet Phys-Semicond., **4**, 1275.

Vossen, J.L. (1971), R.C.A. Review, **32**, 289.

Weiher, R.L. (1962), J. Appl. Phys., **33**, 2834.

Weiher, R.L. and Ley, R.P. (1966), J. Appl. Phys., **37**, 299.

SUMMARY AND CONCLUSIONS

SUMMARY AND CONCLUSION

A systematic study has been carried out in details on the electrical properties of vacuum deposited films of some chalcogenide and oxide with a view to understand the electron transport process and particularly the scattering mechanism and compare with the corresponding properties of the bulk materials.

Consequently, the electrical parameters such as resistivity, Hall effect, thermoelectric power, etc. of deposits formed at different substrate temperatures were measured in a wide range of temperature (78 to 600°K). From these the important parameters like activation energy, TCR, Hall constant carrier concentration, mobility have been evaluated. Further other parameters such as potential barrier height between the grain boundaries, mean free path and possible effective mass of the charge carriers, Fermi energy, etc. have also been deduced. Assuming various types of scattering mechanisms, attempts have been made to evaluate quantitatively the thermoelectric power and compared with observed values at different temperatures. Effective mass is an uncertain quantity for thin films materials. Some attempts have been made to evaluate its magnitude at different temperatures from the observed temperature dependence of thermoelectric power assuming a known

mode of scattering mechanism of the charge carriers vide the relation (cf equation 31a).

It can be mentioned here that these electrical properties were considerably influenced by the evaporation conditions such as substrate and annealing temperatures, crystallients grain boundaries, etc. The structural properties of the films were simultaneously studied by electron diffraction technique which helped not only to confirm the structure but also the study the phase change occurring if any films while depositing them.

The electrical and the structural properties of vacuum deposited MnTe films deposited at 350°C by the thermal evaporation technique were studied in details. The X-ray powder and the electron diffraction analysis of the bulk and films respectively showed that MnTe and NiAs type structure (a = 4.68 and c = 6.82 A°) and the electron diffraction studies showed that these films developed 1-d{10.3} orientations. These films were semiconducting and p-type and hence the majority of the charge carriers were due to the presence of acceptor levels. These deposits would have no doubt necessary grain boundaries as well as other defects such as dislocations, structural disorder, surface asperities, etc. The thermal activation energy evaluated from the both linear portion of the log ρ vs 1/T and log n vs 1/T was found to be varying between 0.1 eV to

0.11 eV with thickness ranging from 10000 A^{o} to 25000 A^{o}. Another important conclusion that follows from the above study is that the mobility increased with increasing temperature and attained a peak at about 315°K and then decreased. The mobility variation suggested that the ionised impurity scattering was predominant below T_p whilst above it scattering mechanism was due to piezoelectric type. Not only ρ, R_H, μ, α but also the potential barrier height were affected by the film thickness. There was good agreement between the observed α and those computed theoretically below T_p. However, there was a sharp deviation in shape of the α-T curves above T_p. This deviation could be caused by several factors and magnon drag might be one of the possible causes. Evaluated m^*_h from the observed thermoelectric power suggested that m^*_h was temperature dependent. Manganese selenide films (1000 to 25000 A^{o}) had much higher resistance (MΩ) and were p-type. The activation energy varied from 0.57 eV to 0.27 eV for thinner to thicker films.

Mercury telluride films formed at 120°C had a cubic structure and developed a 1-d{111} orientation and these were semiconducting. The observed activation energy ($\approx$.08 eV) was very much less than the ΔE_g (=1.13 eV) and was slightly dependent on film thickness. R_H was more or less constant in the low temperature region but it decreased at higher

temperatures. The mobility variation with temperature and thickness was similar to that of MnTe films and the probable scattering mechanism was due to ionised impurities and piezoelectric below and above 310°K respectively. Unlike MnTe, no peak in α was at all observed. Even though a downward trend was expected due to the piezoelectric effect, the saturation tendency was assumed to be due to the superimposition of effect of unionised impurities over the piezoelectric mechanism or due to the considerable increase in effective mass to counterbalance the latter effect. The mean free path was found to be increasing with decreasing temperature and its value obtained at 0°K was about 6.5×10^{-5} cm. Effective hole mass also increased with increasing of temperature.

Tin telluride films showed semimetallic behaviour, similar to the bulk single crystal. All the films were p-type and had positive TCR indicating the overlapping of valence and conduction bands. R_H and ρ variation with temperature showed that these were more or less constant at lower temperature region (78 to 300°K) but a decrease at higher temperature regions. The mobility variation suggested that the atomic lattice and piezoelectric scatterings were dominant above and below 300°K respectively. The thermoelectric power and mean free path for these films were similar to the bulk values. The behaviour of SnSe films, however, differed considerably from those of the bulk.

Lead telluride and lead selenide films showed some peculiar features. Both types of films were semiconducting in nature. Activation energy was a function of film thickness, thinner films had higher activation energy, ρ, R_H and μ etc. changed considerably with the film thickness. The variation of mobilities with temperature for both films was similar i.e. these increased with increasing temperature and followed $\mu \propto T^X$ relation where X varied from 1.5 to 2.2. Another feature noticed was that the dominant scattering mechanism in these films was due to ionised impurities. The calculated thermoelectric power (α–T graph) was of the same nature upto about 300°K but decreased in case of PbTe films. This discrepancy may be due to the effective mass variation at higher temperature. However, there was a good agreement in theoretical and observed α throughout the temperature range in case of PbTe films.

Ga_2Te_3 and Ga_2Se_3 deposits had cubic structure and were n-type and p-type semiconductors respectively. The activation energy observed in case of Ga_2Te_3 was very much less as compared to the bulk while Ga_2Se_3 was near about the bulk value.

The structural analysis of In_2O_3 films showed a b.c.c. type structure with a_o = 10.12 A°. These films (800 to 6000 A°) were semiconducting in nature and ΔE varied between 0.57 to

0.47 eV as thickness varied from thinner to thicker one.

The above studies on the electrical properties of semiconducting, semimetallic and oxide films reveal that the scattering mechanism of the charge carriers and magnitude of these often changed in film state. Some of these can be adduced to factors such as evaporation conditions, annealing, film thickness and much more so to the presence of impurities and defects which are invariably present in the evaporated films, as mentioned earlier. Effects of vacuum of conditions, also cause the phase changes and sometimes with a consequent dissociation. These also change the electrical parameters. The quantitative estimation of thermoelectric and effective carrier mass for thin films would be of great interest. With the precise knowledge of the effective mass along with the other transport properties it would be possible to quantitatively verify a proposed theoretical model for the conduction mechanism in thin films. However, due to a lack in knowledge of the precise value of m^* especially in thin film, it could not be satisfactorily carried out. Despite this deficiency, the present studies definitely showed a variation of the above parameter with temperature and the observed magnitude can at best be treated as artificial one. Whether these have any real significance can only be determined when magnitudes are precisely known.

ACKNOWLEDGEMENTS

The author is extremely grateful to Dr. A. Goswami, Ph.D.(London), D.Sc.(London), Assistant Director, National Chemical Laboratory, Poona-411 008, for his guidance, supervision, encouragement and keen interest in the present investigation.

The author wishes to thank the Director, National Chemical Laboratory, Poona-411 008, for permission to submit this work in the form of a thesis.

He is also grateful to all his colleagues in the Structure and Thin Film Physics Division for their hearty co-operation during the present investigation.

ABMandale

(A. B. MANDALE)